

Supplementary Materials for

The genomic history of the Iberian Peninsula over the past 8000 years

Iñigo Olalde, Swapan Mallick, Nick Patterson, Nadin Rohland, Vanessa Villalba-Mouco, Marina Silva, Katharina Dulias, Ceiridwen J. Edwards, Francesca Gandini, Maria Pala, Pedro Soares, Manuel Ferrando-Bernal, Nicole Adamski, Nasreen Broomandkshobacht, Olivia Cheronet, Brendan J. Culleton, Daniel Fernandes, Ann Marie Lawson, Matthew Mah, Jonas Oppenheimer, Kristin Stewardson, Zhao Zhang, Juan Manuel Jiménez Arenas, Isidro Jorge Toro Moyano, Domingo C. Salazar-García, Pere Castanyer, Marta Santos, Joaquim Tremoleda, Marina Lozano, Pablo García Borja, Javier Fernández-Eraso, José Antonio Mujika-Alustiza, Cecilio Barroso, Francisco J. Bermúdez, Enrique Viguera Mínguez, Josep Burch, Neus Coromina, David Vivó, Artur Cebrià, Josep Maria Fullola, Oreto García-Puchol, Juan Ignacio Morales, F. Xavier Oms, Tona Majó, Josep Maria Vergès, Antònia Díaz-Carvajal, Imma Ollich-Castanyer, F. Javier López-Cachero, Ana Maria Silva, Carmen Alonso-Fernández, Germán Delibes de Castro, Javier Jiménez Echevarría, Adolfo Moreno-Márquez, Guillermo Pascual Berlanga, Pablo Ramos-García, José Ramos Muñoz, Eduardo Vijande Vila, Gustau Aguilera Arzo, Angel Esparza Arroyo, Katina T. Lillios, Jennifer Mack, Javier Velasco-Vázquez, Anna Waterman, Luis Benítez de Lugo Enrich, María Benito Sánchez, Bibiana Agustí, Ferran Codina, Gabriel de Prado, Almudena Estalrich, Álvaro Fernández Flores, Clive Finlayson, Geraldine Finlayson, Stewart Finlayson, Francisco Giles-Guzmán, Antonio Rosas, Virginia Barciela González, Gabriel García Atiénzar, Mauro S. Hernández Pérez, Armando Llanos, Yolanda Carrión Marco, Isabel Collado Beneyto, David López-Serrano, Mario Sanz Tormo, António C. Valera, Concepción Blasco, Corina Liesau, Patricia Ríos, Joan Daura, María Jesús de Pedro Michó, Agustín A. Diez-Castillo, Raúl Flores Fernández, Joan Francès Farré, Rafael Garrido-Pena, Victor S. Gonçalves, Elisa Guerra-Doce, Ana Mercedes Herrero-Corral, Joaquim Juan-Cabanilles, Daniel López-Reyes, Sarah B. McClure, Marta Merino Pérez, Arturo Oliver Foix, Montserrat Sanz Borràs, Ana Catarina Sousa, Julio Manuel Vidal Encinas, Douglas J. Kennett, Martin B. Richards, Kurt Werner Alt, Wolfgang Haak, Ron Pinhasi, Carles Lalueza-Fox, David Reich

This PDF file includes:

Supplementary Text
Figs. S1 to S11
Tables S6 to S22
Caption for Tables S1, S2, S3, S4 and S5

Other Supplementary Material for this manuscript includes the following:

Tables S1, S2, S3, S4 and S5 as excel files
Genotype dataset

46 Table of Contents

47

48	SI 1 -	Archaeological context of newly reported individuals.....	3
49	SI 2 -	Direct AMS ¹⁴ C Bone Dates.....	56
50	SI 3 -	Ancient DNA laboratory work	57
51	SI 4 -	Bioinformatics processing	58
52	SI 5 -	Mitochondrial and Y-chromosome haplogroup determination	58
53	SI 6 -	Kinship analysis.....	59
54	SI 7 -	Genome-wide analysis datasets	60
55	SI 8 -	Principal component analysis	61
56	SI 9 -	<i>f</i> -statistics	61
57	SI 10 -	Estimation of F_{ST} coefficients	61
58	SI 11 -	<i>qpAdm</i> admixture modeling.....	61
59	SI 12 -	Allele frequency estimation of SNPs of phenotypic importance	72
60	SI 13 -	Date of the Carigüela pre-Neolithic individual	73

61

62 **SI 1 - Archaeological context of newly reported individuals**

63 In this section we specify dates in one of two formats. If there is no direct radiocarbon
64 date on the individual analyzed with aDNA, we give a date based on the archaeological
65 context or on the genetic results, in a format like “2500–1700 BCE”. Alternatively, if
66 there is a direct radiocarbon date on the bone being analyzed, we give a date in a format
67 like “95.4% CI calibrated radiocarbon age (Conventional Radiocarbon Age, Lab
68 number)” (an example is “365–204 cal BCE (2215±20 BP, PSUAMS-3466)”). All the
69 dates were calibrated in OxCal 4.2.3 (27) using the IntCal13 calibration curve (28).

70 We thank the Dirección General de Bienes Culturales y Museos de la Consejería de
71 Cultura de la Junta de Andalucía for authorizing the study of the samples held at the
72 Museo Arqueológico y Etnológico de Granada. We thank the Museo de Arqueología de
73 Alava, the Centro de Patrimonio Cultural Mueble GORDAILUA (Irun, Gipuzkoa), the
74 Gobierno Vasco, the Direcció General de Cultura de la Generalitat Valenciana, the
75 Ajuntament de València, the Ajuntament de Bocairent, the Ajuntament de la Font de la
76 Figuera, the Museu de Prehistòria de València, the Museu de Castelló, the Museu de la
77 Valltorta and the Museu d'Alcoi for granting permission to study archaeological remains

78 **Bray Cave (Gibraltar)**

79 *Contact: Clive Finlayson, Francisco Giles, Geraldine Finlayson, Stewart Finlayson*

80 Bray's Cave is located about 330 m. a.s.l. on the western slope of the Rock. The cave
81 formed along the bedding planes of the limestone layers which lie in a north-south
82 orientation dipping to the west, and contains a number of types of speleothem formations,
83 typical of closed cavities with gallery morphology. The current appearance of the cave,
84 before the commencement of the first excavations (29), was caused by the regression of
85 the hillside that led to the opening and collapse of its western wall, with subsequent
86 sealing processes from hillside deposits.

87 A level associated with funerary use of the cave has been attributed to the Bronze Age. It
88 is located in an area of gours (rimstone), soils, and walls of the cavity, forming an
89 organized and hierarchical funerary space, with two separate burial areas (Burials 1 and
90 2). The fact that certain speleothems show signs of having continued in their
91 development, as well as the stratigraphic position of the collapse of the walls of the cavity,
92 indicate a closed cave environment, which would have only had a small entrance at the
93 time of the burials. Both burials show anthropic adaptations of the karstic formations to

94 shape the tombs, and areas of re-interment of the bone remains. The latter are the product
95 of the removal of soil and the reuse of the burial sites. Two dates have been obtained for
96 these burials: 1664–1459 cal BCE (3290±40 BP, Beta-181890) (carbon) and 1900–1691
97 cal BCE (3480±40 BP, Beta-181891) (bone) (30, 31). We analyzed 3 individuals from
98 this site:

99 • I10939/119: 1900–1400 BCE

100 • I10940/121: 1900–1400 BCE

101 • I10941/120: 1900–1400 BCE

102 **Europa 1 (Gibraltar)**

103 *Contact: Clive Finlayson, Francisco Giles, Geraldine Finlayson, Stewart Finlayson*

104 The cave known as Europa 1 is located at the southernmost tip of Gibraltar, in the area
105 known as Deadman’s Beach. The cave formed along a fault gap in the limestone of the
106 Rock, and its entrance is currently at approximately 5 m a.s.l., on the cliff below the
107 marine platform known as Europa Point (15 -17 m a.s.l.), where there is a series of cavities
108 located between 11 and 8.5 m a.s.l. which are all that remain after the erosion of a larger
109 cave, and most are filled with marine conglomerate with remains of fauna and algal
110 formations. Below these caves, filling a vertical karst channel, a marine conglomerate
111 with fauna is located at 5.25 m a.s.l., and has been dated at 92.5 ± 1.5 Ka. It is covered
112 by a parietal, vadose zone and polycyclic stalagmite crust, which has been dated at 76 Ka
113 at its base, and 41 Ka at its top. Above the marine deposit, and interspersed between the
114 different stages of stalagmitic formation, there are karstic gaps with a reddish clay matrix,
115 in which an erosive phase that affects both these materials and the marine ones can be
116 observed. On top of this, new stalagmite growth is interspersed with karstic materials
117 with a reddish clay matrix. Below the cave, there is a platform created by marine erosion
118 at + 3 m a.s.l. and an undercut at + 1 m a.s.l. These stalagmitic crusts correspond to vadose
119 speleothems which must have been formed inside a cave, showing that the deposits were
120 formed inside a small cavity, elements of which are conserved in their innermost part
121 (32).

122 Although no remains of these deposits are found in Europa 1, and given that they may
123 remain below the archaeological levels, at +5 m a.s.l., evidence of borings by *Lithophaga*
124 inside the cave, indicates that the sea level reached that height, and clearly related to the
125 external marine deposit. The archaeological sediments are not sealed by any stalagmite

126 crust, with which it can be inferred that there were some major erosive conditions that
127 formed this marine cave by breaking into an existing prehistoric karst system, which has
128 subsequently been filled by archaeological deposits after 40 Ka.

129 The mouth of the cave had been blocked by 19th century masonry work until its discovery
130 in 1996. After entering through a 1.40 m passageway, a small antechamber is accessed
131 that extends across the general direction of the cave, and which via a narrow passage,
132 opens into a small chamber which is filled almost entirely by marine deposits and a
133 sedimentary accumulation containing archaeological and faunal remains that, due to its
134 inclination, seems to originate from outside. The size of the cave precludes its use as a
135 place of habitation.

136 Level 5 of the cave contained Black earth with limestone clasts, fauna (rabbit, deer,
137 carnivores, birds, etc.), handmade ceramics (Neolithic), human bones (metatarsals, skull,
138 phalanges) and lithic pieces of flint and jasper (33).

139 We analyzed one individual from this site:

- 140 • I10942/122: 5500–4500 BCE

141 **Cabezo Redondo (Villena, Alacant/Alicante, Valencian Community, Spain)**

142 *Contact: Gabriel García Atienzar, Mauro Hernández, Virginia Barciela González,*
143 *Domingo C. Salazar-García*

144 Cabezo Redondo is located about 2 km away from the town center of Villena on a circular
145 hill whose summit is about 40 m above the surrounding land and 579 m a.s.l.. It is located
146 in the center of the so-called "Villena basin", in which several natural corridors converge
147 and connect the Mediterranean coast with the interior of the Iberian Peninsula and the
148 highlands of Andalusia and Murcia with the interior of the Valencian region.

149 In 1949 J. M^a Soler began excavations at Cabezo Redondo. These were interrupted by the
150 exploitation of the hill for gypsum quarries. In 1987, the excavations at Cabezo Redondo
151 were resumed, with field work on the western side (34).

152 This site has yielded 50 radiocarbon dates from domestic and funeral contexts. These
153 dates and stratigraphic relationships define two moments of occupation. The first one is
154 located at the top of the hill, where the first occupations date back to around 2100 BCE.
155 This phase must have lasted until 1700 BCE, when this sector of the settlement was
156 reorganized.

157 In a second phase, the region of habitation expanded to include the western slope. During
158 this period (1700–1300 BCE; Late Bronze Age) an important architecture was developed
159 on this slope; domestic structures built with mud. It also stands out for its urban
160 complexity, which makes Cabezo Redondo one of the most important settlements in the
161 east of the Iberian Peninsula. At this time, the funerary material was located under the
162 floor of some houses, but also inside many of the cracks and small cavities of the hill.
163 These burials follow different rituals and present different grave goods, always rare.

164 Among the archaeological materials associated with funerary and domestic contexts,
165 there are gold objects, glass ornaments, ivory and bronze objects, and decorated ceramic
166 vessels. These pieces connect the inhabitants of the village with the inhabitants of the
167 Iberian Plateau, the Mediterranean and the European commercial circuits. The
168 abandonment of the village must have taken place during the 13th century BCE, before
169 the beginning of the Final Bronze Age.

170 A preliminary review of the human remains of the Cabezo Redondo shows the different
171 conservation of the remains according to the burial space. The burials deposited in *pithos*,
172 cists, and individual graves show a good state of conservation, while those found in caves
173 are more disturbed. Demographically, at least 61 individuals are identified, with children
174 being the best represented age range at the site. The number of juveniles is low, as is the
175 number of adults, with a predominance of those who died between 30 and 39 years old.
176 The abundance of children is interpreted as evidence of a high birth rate and a higher
177 number of deaths in the early stages of life.

178 The identification of evidence of disease or injury to teeth and bones is skewed by partial
179 bone preservation. Among the children remains there are some teeth with enamel
180 hypoplasia. There are also some cases of orbital sieve related to anemia of different origin.
181 In the adult population, there are signs that indicate intense physical activity in the arms
182 and legs, typical of a population dedicated to cultivating the land and caring for animals.
183 The microscopic dental analysis of Cabezo Redondo shows that the density of micro-
184 striae is low. There are no differences between children or adults, indicating a similar
185 consumption of food types. These data correspond to a type of diet with an important
186 meat component and with refined cereal processing to obtain flour. Evidence of the use
187 of teething for non-food activities is noteworthy. The presence of grooves in the anterior
188 teeth of some individuals shows one of the few documented cases during recent prehistory
189 related to textile activities (35).

190 The evidence related to social prestige in Cabezo Redondo is abundant and appears to be
191 associated with habitation areas and funerary deposits. Interestingly, the presence of
192 ornamental objects in only a few burials of adult individuals and, in particular, of a few
193 children, reveals social differences between the inhabitants of the village and the
194 hereditary nature of some privileges. Some ornaments are exceptional beyond their raw
195 material. The gold and silver truncated cones, as well as the ivory combs and glass beads,
196 reveals connections with the El Argar culture. We analyzed three individuals from this
197 site:

198 • I3486/S-EVA 26078: 1700–1500 BCE [based on other dates in the second phase of
199 occupation]

200 • I3488/S-EVA 22926: 1700–1500 BCE [based on other dates in the second phase of
201 occupation]

202 • I3487/S-EVA 26688: 1734–1617 cal BCE (3365±20 BP, PSUAMS-2161)

203 **Les Llometes (Alcoi, Alacant/Alicante, Valencian Community, Spain)**

204 *Contact: Domingo C. Salazar-García, Oreto García-Puchol*

205 Les Llometes includes two cavities, a cave and a crevice, situated within 15m of each
206 other, and is located within the municipality of Alcoi, at the exit of the Barranc del Cinc
207 ravine environment, towards the southeast of the Mariola Mountains in the province of
208 Alacant/Alicante. A radiocarbon dataset has been recently produced on most of the skulls
209 available to date, confirming a tight chronology of use of this site as a burial ground
210 during the Late Neolithic and comprising the earliest evidence of cave collective burials
211 in Eastern Iberia (36).

212 Les Llometes Cave has a stratigraphical sequence spanning at least two levels, reaching
213 1.8 m in depth from the surface. The first level included six skeletons (placed in prone
214 position) and grave goods consisting mainly of pottery and metal weapons. The second
215 level revealed 18 skeletons, positioned laterally and containing various remains including
216 pottery, polished stone tools, large flint blades and flint arrowheads, as well as ornaments,
217 although no metal artifacts were recorded (37). Most of the skeletal remains and grave
218 goods recovered from Les Llometes Cave were dispersed among various private
219 collections and later lost. However, five skulls were stored in the Archaeological Museum
220 of Alcoi and the National Archaeological Museum of Madrid.

221 Les Llometes Crevice was narrow and difficult to access. The orientation of the human
222 remains found in Les Llometes Crevice was not recorded, and the archaeologist described
223 them as being completely commingled and desarticulated (37).

224 We analyzed three individuals from the cave:

- 225 • I7647/LL9: 4050–3340 cal BCE (5180±24 BP, MAMS-16335)
- 226 • I7601/LL10: 3660–3520 cal BCE(4810±22 BP, MAMS-16354)
- 227 • I7642/LL27: 2907–2761 cal BCE (4240±23 BP, MAMS-16338)

228 We analyzed nine individuals from the crevice:

- 229 • I7645/LL5: 3990–3550 cal BCE (5120±25 BP, MAMS-16340)
- 230 • I7646/LL7: 3710–3630 cal BCE (4880±28 BP, MAMS-16339)
- 231 • I7643/LL3: 3960–3710 cal BCE (5040±33 BP, MAMS-16344)
- 232 • I7600/LL12: 4100–2700 BCE [based on other dates in the same context]
- 233 • I7644/LL4: 3640–3380 cal BCE (4760±22 BP, MAMS-16353)
- 234 • I7594/LL2: 3519–3370 cal BCE (4670±22 BP, MAMS-16356)
- 235 • I7595/LL11: 3519–3370 cal BCE (4670±23 BP, MAMS-16332)
- 236 • I7597/LL24: 4100–2700 BCE [based on other dates in the same context]
- 237 • I7598/LL25: 3630–3370 cal BCE (4710±22 BP, MAMS-16346)

238 **Alto de la Huesera (Laguardia, Araba/Álava, Basque Country, Spain)**

239 *Contact: Javier Fernández-Eraso, José Antonio Mujika-Alustiza*

240 This site was described in Lipson et al. 2017 (13). We analyzed three new individuals:

- 241 • I1845/LHUE-Pet1, LHUE-2010, CUADRO KII, Sector 7, L-IV.: 3014–2877 BCE
242 [3011–2877 cal BCE (4290±30 BP, Beta-301226), 3014–2891 cal BCE (4320±30 BP,
243 Beta-301223), 3010–2970 cal BCE (4350±30 BP, Beta-301222)]
- 244 • I1846/LHUE-Pet3: LHUE-2010, CUADRO K12, Lecho 5: 3014–2877 BCE [3011–
245 2877 cal BCE (4290±30 BP, Beta-301226), 3014–2891 cal BCE (4320±30 BP, Beta-
246 301223), 3010–2970 cal BCE (4350±30 BP, Beta-301222)]

247 • I1978/LHUE-Pet2: LHUE-2010, CUADRO K10, Sector 5: 3014–2877 BCE [3011–
248 2877 cal BCE (4290±30 BP, Beta-301226), 3014–2891 cal BCE (4320±30 BP, Beta-
249 301223), 3010–2970 cal BCE (4350±30 BP, Beta-301222)]

250 **El Sotillo (Laguardia, Araba/Álava, Basque Country, Spain)**

251 *Contact: Javier Fernández-Eraso, José Antonio Mujika-Alustiza*

252 This site was described in Lipson et al. 2017 (13). It is a megalithic tomb used during the
253 Late Chalcolithic, and after a hiatus of about 500 years it was reused during the Middle-
254 Late Bronze Age. We analyzed six new individuals from the Bronze Age phase of the
255 site:

256 • I2469/ES.2/4-3: 910–840 cal BCE (2740±30 BP, Beta-299308)

257 • I2471/ES.3/4-2: 1630–1497 cal BCE (3280±30 BP, Beta-299311)

258 • I1977/ES.2/4-4: 1660–1454 cal BCE (3260±30 BP, Beta-299312)

259 • I2472/ES.3/4-4: 1605–1425 cal BCE (3220±30 BP, Beta-299309)

260 • I2470/ES.3/4-1: 1411–1231 cal BCE (3060±30 BP, Beta-299307)

261 • I1840/ES.2/4-1: 1660–1454 cal BCE (3260±30 BP, Beta-299302)

262 **La Hoya (Laguardia, Araba/Álava, Basque Country, Spain)**

263 *Contact: Armando Llanos*

264 This site was described in Nuñez et al. 2016 (38). We analyzed three adult individuals
265 from the Celtiberian period of the site.

266 • I3757/LHY 142-T: 400–300 BCE

267 • I3759/LHY073: 361–195 cal BCE (2195±25 BP, PSUAMS-2078)

268 • I3758/LHY136: 365–204 cal BCE (2215±20 BP, PSUAMS-3466)

269 **Las Yurdinas II (Peñacerrada-Urizaharra, Araba/Álava, Basque Country, Spain)**

270 *Contact: Javier Fernández-Eraso, José Antonio Mujika-Alustiza*

271 This site was described in Lipson et al. 2017 (13). We analyzed one new individual:

272 • I1842/LY.II.A.10.15064: 3350–2750 BCE [3022–2779 cal BCE (4290±40 BP, Beta-
273 137895), 3090–2900 cal BCE (4360±40 BP, Beta-137896), 3310–2904 cal BCE
274 (4390±40 BP, Beta-148054) three dates of the whole stratigraphy of the site]

275 **Cueva de la Paloma (Soto de las Regueras, Asturias, Spain)**

276 *Contact: Almudena Estalrrich, Antonio Rosas*

277 The cave site is situated approximately 16 km from the coastline and 12 km from Oviedo,
278 the capital of the Asturias region. During the earliest Holocene, the northern Spanish
279 coastline was situated around 6 km offshore (39).

280 The cave was discovered in 1912, and excavated between 1914 and 1915 by Eduardo
281 Hernández Pacheco (40). The stratigraphic units of the cave contain archaeological
282 materials, and the study of the lithic and bone artifacts classified the samples of La Paloma
283 as belonging to the Magdalenian and Azilian cultures (40–42).

284 More than 5800 mammal bone remains have been recovered, with *Cervus elaphus* as the
285 most dominant taxa (43, 44). Other species present included *Rupicapra rupicapra*,
286 *Capreolus capreolus*, *Equus ferrus*, *Sus scrofa*, *Canis lupus*, *Panthera cf. leo*, *Vulpes*
287 *vulpes*, and *Ursus arctos* (44, 45).

288 Bone samples from 4 adult right tibias are analyzed in this study, out of the 91
289 anatomically modern human remains originally recovered at the site. The new dating of
290 the analyzed human remains, however, does not correspond to an Azilian archeological
291 and chronological context as originally published (40–42, 46), but instead to a Late
292 Neolithic-Chalcolithic chronology. In fact, it was already noted that the superficial levels
293 of the site were removed by looters (40), mixing the sediments and altering the
294 stratigraphic units.

295 The analyzed individuals are:

- 296 • I3214/TDPAD-01: 3400–3100 BCE
- 297 • I3243/TDPAD-03: 2500–2200 BCE
- 298 • I3239/TDPAD-02: 2500–2200 BCE
- 299 • I3238/TDPAD-04: 2500–2200 BCE

300 **Cova de la Guineu (Font-rubí, Barcelona, Catalonia, Spain)**

301 *Contact: Marina Lozano, Artur Cebrià, Juan Ignacio Morales, Xavier Oms, Josep Maria*
302 *Fullola*

303 The Cova de la Guineu site is in Font-Rubí (Barcelona, NE Iberian Peninsula), c. 730m
304 amsl, excavated since the 1980's by the SERP group of the University of Barcelona (47,
305 48). In this site, a long sequence covering the Late Upper Pleistocene and the Holocene
306 has been uncovered, providing data on occupations from the Upper Paleolithic to the Late
307 Bronze Age populations. In the Late Neolithic-Chalcolithic, the cave was used as an
308 individual and successive burial place (47, 48). According to the dental data, a minimum
309 number of 70 individuals of different age, including perinatal, subadults and adult
310 individuals, were identified from a commingled funerary context. Some scarce grave-
311 goods has been recovered (Bell-Beaker and plain vessels, lithics and shell-beads). Three
312 dates on human bones are available for the Late Neolithic-Chalcolithic occupation: 2871–
313 2505 cal BCE (4110±38 BP, OxA-16881); 3091–2916 cal BCE (4385±32 BP, OxA-
314 16966); 3353–3099 cal BCE (4513±30 BP, OxA-29636).

315 We analyzed 13 individuals from this site:

- 316 • I10277/GN.08.Data:27/4; Nivell:Rx.Q:F3.n3: 3400–2500 BCE
- 317 • I10278/GN.88.E3.32: 3400–2500 BCE
- 318 • I10280/GN.89.E2.379a: 3400–2500 BCE
- 319 • I10282/GN.90.Remenat.General.n.5: 3400–2500 BCE
- 320 • I10283/Guineu.08.RemenatF3-4: 3400–2500 BCE
- 321 • I10284/Guineu.82.5.: 3400–2500 BCE
- 322 • I10285/Guineu.88.Rem.Cala123a: 3400–2500 BCE
- 323 • I10286/Guineu.89.Rem.Ext.3611a: 3400–2500 BCE
- 324 • I10287/Guineu.90.Rem.Ext.4001/Guineu.M.56.: 3400–2500 BCE
- 325 • I11303/Guineu.90.Rem.Ext.4002: 3400–2500 BCE
- 326 • I11304/Guineu.94.C5.125: 3400–2500 BCE
- 327 • I11305/Guineu.95.B7.424.: 3400–2500 BCE

328 • I11306/Guineu.95.Rem.Ext.4000: 3400–2500 BCE

329 **Turó de Ca n'Oliver (Cerdanyola, Barcelona, Catalonia, Spain)**

330 *Contact: Joan Francès Farré*

331 The Iberian settlement of Turó de Ca n'Oliver is located on the mountain ranges of the
332 Collserola's slope in Cerdanyola del Vallès. Excavations in 2017 revealed the urban
333 evolution and the chronology of the settlement on the hill, believed to have occupied 2
334 hectares. Settlement evolution can be summarized as spanning 4 phases:

335 The first occupation of the hill (phase 0) is represented by a previous initial phase to the
336 urban one formed by an aggrupation of huts situated on the natural rock, for which only
337 some rock cut-outs and stick holes are preserved. Generally, the patterns of the post-holes
338 suggest rectangular or subrectangular constructions without specific typology. Because
339 of the lack of associated materials clearly differentiated from Phase 1, it is very difficult
340 to date them. Despite this, Phase 0 can roughly be dated to the last quarter of 6th century
341 BCE.

342 The first main urban phase of the settlement (Phase 1) is dated to between the last quarter
343 of 6th century BCE and middle 5th century BCE, in an unequivocally Iberian cultural
344 context. This phase is characterized by ceramics painted with bands and circle motifs,
345 and reduced firing ceramics characterized by indigenous forms and other Mediterranean
346 influence, along with handmade artifacts of an early Iberian culture attribution. The layout
347 was characterized by techniques of the early Iberian period, with houses built into deep
348 rock cut-outs, rectangular houses, modest dimensions and a great simplicity
349 compartmentalized with walls made of stone sockets and adobe.

350 In the middle of the 5th century BCE the settlement was widely reformed and experienced
351 a radical change in the conception of the habitation space (Phase 2). In this period the
352 ancient cutout in the natural rock occupied by the chambers of the previous phase was
353 filled. The filling of the cut allowed for larger houses that rested on a prominent wall that
354 enclosed the village. The first human skull remains were found under this wall connected
355 with horse remains in what seems like a ritual offering.

356 During Phase 3, dated to between the end of 4th century BCE or early 3rd century BCE
357 and the end of the 3rd century BCE, new reformations of the town took place. Those
358 changes must be related to the consolidation of the settlement as the main center of an
359 extensive territory and with an important storage capacity as evidenced by new field of

360 silos. Ca n'Oliver was refortified with the construction of new accesses and possibly with
361 a set of outer defences as reflected in excavated sections of the settlement moat. A
362 fundamental element of this town is the silos field. It extends from the west side of the
363 south gate to south, although only a small portion has been excavated. These are deposits
364 of considerable volume and about three meters deep, which in some cases can reach 5.25
365 meters (ST-738). As regards the chronology, the oldest deposit must be dated to the end
366 of the 4th century or the beginning of the 3rd century BCE and the date of abandonment
367 of the silos field to 50 BCE. The structures appear on each side of the pit although they
368 are more abundant outside its limits. Several of these moats contained human remains
369 (skulls, mandibles) that must be linked to the so-called "cult of the skull" documented at
370 this time in the Celtic world as well as in the Iberian.

371 We analyzed one individual from Phase 3 of the site:

- 372 • I3496/MC-1573: 300–200 BCE

373 A last phase, already reflecting Roman influence (Phase 4), dated from the first decades
374 of the 2nd century BCE, and was characterized by a new urban reorganization affected
375 by the events of the Second Punic War. This includes the construction of a new wall that
376 did not exactly follow the layout of the previous one, and the expansion and continuity of
377 the silos field as well as the construction of new houses, now extending beyond the
378 perimeter of the settlement. The settlement was abandoned definitively around 50 BCE.

379 **Mas d'en Boixos-1 (Pacs del Penedès, Barcelona, Catalonia, Spain)**

380 *Contact: Tona Majó, F. Javier López-Cachero*

381 Mas d'en Boixos is a site located in the Catalan Prelitoral depression in the Penedès region
382 (Barcelona). Several excavation seasons have been undertaken since 1997 with more than
383 450 structures uncovered, most of them storage silos. There are stratigraphic layers
384 ranging from the Early Neolithic until modern times with an especially intense occupation
385 period during the Early Iron Age. The human remains retrieved from that period are
386 scarce -two sub-adults, two adults and one infantile- although they are quite exceptional
387 due to the fact they are inhumation burials. In addition, there are cremation remains
388 belonging to one additional adult individual in a nearby silo structure. We analyzed three
389 individuals from this site, two from structure E-448 and one from structure E-449:

- 390 • I12410/MB1 '08 E-448 Ind 1: 515–375 cal BCE (2350±30 BP, Beta-495153)

- 391 • I12877/MB1 '08 E-448 Ind 2: 515–375 BCE

392 • I12878/MB1 '08 E-449 Ind 1: 507–366 cal BCE (2340±30 BP, Beta-495155)

393 **Hort d'en Grimau (Castellví de la Marca, Barcelona, Catalonia, Spain)**

394 *Contact: Tona Majó, F. Javier López-Cachero*

395 Hort d'en Grimau site is located in the Alt Penedés region (Barcelona). During the 1980s,
396 different archaeological structures were excavated, most of them dated from the Middle
397 Neolithic. Only two features date from the Early Iron Age: a hut floor and a storage silo
398 containing the partially cremated remains of an adult woman and a complete male horse
399 skeleton, still in anatomical connection. The finding of the horse is exceptional in the
400 Iberian context during this period. We analyzed a tooth from the adult woman:

401 • I12879/HG-E10: 728–397 cal BCE (2390±30 BP, Beta-495156)

402 **Can Roqueta-Can Revella and Can Roqueta II (Sabadell, Barcelona, Catalonia,**
403 **Spain)**

404 *Contact: Tona Majó, F. Javier López-Cachero*

405 Can Roqueta is an excavation area within a large archaeological complex that covers 2.5
406 km² outside the town of Sabadell, 30 km away from Barcelona. This settlement area
407 occupied from the Neolithic to the Middle Ages presents structures of different functions
408 and typologies.

409 In the sector Can Roqueta II, The Early Bronze Age structures are dated between 2300–
410 1300 cal BCE, with several radiocarbon dates pointing to the primary occupational
411 period, between 2153–1734 cal BCE and 1638–1435 cal BCE (49, 50). Archaeological
412 work between 1999 and 2000 documented 121 graves in a landscape of 11 hectares. The
413 site was occupied by farming groups that used a sophisticated bronze technology; there
414 is evidence of crucibles, metal casts and cooper smelting. The pottery is diverse, with
415 Epi-Bell Beaker traits. There are numerous funerary structures that were sometimes re-
416 used with several, successive burials, sometimes accompanied by dog skeletons. There
417 are also functionally complex, semi-excavated structures where human bones have been
418 found in fillings as well as in places deliberately designed as graves (51, 52).

419 We analyzed four individuals from the Bronze Age period of the Can Roqueta II sector:

420 • I1311/E-498; N°617: 2000–1400 BCE [1930–1634 cal BCE (3465±60 BP, UBAR-
421 697), 1867–1526 cal BCE (3370±50 BP, UBAR-670), 1736–1453 cal BCE (3305±55 BP,

422 UBAR-671), 1877–1526 cal BCE (3380±60 BP, UBAR-672), four dates of the whole
423 stratigraphy of the site]

424 • I1312_d/E-459_No6: 2000–1400 BCE [1930–1634 cal BCE (3465±60 BP, UBAR-
425 697), 1867–1526 cal BCE (3370±50 BP, UBAR-670), 1736–1453 cal BCE (3305±55 BP,
426 UBAR-671), 1877–1526 cal BCE (3380±60 BP, UBAR-672), four dates of the whole
427 stratigraphy of the site]

428 • I1313_d/E-459_No147: 2000–1400 BCE [1930–1634 cal BCE (3465±60 BP, UBAR-
429 697), 1867–1526 cal BCE (3370±50 BP, UBAR-670), 1736–1453 cal BCE (3305±55 BP,
430 UBAR-671), 1877–1526 cal BCE (3380±60 BP, UBAR-672), four dates of the whole
431 stratigraphy of the site]

432 • I1310/E-459_No148: 2000–1400 BCE [1930–1634 cal BCE (3465±60 BP, UBAR-
433 697), 1867–1526 cal BCE (3370±50 BP, UBAR-670), 1736–1453 cal BCE (3305±55 BP,
434 UBAR-671), 1877–1526 cal BCE (3380±60 BP, UBAR-672), four dates of the whole
435 stratigraphy of the site]

436 In the sectors of Can Roqueta II and Can Revella we also sampled four Iron Age
437 inhumations, contemporaneous to the nearby necropolis of Can Piteu-Can Roqueta with
438 more than a thousand cremation burials (49). In this context, the Iron Age inhumations
439 from Can Roqueta II and Can Revella represent exceptions to the dominant funerary rite.

440 Can Revella:

441 • I12640/CRCRV285-ADNUB50: 696–540 BCE (dating on Equus bones buried
442 alongside the human skeleton)

443 • I12641/CRCRV110-ADNUB52: 791–540 cal BCE (2510±30 BP, Beta 449093)

444 Can Roqueta II:

445 • I12642/CRII-193-ADNUB54: 731–399 cal BCE (2400±30 BP, Beta 463858)

446 • I12643/CRII-107-ADNUB55: 758–429 cal BCE (2460±30 BP, Beta 449091)

447 **Cova del Gegant (Sitges, Barcelona, Catalonia, Spain)**

448 *Contact: Joan Daura, Montserrat Sanz Borràs*

449 Cova del Gegant is a cave located in the northeast of the Iberian Peninsula, ~40 km south
450 of Barcelona. It consists of a principal chamber (GP), now eroded by wave action, and its
451 inner part (GP1 and GP2), where a small conduit (GLT) leads to the adjacent Cova Llarga.

452 Two galleries branch off of the right side of GP, one more interiorly (GL2) and another
453 near to the sea (GL1). At least eight site formation episodes from the Upper Pleistocene
454 (Episodes 0-3) to the Holocene (Episodes 4-7) have been recognized in the Cova del
455 Gegant stratigraphic sequence, alternating between continental sediment deposition and
456 periods of marine erosion followed by the accumulation of beach deposits (53). The first
457 Holocene deposition in GP2 corresponds to layer XXV (Episode 4). This archaeological
458 layer is ascribed to the Bronze Age and mainly corresponds to a collective burial
459 radiocarbon dated to the Middle Bronze Age, 1600-1400 cal BCE. The funerary context
460 that also yielded numerous fragments of Late Bell Beaker pottery, gold and amber
461 ornaments and human remains (MNI=19). This layer has been dated on the basis of three
462 human teeth yielding an age of 1622–1460 (3270±30 BP, Beta-312860), 1521–1417
463 (3200±30 BP; Beta-312861) and 1604–1430 (3225±27 BP; OxA-29612) (54). One
464 human remain, corresponding to an isolated lower left permanent incisor (I₁) from a
465 Bronze Age individual was successfully analyzed for ancient DNA and radiocarbon
466 dated:

- 467 • I1836/CG13-5135: 1682–1505 cal BCE (3310±35 BP, Poz-83482)

468 **Font de la Canya (Avinyonet del Penedés, Barcelona, Catalonia, Spain)**

469 *Contact: Marta Merino Pérez, Daniel López-Reyes*

470 The prehistoric site of Font de la Canya is an emblematic site for archaeological research
471 in Catalonia. With a sequence of more than 15 years of consecutive archaeological
472 campaigns (1999–2017), the volume of data is exceptional both in quality and quantity
473 and represents an important contribution to the knowledge of the early Iron Age and of
474 the Iberian culture

475 Font de la Canya was a trading center belonging to the Iron Age Iberian culture and
476 located in the middle of the Penedés region. It was inhabited between the 7th-1st centuries
477 BCE. The storage and distribution of cereals, extremely important for the agriculture and
478 diet of the time, was the main economic activity at the site. This is demonstrated by the
479 finding of hundreds of “silos” or cereal deposits, as well as several working spaces
480 dedicated to the managing of cereals and other goods.

481 The rich archaeological materials recovered inform us about the economy of the Iberian
482 culture and trading with other Mediterranean civilizations such as the Phoenicians,
483 Greeks, Carthaginians and Romans. The exchanges highlight the cosmopolitan and
484 commercial orientation of the people who lived at the site. For instance, archaeological

485 excavations have identified evidence of the earliest wine production in the territory during
486 the 7th century BCE, associated with contacts with the Phoenicians.

487 We analyzed one individual from this site:

- 488 • I4556/TFC-16.SI.204.Ind 2 (tooth 31 + 32): 700–500 BCE

489 **L'Esquerda (Roda de Ter, Barcelona, Catalonia, Spain)**

490 *Contact: Imma Ollich-Castanyer, Antònia Díaz-Carvajal*

491 L'Esquerda is an archaeological site located in a peninsula created by the river Ter in
492 Roda de Ter. This location creates strategic features that explain the continuity of
493 settlement from the end of the Bronze Age to the 14th century CE. From the oppidum of
494 the Ausetani tribe to the Roda Civitas of the Visigoths and Carolingians, its walls
495 demonstrate the importance of the site as a fortress that witnessed the establishment of
496 different peoples (55).

497 With the establishment of the Carolingians at the end of the 8th century CE over the ruins
498 of the old Iron Age Iberian fortress and making use of the Visigoth wall, an initial
499 settlement was formed. It was consolidated during the 9th and 10th centuries CE around
500 a church called Sant Pere de Roda. During the first half of the 11th century CE, a new
501 church was built in the same location, whose remains can still be seen. A necropolis was
502 created around the church with burials in three different levels. The lowest level was
503 characterized by anthropomorphic tombs excavated in the rock and dated to the end of
504 the 8th century CE and the beginning of the 10th century CE. We analyzed five
505 individuals from this level:

- 506 • I7674/T-143: 785–801 CE [between conquest of Girona and conquest of Barcelona]
- 507 • I7672/T-120-1: 785–801 CE [between conquest of Girona and conquest of Barcelona]
- 508 • I7676/T-191: 785–801 CE [between conquest of Girona and conquest of Barcelona]
- 509 • I7675/T-194: 785–801 CE [between conquest of Girona and conquest of Barcelona]
- 510 • I7673/T-120-2: 785–801 CE [between conquest of Girona and conquest of Barcelona]

511 The second level was characterized by slab tombs corresponding to the 11th–13th
512 centuries CE when the Romanic church was in use.

513 The third and more superficial level dated between the end of the 13th century CE to the
514 end of the 14th century CE, with burials in a simple or complex pit (56).

515 Beside the already mentioned necropolis, a different burial place was found outside the
516 wall, radiocarbon dated to the second half of the 7th century CE (57). A total of 13 simple
517 pit and slab tombs have been identified, with male adults and male and female infants.
518 We analyzed five individuals from this burial place:

519 • I3778/T-269: 600–700 CE

520 • I3776/T-267: 600–700 CE

521 • I3866/T-264: 600–700 CE

522 • I3775/T-266: 600–700 CE

523 • I3777/T-268: 600–700 CE

524 **El Hundido (Monasterio de Rodilla, Burgos, Castilla y León, Spain)**

525 *Contact: Javier Jiménez Echevarría, Carmen Alonso*

526 This site was described in Szécsényi-Nagy et al (58). We analyzed two individuals from
527 this site:

528 • EHU001/UE 750: 2287–2044 cal BCE (3760±30 BP, Beta-492280)

529 • EHU002/UE 450: 2562–2306 cal BCE (3933±32 BP, CSIC-1896)

530 **El Cerro (La Horra, Burgos, Castilla y León, Spain)**

531 *Contact: Domingo C. Salazar-García, Ángel Esparza Arroyo, Javier Velasco Vázquez,*
532 *Germán Delibes de Castro*

533 The site of El Cerro, like other “Campos de hoyos” of the archaeological culture Cogotas
534 I (Central Iberian Meseta Middle-Late Bronze Age, ca. 1850–1150 cal BCE), presents
535 some remains of some shacks as well as numerous dug structures filled with waste
536 material (potsherds, animal bones, ashes) that were originally grain storage pits. A triple
537 burial was excavated and contained three subadults, whose death must have resulted in
538 the ritualized abandonment of the site (59–61).

539 We analyzed one individual from this site:

540 • I3490/S-EVA 9674: 1850–1150 BCE

541 **Virgatal (Tablada de Rudrón, Burgos, Castilla y León, Spain)**

542 *Contact: Germán Delibes de Castro, Elisa Guerra*

543 This site was described in Olalde et al. 2018 (9). We analyzed one new individual dated
544 to the Bronze Age:

- 545 • I6470/RISE912: 1753–1549 cal BCE (3375±35 BP, Poz-49177)

546 **Valdescusa (Hervías, La Rioja, Spain)**

547 *Contact: Javier Jiménez Echevarría, Carmen Alonso*

548 This site was described in Szécsényi-Nagy et al (58). We analyzed five individuals from
549 this site:

- 550 • VAD001/E45: 1867–1616 cal BCE (3400±35 BP, Ua-36345)

- 551 • VAD002/E47: 1689–1528 cal BCE (3330±30 BP, Beta-479536)

- 552 • VAD003/E69: 1689–1528 cal BCE (3330±30 BP, Beta-479534)

- 553 • VAD004/E74: 1673–1255 BCE

- 554 • VAD005/E77: 1742–1546 cal BCE (3360±30 BP, Beta-479535)

555 **Campo de Hockey (San Fernando, Cádiz, Andalusia, Spain)**

556 *Contact: Eduardo Vijande Vila, José Ramos Muñoz, Pablo Ramos-García, Adolfo*
557 *Moreno-Márquez*

558 The Campo de Hockey site is located in the Bay of Cádiz, the southernmost region of the
559 Iberian Peninsula. Geo-archaeological studies have confirmed that, during the Neolithic,
560 this marshy area was mostly under the sea, with the most elevated areas both in the city
561 and its immediate hinterland forming small islets (62).

562 In 2007, the construction of a hockey stadium exposed the remains of this late Neolithic
563 settlement, dated to the turn of the 4th millennium BCE (63).

564 The excavation revealed the existence of three areas of activity. The highest, westernmost
565 sector was the domestic area. The middle sector contained five features cut into the
566 tertiary marl soil which, based on typology, have been interpreted as ‘pits’. The size of
567 these structures suggests their use for storage, for example as grain silos. Finally, the
568 necropolis was found in the lowest area. The funerary ritual attested in this necropolis has

569 characteristics that have not been described elsewhere in the region during this period.
570 Most graves contain only one individual, which allows us to infer social differences, also
571 reflected on the typology of the tomb and the grave offerings, as well as to collect data
572 concerning gender and age distribution (64) (often an impossible task with collective
573 tombs in which bones are mixed).

574 Different types of grave exist, from simple burial pits to burial mounds or more elaborate
575 graves (63, 64). A total of 60 graves have been excavated to date, including 49 (82%)
576 individual graves, eight double graves and 2 quadruple graves, amounting to a total of 73
577 individuals. The presence of rich grave offerings (beads made of amber, variscite and
578 turquoise, and imported polished axes) in the most elaborate graves is a clear indication
579 of social inequality.

580 We sampled six individuals from this site:

- 581 • I7160/CH-08-C15-UE1514-E16: 4039–3804 cal BCE (5140±35 BP, CNA4579.1.1)
- 582 • I7679/CH-08-C14A-UE1402-E21: 4300–3700 BCE [from layer dates on different
583 skeletons: 3948–3708 cal BCE (5020±50 BP, CNA360); 4221–3990 cal BCE (5650±40
584 BP, CNA664); 4244–3983 cal BCE [5665±50 BP, CNA833]]
- 585 • I7547/CH-08-C12-UE1210-E2: 4300–3700 BCE [from layer dates on different
586 skeletons: 3948–3708 cal BCE (5020±50 BP, CNA360); 4221–3990 cal BCE (5650±40
587 BP, CNA664); 4244–3983 cal BCE [5665±50 BP, CNA833]]
- 588 • I7549/CH-08-C12-UE1214-E6: 4300–3700 BCE [from layer dates on different
589 skeletons: 3948–3708 cal BCE (5020±50 BP, CNA360); 4221–3990 cal BCE (5650±40
590 BP, CNA664); 4244–3983 cal BCE [5665±50 BP, CNA833]]
- 591 • I7550/CH-08-C15-UE1502-E4: 4300–3700 BCE [from layer dates on different
592 skeletons: 3948–3708 cal BCE (5020±50 BP, CNA360); 4221–3990 cal BCE (5650±40
593 BP, CNA664); 4244–3983 cal BCE [5665±50 BP, CNA833]]
- 594 • I8134/CH-08-C17A-UE1709-E4: 4300–3700 BCE [from layer dates on different
595 skeletons: 3948–3708 cal BCE (5020±50 BP, CNA360); 4221–3990 cal BCE (5650±40
596 BP, CNA664); 4244–3983 cal BCE [5665±50 BP, CNA833]]

597 **Loma del Puerco (Chiclana de la Frontera, Cádiz, Andalusia, Spain)**

598 *Contact: Eduardo Vijande Vila, José Ramos Muñoz, Pablo Ramos-García, Adolfo*
599 *Moreno-Márquez*

600 The necropolis of Loma del Puerco is 8 km away from the town of Chiclana de la
601 Frontera, in the Bay of Cádiz. The funerary structures are 400 m from the coastline, in a
602 gentle southwest-facing slope.

603 The first excavation season took place in 1991, when four graves were excavated. These
604 are collective graves, circular or oval in shape, cut into the tertiary marl soil and lined by
605 large vertical slabs of sandstone, fit in with small and middle-sized stones (65). These
606 four graves contained a total of 14 individuals and very poor grave offerings.

607 A second excavation season was undertaken in 2016. Two more graves were identified.
608 The most interesting of these features (UE 1038) was a rectangular pit, 2 x 1.20 m in size,
609 cut into the tertiary marl soil and lined by large vertical slabs. Inside this grave, three
610 anatomically articulated adult individuals were found, along with the scattered remains
611 of a sub-adult individual. Individual number 1 (who was sampled for this study)
612 corresponds to a woman, and was the only one to carry any kind of grave goods (two
613 gypsum beads and a shell fragment):

614 • I7162/LM-16-Sep1: 1932-1697 cal BCE [1932–1756 cal BCE (3524±30 BP,
615 CNA4237.1.1), 1880-1697 cal BCE (3465±20 BP, PSUAMS-4262)]

616 **Els Estrets de la Rata (Vilafamés, Castelló/Castellón, Valencian Community, Spain)**

617 *Contact: Domingo C. Salazar-García*

618 This site is located in the pre-coastal mountain ranges in the province of
619 Castelló/Castellón, overlooking the plain of Vilafamés and the pass of “la rambla de la
620 viuda”.

621 The settlement is delimited by a wall with a circular tower at its most accessible corner.
622 It is dated to the “Iberian” period between 3rd-2nd centuries BCE by the different type of
623 ceramics: Roman, local Iberian and importation ceramics. The defensive structure
624 encloses a space with several rectangular compartments built with masonry that could
625 have served as storage spaces. Under the rooms, two newborn burials were found (66).
626 We analyzed both individuals:

627 • I3321/S-EVA 9303; Ind 2: 300–100 BCE

628 • I3320/S-EVA 9305; Ind 1: 300–100 BCE

629 **Puig de la Misericordia (Vinarós, Castelló/Castellón, Valencian Community, Spain)**

630 *Contact: Domingo C. Salazar-García, Arturo Oliver Foix*

631 This site is located at the top of a hill in the middle of the coastal plain of Vinaròs,
632 controlling the coast and the access to the plain delimited by the foothills of “Serra d'Irta”,
633 “Montsià”, “Maestrazgo” and “Tinença de Benifassar”.

634 The site contains four occupations from Late Bronze Age to the Late Iron Age. Between
635 700 and 400 BCE the settlement was used as a fortified residence, with evidence of
636 trading with Phoenicians and Greeks (67). Newborn burials were located under one of
637 the settlement rooms and dated to the early stage of the “Iberian culture” around the 6th
638 century BCE. The latest phase of the site corresponds to the second half of the 2nd century
639 BCE during the Roman Republic, during which a building related to the agricultural
640 colonization was built, beginning the Roman domination in the area. We sampled one
641 individual from this site:

642 • I3322/S-EVA 9307: 600–500 BCE

643 **Cingle del Mas Nou (Ares del Maestre, Castelló/Castellón, Valencian Community,**
644 **Spain)**

645 *Contact: Domingo C. Salazar-García*

646 Cingle del Mas Nou is an open-air site close to a rock shelter situated in the town of Ares
647 del Maestre. It is on the southern side of Serra d'En Seller, close to the valleys of Cirerals
648 and Molero, at 940 m above sea level. The site was discovered in 1975, and excavations
649 ran from 1986 to 1999. The stratigraphic sequence of the site is divided into five levels,
650 grouped in two occupation phases: Levels I and II are associated with the Early Neolithic,
651 Levels III and IV to the Geometric Mesolithic, and Level 5 is sterile. The analysis of the
652 excavated remains is ongoing (68). Nine human individuals dating to the Mesolithic have
653 been described: 2 adults and 7 children of different ages (69).

654 We analyzed one Mesolithic individual:

655 • I3209/Q4[-125/-144]: 5976-5783 cal BCE (6980±25 BP, PSUAMS-4414)

656 **Castillejo del Bonete (Terrinches, Ciudad Real, Castilla-La Mancha, Spain)**

657 *Contact: Domingo C. Salazar-García, Luis Benítez de Lugo Enrich, María Benito*
658 *Sánchez*

659 Castillejo del Bonete was a ceremonial site used for more than one thousand years during
660 the Copper and Bronze Ages. It is located in the interior of the Iberian Peninsula, on the
661 southern edge of the Castilian Meseta, on top of a hill with great visibility controlling a
662 natural pass along the southeast of Ciudad Real province. It holds a strategic position
663 between the river basins of the Guadiana and the Guadalquivir. Excavations at this site
664 began in 2003 and are still ongoing. Rites performed at this site were related to death and
665 resurrection of the sun, human death, and veneration of ancestors. Some examples are
666 feasting rites, offerings to the dead, and architecture oriented towards the winter solstice
667 (70, 71). A natural cave was monumentalized and used as funerary chamber, building a
668 large tumulus and creating cave art. This main tumulus is connected with others though
669 several corridors.

670 Several radiocarbon dates have been obtained on human and non-human material, all
671 yielding dates between 2465–1565 cal BCE (72, 73).

672 Burials have been found in the tumulus and its surroundings, both primary (in fetal
673 position and lateral decubitus position on the right side) and secondary deposits, which
674 indicates the reuse of the funerary space. A good example of this pattern is Tumba 1
675 which, although altered, still preserved the remains of a 30-35-year-old male individual
676 that was sampled for DNA analysis:

677 • I3756/TEBO'03, D8 UE12; Tumba 1: 2014–1781 cal BCE (3565±25 BP, PSUAMS-
678 2077)

679 Another good example is Tumba 4, the only multiple burial in this site with a 40-50-year-
680 old male and a 30-40-year-old female who was buried with two ivory buttons and who
681 had a marine diet, suggesting a non-local origin (74). We sampled both individuals from
682 Tumba 4:

683 • I3484/TEBO'04 Tumba 4 Ind 2: 2271–1984 cal BCE (3720±70 BP, Rome-1687)

684 • I3485/TEBO'04 Tumba 4 Ind 1: 2300–1900 BCE

685 Tumba 5, also located in the main tumulus, belonged to a 40-50-year-old male with
686 degenerative signs such as osteoarthritis and dorsal Kyphoscoliosis. This individual also

687 presented muscle stress signs on the upper limbs and shoulder girdle suggesting activities
688 related to archery:

- 689 • I12809/TE'15 BO 1257-56, Tumba 5: 1880–1770 BCE

690 The last individual analyzed here was a young male found inside the monumentalized
691 sepulchral cave with a large burial mound; specifically, in Gallery 3 (subsector 3.1.7).
692 This is an area that remained closed and sealed from Prehistory to the present-day. Human
693 bones from a minimum of two individuals were found, but most of the remains belonged
694 to one of them (Individual 1), who was analyzed here:

- 695 • I12855/TE'17 BO UF73: 1880–1770 BCE

696 This burial appeared without strict anatomical connection, except for some bones that
697 were found articulated (spine and some ribs). The bones that had lost the strict articulation
698 were in their anatomical place, which implies a primary burial in fetal position and a later
699 anthropic removal. In this tomb, a limestone funerary stele with 15 bivalve fossils
700 (*Pectinidae*) has been found. The rock was moved inside this cave from a distance of 40
701 km (75). The two individuals were likely deposited on the bottom of the cave in this
702 closed place, without being buried in a pit; as no excavation of any pit has been detected.
703 Gallery 3 is a rocky cavity where there is no soil with sufficient land to house a burial.

704 Castillejo del Bonete acts as a karstic system of funerary galleries (72) that were
705 artificially sealed, suggesting sociocultural stratification. Outside the main tumulus 6
706 individuals were found in 5 graves, whereas inside the funerary cave there was a
707 minimum of 11 individuals (6 adults and 5 subadults). Although anthropological analyses
708 are still ongoing, we can conclude that this is a small number of individuals given the
709 long period of use of this monument. This could be explained by cultural hierarchy or by
710 the social role played by the buried individuals.

711 **Sima del Ángel (Lucena, Córdoba, Andalusia, Spain)**

712 *Contact: Enrique Viguera, Cecilio Barroso, Francisco J. Bermúdez*

713 Ángel Cave (Lucena, Córdoba, Spain. 37° 22' 11" N; 4° 28' 44" W; 608 m.a.s.l.) is an
714 important Middle Pleistocene site located in the south of Iberian Peninsula. It is a karst
715 system made up of several units (76). The main site, excavated beginning in 1995, is
716 open-air, the remainder of a former cave that collapsed. The most striking feature of the
717 site is the presence of one of the largest hearths in Europe, which covers the entire
718 stratigraphic sequence, without a single hiatus, at a depth of 5 m. The assemblage is

719 composed of more than 5000 tools (mainly flake and retouched tools, in addition to nearly
720 50 handaxes), conforms to Final Acheulean, with the special presence of bone retouchers
721 (77). The vast majority of the *ca.* 9,000 fossil remains (mainly equids, large bovids and
722 cervids) are burnt and highly fragmented due to marrow extraction activities, and a good
723 number of them displayed cut marks (76, 77). Stratigraphic and archaeological data, along
724 with new radiometric dating, indicate an uninterrupted occupation of the site between 320
725 and 180 ka BP (78).

726 Close to the main site there is a small cave. In order to relate its archaeology to that of the
727 Paleolithic cave, it was cleared between 2013 and 2016 and an extraordinary number of
728 human remains and archaeological materials were discovered. That record was out of
729 stratigraphic context but it denotes the use of the cave as a burial place in recent
730 Prehistory. From this cave, two narrow holes lead to a larger cavity, the ‘Sima’, where
731 the sample for the present study was recovered. It is a 60 m deep vertical fracture that
732 hosts a pyramidal sedimentary package made up by materials brought from outside the
733 site. An area on the southeastern slope of this deposit, with an inclination of *ca.* 40°, has
734 been excavated since 2013. The profuse archaeological record recovered at ‘Sima del
735 Ángel’ reveals a continuous use of the karst system for burials for a long period of recent
736 prehistory between the VI and II millennia BCE. Even though it is difficult to arrange the
737 deposits in a precise chronostratigraphic sequence, it can be deduced from the
738 archaeological record and available dating that the ‘Sima’ was used as an immense natural
739 ossuary, into which human remains and grave goods placed in the upper cave were
740 gradually thrown down, with an especially intense use in Neolithic and Chalcolithic
741 times.

742 The Neolithic pottery record from ‘Sima del Ángel’ ranges from the VI to V millennia
743 BCE. It is mainly composed of fragments of bowls and globular vessels decorated with
744 incisions and/or impressions and red ochre *engobe*, while *Cardium* pottery has also been
745 collected. Chalcolithic ceramics are well exemplified by fragments of plates and dishes
746 with incised and impressed decoration. Thickened rim plates are characteristic of this
747 period and are datable to between 2800 and 2200 BCE. In addition, there are some Bell
748 Beaker pottery fragments. The stone tool assemblage is primarily composed of flint
749 blades, but there are also ground stone axe heads and gouges. Finally, many personal
750 ornaments, such as stone bracelets, plenty of beads (made of shell, stone and bone) and
751 shell pendants, have been recovered.

752 Up to now around 2,500 human remains (bones, bone fragments and isolated teeth) have
753 been exhumed. Due to environmental conditions and geologic dynamics within the site,
754 the state of preservation of anthropological remains is poor. Anatomical connections have
755 not been reported and, for the moment, a minimal number of more than 40 individuals
756 has been estimated (among which 1/3 are subadults). Traces of deliberate manipulation
757 have been detected in minority of the human remains, and they include cut marks,
758 scratches and heat induced changes, which may result from a secondary funerary rite.
759 However, the evidence of some bone fractures and marrow extraction on human bones
760 agrees with a cannibalistic practice.

761 The samples analyzed in this paper were recovered in the 2016 excavation.
762 Environmental conditions within the cave are favorable for ancient DNA preservation,
763 and human remains were collected and handled following an anti-contamination process
764 and then stored at 4°C. The current sample comes from the Chalcolithic horizon in ‘Sima
765 del Ángel’, radiocarbon dated with ages of 2862–2500 cal BCE (4096±31 BP, OxA-
766 32885) and 2831–2474 cal BCE (4040±28 BP, OxA-35790). It consists of teeth and
767 petrous portions of the temporal bone belonging to 16 individuals. There are at least 6
768 males and 5 females among them. Some of the remains are those of subadult individuals:
769 I8154 is the maxillary first deciduous molar of a ~7-year-old girl; I8158 is the shovel
770 shaped lateral deciduous incisor of a ~4-year-old boy; I8198 is the left temporal bone of
771 a ~5-year-old girl. Generally, the teeth from adult individuals are highly worn and some
772 of them have slight cervical carious lesions. Analyzed individuals are listed below:

- 773 • I7588/SIMA107: 2900–2500 BCE
- 774 • I7587/SIMA10,181: 2900–2500 BCE
- 775 • I8148/11801: 2900–2500 BCE
- 776 • I8149/11813: 2900–2500 BCE
- 777 • I8150/11849: 2900–2500 BCE
- 778 • I8153/11802: 2900–2500 BCE
- 779 • I8154/11831: 2900–2500 BCE
- 780 • I8155/11832: 2900–2500 BCE
- 781 • I8156/11807: 2900–2500 BCE

- 782 • I8157/11800: 2900–2500 BCE
- 783 • I8158/11803: 2900–2500 BCE
- 784 • I8197/11834: 2900–2500 BCE
- 785 • I8198/11838: 2900–2500 BCE
- 786 • I8199/11853: 2900–2500 BCE
- 787 • I8364/11836: 2706–2569 BCE
- 788 • I8365/11837: 2706–2569 BCE

789 **Empúries (Girona, Catalonia, Spain)**

790 *Contact: Marta Santos, Pere Castanyer, Joaquim Tremoleda*

791 The archaeological site of Empúries is composed by the remains of the ancient Greek
792 colony of Emporion—founded by the Phocaeans in the first half of the 6th century BCE
793 (19)—and by the remains of a Roman city created at the beginning of the 1st century BCE
794 on an area previously occupied by a fortified camp built after the earliest Roman presence
795 in the area. Both town were later integrated into the *municipium Emporiae*, which was
796 founded at the beginning of the Roman imperial period.

797 Several sites in the vicinity of Empúries attest the previous occupation of the area—
798 located in the southern of the Gulf of Rosas—from the Neolithic and specially during the
799 Final Bronze Age and the Early Iron Age. Other sites demonstrate the habitation of the
800 area during de Late Antiquity and Medieval Period, after the abandonment of the Roman
801 city in the 3rd century CE.

802 The Greek and Roman towns were surrounded by several funerary areas, some of which
803 suffered from intense pillage before the beginning of excavations under the initiative of
804 the “Junta de Museus de Barcelona” in 1908. In other cases it was possible to carry out
805 excavations documenting the numerous tombs—both inhumations and cremations—
806 published by Martín Almagro in two volumes in 1953 and 1955. However, besides the
807 study of the funerary materials associated with those tombs and general descriptions of
808 the characteristics of the burials, until very recently the anthropological information has
809 been extremely incomplete because in most of the cases the remains have not been
810 preserved.

811 Together with the new burials documented in the 80s in the parking area of the site, other
812 more recent interventions in specific areas located south of the Greek town have
813 recovered a group of funerary structures that increase our knowledge of the necropolises
814 on the eastern slope of Empúries hill, next to the tracks leading to the town. We have
815 analyzed a total of 24 individuals from these latest excavations.

816 A first group of burials correspond to an area of the necropolis excavated in 2010 due to
817 the construction of a new reception building of the MAC- Empúries. This area, south of
818 the Greek town, was identified as 10-SU-28-D1. The southern part of this area was
819 occupied by tombs associated to the Greek town, mainly inhumations on the rock or
820 taking advantage of the substrate depressions. Although some of these tombs lacked grave
821 goods, the recovered materials in other tombs date the use of this necropolis during the
822 5th and 4th centuries BCE. We have analyzed 10 individuals from this area:

- 823 • I8211/10-SU-28-D1-E-96: 500-450 BCE
- 824 • I8213/10-SU-28-D1-E-60: 500-400 BCE
- 825 • I8344/10-SU-28-D1-E-74: 500-400 BCE
- 826 • I8209/10-SU-28-D1-E-99: 450-400 BCE
- 827 • I8214/10-SU-28-D1-E-82: 400-350 BCE
- 828 • I8215/10-SU-28-D1-E-76: 400-350 BCE
- 829 • I8210/10-SU-28-D1-E-91: 500-350 BCE
- 830 • I8212/10-SU-28-D1-E-46: 500-350 BCE
- 831 • I8340/10-SU-28-D1-E-63: 500-350 BCE
- 832 • I8341/10-SU-28-D1-E-62: 500-350 BCE

833 Further south, and without disturbing the old cemetery, this area was used again as
834 necropolis during the Roman Period, specially during the 2nd century CE, with pit burials
835 and tombs with *tegulae* cover. We analyzed 7 individuals from this group of tombs:

- 836 • I8216/10-SU-28-D1-E-35: 57–208 cal CE (1895±20 BP, PSUAMS-4212)
- 837 • I8474/10-SU-28-D1-E-47: 100-200 CE
- 838 • I8475/10-SU-28-D1-E-16: 100-200 CE

- 839 • I8338/10-SU-28-D1-E-15: 100-200 CE
- 840 • I8339/10-SU-28-D1-E-8: 100-200 CE
- 841 • I10865/10-SU-28-D1-E-37: 100-200 CE
- 842 • I10866/10-SU-28-D1-E-20: 43 cal BCE–51 cal CE (2005±15 BP, PSUAMS-5281)

843 The second area, located quite far south from the limits of the Greek city, corresponds to
 844 the so-called Granada Necropolis, partially excavated and published by Martín Almagro.
 845 More recently, due to the urbanization of this area identified as SU-33-A4, preventive
 846 archaeological excavations have described the sequence of use of this cemetery. Although
 847 this space was used since the 5th century BCE, the burials analyzed here date to a period
 848 between the 3rd and 2nd centuries BCE, which is well documented in the new
 849 excavations. They correspond to inhumations excavated in the rock or in the sand layer
 850 above the rock, oriented west-east, often marked by a simple stone mound and containing
 851 only ointment cases deposited next to the bodies. We analyzed five individuals from this
 852 area:

- 853 • I8203/02-SU-33-A4-T1058: 300–100 BCE
- 854 • I8204/12-SU-33-A4-600: 300–100 BCE
- 855 • I8205/12-SU-33-A4-T180: 300–100 BCE
- 856 • I8206/12-SU-33-A4-T680: 300–100 BCE
- 857 • I8208/12-SU-33-A4-T510: 370-204 cal BCE (2220±20 BP, PSUAMS-4277)

858 A new phase of this necropolis, associated with the cremation rite and dated between the
 859 1st century BCE and the 1st century CE, has been documented. Finally, the most recent
 860 phase of the necropolis involved the return to the inhumation rite, although within the
 861 excavated part only one burial was found. The tomb was south-north oriented and dates
 862 to the 2nd century CE or later. The analyzed individual is:

- 863 • I8202/02-SU-33-A4-T1077: 100–300 CE

864 The last individual belonged to one of the Late Roman cemeteries located in the lower
 865 part of the western side of the Empúries hill, related to funerary or worship buildings.
 866 Specifically, the tomb was excavated in 2005 together with other tombs in the area called
 867 Santa Magdalena, which belongs to the necropolis created next to an old mausoleum
 868 transformed into a church. This necropolis was also used during the Medieval period. The

869 tomb corresponds to an individual inhumation inside a pit delimited by stones and without
870 a preserved cover, dated to the 6th century CE:

- 871 • I8343/05-SMG-8075: 500–600 CE

872 **Puig de Sant Andreu (Ullastret, Girona, Catalonia, Spain)**

873 *Contact: Gabriel de Prado, Bibiana Agustí, Ferran Codina*

874 The Iberian culture town of Ullastret (6th-2nd centuries BCE) is located in the Ampurdán
875 (Girona) plain and constitutes one of the most important archaeological sites of the Iron
876 Age in the northwest Mediterranean. This large urban area was formed by two inhabited
877 sites, Puig de Sant Andreu and la Illa d'en Reixac, separated by 300 meters and
878 representing a true *dipolis*. The combined sites occupied more than 15 hectares after the
879 4th century BCE and were the capital of the Iberian culture Indigetes (or Indiketes) tribe,
880 which is cited in classical sources including Avienus, Ptolemy and Strabo

881 The Iberian culture practiced the funerary ritual of body cremation, which resulted in a
882 very small number of human remains for study. In this sense, the site of Ullastret is unique
883 because excavations have identified remains from more than 40 individuals, mostly
884 mandibles, skulls and isolated teeth. In most of the cases, these remains present evidence
885 of violence and could correspond to the heads of enemies beheaded in combat that were
886 exhibited as war trophies in public spaces. This ritual is archaeologically documented in
887 the northeast corner of Iberia and in southern Gaul where archaeological evidence,
888 iconography and classic sources are available.

889 The remains analyzed in this study correspond to a group of 34 isolated fragments from
890 a minimum of 8 individuals. They were found on the floor of the main street (zone 13)
891 near a large aristocratic building (zone 14). They were directly covered by the ruins of
892 the building and the city which was abandoned around 200 BCE. Their location and
893 characteristics suggest that they represented enemies' heads exhibited at the building's
894 entrance together with their weapons. After being exposed for some time, maybe years,
895 they finally dropped to the street floor before the abandonment of the city, by which time
896 they likely had already lost their significance.

897 We analyzed five samples from this site that corresponded to four different individuals:

- 898 • I3326/4979: 250–200 BCE
- 899 • I3327/4980: 250–200 BCE

- 900 • I3324/4976: 360–193 cal BCE (2190±20 BP, PSUAMS-2159)
- 901 • I3323/4975+4977: 365–204 cal BCE (2215±20 BP, PSUAMS-2158)

902 **Sant Julià de Ramis (Girona, Catalonia, Spain)**

903 *Contact: Neus Coromina, Josep Burch, David Vivó*

904 The necropolis of Sant Julià de Ramis is located on the top of the mountain of the same
905 name (79). The first stable habitat established in this place was an Iberian Iron Age
906 settlement in the mid/second half of the 6th century BCE. When it was abandoned, a small
907 rural establishment was constructed at the bottom of the mountain that survived, with
908 successive alterations, until the mid-4th century CE. This period coincided with the
909 building of a large fort on the top of the mountain, whose strategic situation should be
910 considered in light of the fact that it was adjacent to the Via Augusta and close to the city
911 of *Gerunda*. Even when the Western Roman Empire fell, the fort was not deserted.
912 Instead, it underwent extensive remodeling. Subsequently, in association with the fort, a
913 group of houses were built on top of the mountain and over time were organized around
914 a chapel built in the same period.

915 The Muslim conquest of the area at the beginning of the 8th century led to the
916 abandonment of the fort which rapidly became a ruin, as described in documentary
917 sources from the 9th century CE. However, the archaeological excavations completed to
918 date have revealed that in the second half/end of the 8th century, a cemetery developed
919 around the chapel that would be in use until the start of the 21st century. The vitality of
920 the place, which became the center of a parish in the medieval period, is further reflected
921 in the construction of a new church at the end of the 10th century-start of the 11th century,
922 dedicated to Sant Julià.

923 We analyzed seven individuals from this site:

- 924 • I10851/SJR'15-1669: 887–1013 cal CE (1100±30 BP, Beta-458691)
- 925 • I10852/SJR'14-1670: 973–1150 cal CE (1010±30 BP, Beta-458692)
- 926 • I10853/SJR'15-1796: 989–1153 cal CE (990±30 BP, Beta-448950)
- 927 • I10854/SJR'15-1820: 973–1150 cal CE (1010±30 BP, Beta-448952)
- 928 • I10892/SJR'15-1846: 770–1200 CE (based on dates in the same context)
- 929 • I10895/SJR'15-1828: 777–981 cal CE (1140±30 BP, Beta-448953)

930 • I10897/SJR'17-2099: 1033–1204 cal CE (910±30 BP, Beta-477258)

931 **Pla de l'Horta (Sarrià de Ter, Girona, Catalonia, Spain)**

932 *Contact: Neus Coromina, Josep Burch, David Vivó*

933 The Pla de l'Horta villa is located in Sarrià de Ter, around four kilometers from the city
934 of Girona, and therefore it should be considered a *fundus* that belonged to the *suburbium*
935 of *Gerunda* (80). It was constructed in the middle of the 1st century BCE. The residential
936 part underwent substantial alterations in the Flavian and Severan periods, on both
937 occasions with notable use of mosaic floors. In the industrial district of this settlement
938 we can identify the area of the wine presses, especially from the 4th century CE, which
939 is the last phase for which there is evidence on the villa. However, due to the villa's
940 considerable size, we can deduce that it probably had a large industrial area that has not
941 yet been excavated to the north of the structures that have been discovered.

942 Immediately to the north of this area, a necropolis associated with the villa has been
943 found, with a funerary building and a series of tombs. This site clearly belongs to the
944 villa, which would subsequently be extended in the Visigoth period. The samples that
945 have been analyzed correspond to this Visigothic phase. Several types of burials can be
946 seen, from a simple grave to a cist. The number of burials identified (58), as well as the
947 results of the analysis, demonstrate the persistence and importance of the habitat, even
948 though it has not yet been identified archaeologically. The grave goods and the typology
949 of the tombs point to a Visigothic origin of the individuals.

950 We analyzed nine individuals from this site:

951 • I12029/PH'06-1144: 500–600 CE

952 • I12030/PH'06-1169: 500–600 CE

953 • I12031/PH'06-1172: 500–600 CE

954 • I12032/PH'06-1183: 500–600 CE

955 • I12033/PH'06-1192: 500–600 CE

956 • I12034/PH'06-1207: 500–600 CE

957 • I12162/PH'06-1163: 500–600 CE

958 • I12163/PH'06-1166: 500–600 CE

959 • I12164/PH'06-1157: 500–600 CE. First degree relative of I12032.

960 **Cueva de la Carigüela (Piñar, Granada, Andalusia, Spain)**

961 *Contact: Juan Manuel Jiménez Arenas, Isidro Jorge Toro Moyano*

962 The anatomically modern human mandible of Carigüela (Car1) was found during the field
963 seasons led by J.P. Spahni during the 50s of the last century. Initially, it was almost
964 complete although at present only the right half mandible with three molars is conserved.
965 The stratigraphic position is level III, associated with pre-neolithic lithic industry and a
966 fragment of parietal bone. Car1 was described and measured by García Sánchez (81) who
967 focused on the presence of ancestral features. In that paper, a close affinity of Car1 with
968 the male mandible from Combe Capelle was concluded.

969 Relevant features of Car1 include the presence of a retromolar space, a well-defined
970 mylohyoid line and deep submandibular fossa, and the presence of a goniac extroversion.

971 We analyzed a tooth from this mandible:

972 • I10899/Car1: 9700–5500 BCE (see SI 13)

973 **Cerro de la Virgen (Orce, Granada, Andalusia, Spain)**

974 *Contact: Juan Manuel Jiménez Arenas, Isidro Jorge Toro Moyano*

975 The site of Cerro de la Virgen is located in Orce (northeast Granada province), in a
976 flattened spur that was subsequently affected by agricultural activities, a building
977 construction now demolished, and a small church at the highest point of the hill. The site
978 is delimited by the river Orce in the north and by two gullies in the east and west. All the
979 recovered materials are attributed to the Bronze Age and show connections to the El Argar
980 culture (82). This site includes 36 individual and double cist burials inside the habitational
981 units.

982 We analyzed two individuals from this site:

983 • I8144/8: 1877–1636 cal BCE (3426±34 BP, Ua-39403)

984 • I8136/19: 1606–1418 cal BCE (3216±33 BP, Ua-39408)

985 **Cerro de la Encina (Monachil, Granada, Andalusia, Spain)**

986 *Contact: Juan Manuel Jiménez Arenas, Isidro Jorge Toro Moyano*

987 Cerro de la Encina is a site located 7 kilometers from the city of Granada, on the right
988 bank of the Monachil river, in one of the valleys leading to Sierra Nevada. The settlement
989 spread over a wide hill that clearly stands out from its surroundings. It has a strategic
990 location due to its natural defenses that limit access to the settlement, and due to its control
991 of La Vega de Granada and the access to Sierra Nevada.

992 The habitation spaces are located on the hillsides and adjacent plateaus, with the
993 fortification as the central element around which the settlement is articulated. The burials
994 are located under the house floors.

995 We analyzed one individual from this site:

- 996 • I8140_d/13: 2117–1779 cal BCE (3590±40 BP, Beta-230003)

997 **La Navilla (Arenas del Rey, Granada, Andalusia, Spain)**

998 *Contact: Juan Manuel Jiménez Arenas, Isidro Jorge Toro Moyano*

999 La Navilla is part of a group of collective burials (megaliths) located in the Alhama region
1000 in the southwest of the Granada province (83). It is a corridor tomb with a trapezoidal
1001 chamber located in the right bank of the Cacán river and containing 34 burials. It is
1002 surrounded by a group of orthostats.

1003 We analyzed three individuals from this site:

- 1004 • I8048/13: 2200–2000 BCE

- 1005 • I8141/7: 2200–2000 BCE

- 1006 • I8142/8: 2200–2000 BCE

1007 **Necrópolis de Cobertizo Viejo (La Zubia, Granada, Andalusia, Spain)**

1008 *Contact: Juan Manuel Jiménez Arenas, Isidro Jorge Toro Moyano*

1009 Cobertizo Viejo is a singular building located along the road from Granada to La Zubia.
1010 The first two phases of the building are dated to the Nazari period (14th-15th centuries
1011 CE) by the associated ceramic material (84). The building originally had a religious

1012 purpose, acting as the tomb of a Marabout, and was later enlarged with other constructions
1013 (including a cemetery) as the main tomb became increasingly important.

1014 The three analyzed tombs were excavated from the cemetery north of the main building:

1015 • I8145/sepultura 1: 1300–1500 CE

1016 • I8146/sepultura 4: 1300–1500 CE

1017 • I8147/sepultura 18: 1300–1500 CE

1018 **Calle Panaderos 21-23 (Granada, Andalusia, Spain)**

1019 *Contact: Juan Manuel Jiménez Arenas, Isidro Jorge Toro Moyano*

1020 This site is located in the city of Granada and was excavated in 2005 (85). The level of
1021 the Islamic necropolis is marked by a stratum of loose reddish-brown soil that appeared
1022 in the central part of the site, south of the jar E-17 and near the southwest limit. This
1023 stratum was irregularly distributed and covered burials CEF-20, CEF-43, CEF-36, CEF-
1024 37, CEF-40, CEF-25, CEF-47, CEF-28, CEF-29, CEF-23, CEF-24 and CEF-56. The
1025 bodies were oriented towards the southeast and in lateral decubitus position on the right
1026 side, following the Islamic tradition, with various degrees of limb flexion. Radiocarbon
1027 dating at the “Centro de Instrumentación Científica de la Universidad de Granada”
1028 confirmed that these burials belonged to the period of Muslim rule, more specifically to
1029 period of the Caliphate of Cordoba during the 10th century CE.

1030 We analyzed one individual from this site:

1031 • I7427/CEF-43: 900–1000 CE

1032 **Casa Cuartel Guardia Civil (Alhama de Granada, Granada, Andalusia, Spain)**

1033 *Contact: Juan Manuel Jiménez Arenas, Isidro Jorge Toro Moyano*

1034 In 2009, during construction works for the new headquarters of the “Guardia Civil” in
1035 Alhama de Granada, a medieval necropolis was discovered. More than 20 individuals
1036 were found, all buried with a southeast-northwest orientation and in lateral decubitus
1037 position on the right side, following the Islamic tradition. The associated ceramics place
1038 the necropolis within the 12th and 13th centuries CE. We analyzed 2 individuals from
1039 this site:

1040 • I7458/CEF0073/UEI513: 1100–1300 CE

1041 • I7457/CEF0010/UEI211: 1100–1300 CE

1042 **Cueva Romero (Huéscar, Granada, Andalusia, Spain)**

1043 *Contact: Juan Manuel Jiménez Arenas, Isidro Jorge Toro Moyano*

1044 The site occupies a wide area along the fluvial terraces located on the banks of the
1045 Huéscar river. Archaeological analysis has documented several phases of occupation
1046 (86). The earliest one dates to the Late Neolithic-Early Copper Age and is defined by a
1047 silo associated with a circular hut, the second corresponds to an Iron Age horizon in the
1048 context of secondary deposition and the third corresponds to a short occupation during
1049 the Roman period. Finally, a medieval necropolis with nine pit burials has been
1050 documented.

1051 We analyzed three individuals from the medieval necropolis:

1052 • I7497/Burial 2 (no. 1003): 1000–1100 CE. This burial includes a mixed cover made
1053 of sandstone and conglomerate. The body was in lateral decubitus position on the right
1054 side, legs slightly flexed, arms resting on the pubis and face oriented to the southeast. The
1055 burial was oriented on the southwest-northeast axis. Based on these characteristics the
1056 burial can be dated to the Medieval period.

1057 • I7498/Burial 9 (no. 8016): 1000–1100 CE. This is a single pit burial with a cover
1058 made with three sandstone slabs and large conglomerates. The space between the slabs
1059 was filled with small sandstone pieces and silex pebbles. The body was in lateral
1060 decubitus position on the right side, arms resting on the pubis and legs slightly flexed.
1061 The associated materials, including numerous fragments of cooking pots and ceramic
1062 platters with the imprints of fingers, places the burials around the 11th century CE. At the
1063 constructive level, the pit covers made with sandstone slabs are the most reliable indicator
1064 for the dating of the burials within the Zirid period.

1065 • I7499/Sepultura 7 (no. 5019): 1000–1100 CE. This is a single pit burial with a cover
1066 made of six sandstone slabs and large conglomerates. The space between the slabs was
1067 filled with small sandstone pieces and silex pebbles. The body was in lateral decubitus
1068 position on the right side following a southwest-northeast axis, arms resting on the pubis
1069 and extended legs.

1070 **El Castellón (Montefrío, Granada, Andalusia, Spain)**

1071 *Contact: Juan Manuel Jiménez Arenas, Isidro Jorge Toro Moyano*

1072 This site is located at the El Castellón hill, occupying a strategic area dominating the
1073 valley. Between 1977 and 1985 the excavation uncovered 115 well-preserved cist burials
1074 with large slabs, oriented on a north-south axis and reused several times (87). The simple
1075 burials generally correspond to young individuals. Grave goods were found in 16 graves,
1076 including earrings, bronze rings, glass beads, four Visigothic buckles, one bronze belt
1077 with two animal figures holding a large cup (interpreted as having a Byzantine origin),
1078 and ceramic olpes (flask). These objects place the cemetery within the 6th and 7th
1079 centuries CE, although the available date indicates a slightly earlier chronology.

1080 We analyzed nine individuals from this necropolis:

1081 • I3577/sepultura 31: 400–600 CE

1082 • I3574/sepultura 48: 400–600 CE

1083 • I3579/sepultura 2: 400–600 CE

1084 • I3583/sepultura 80: 400–600 CE

1085 • I3578/sepultura 29: 400–600 CE

1086 • I3575/sepultura 44 individuo 1: 400–600 CE

1087 • I3582/sepultura 77: 400–600 CE

1088 • I3581/sepultura 71: 400–600 CE

1089 • I3576/sepultura 27: 408–538 cal CE (1595±25 BP, PSUAMS-2117)

1090 **El Maraute (Torrenueva, Granada, Andalusia, Spain)**

1091 *Contact: Juan Manuel Jiménez Arenas, Isidro Jorge Toro Moyano*

1092 This necropolis is located on top of a hill within the Torrenueva town limits (88). The
1093 bodies were in lateral decubitus position on the right side oriented west-east, facing the
1094 south and with flexed limbs, except one adult individual found in a prone position with
1095 the head oriented south, hands united below the body and crossed legs. This generally
1096 corresponds to the Islamic funerary rite.

1097 In the same stratigraphic level, a trapezoidal house with internal divisions was
1098 documented. This house had a kitchen area and a space with lime floor with abundant

1099 ceramics for presenting food dated to the 10th and 11th centuries CE, such as “ataifores”
1100 with green and manganese epigraphy (al-mulk) and fragments of kitchen ceramics.

1101 We analyzed one individual from this site:

- 1102 • I7500/Individuo 2: 900–1100 CE

1103 **Paseillos universitarios-Fuentenueva (Granada, Andalusia, Spain)**

1104 *Contact: Juan Manuel Jiménez Arenas, Isidro Jorge Toro Moyano*

1105 The villa of the “Paseillos universitarios” is located in the city of Granada. The earliest
1106 phase has a Late Roman chronology (3rd-5th centuries CE) featuring an *horreum*, silos
1107 and one *torcularium* (89), and is associated to a necropolis from which the individuals
1108 analyzed in this study were sampled:

- 1109 • I3980/Individuo 221: 432–601 cal CE (1520±20 BP, PSUAMS-2110)
- 1110 • I3981/Individuo 234: 400–600 CE

1111 **Nécropolis de Torna Alta (Mondújar (Lecrín), Granada, Andalusia, Spain)**

1112 *Contact: Juan Manuel Jiménez Arenas, Isidro Jorge Toro Moyano*

1113 A few meters from the Cerrillo de Mondújar, in the field known as Torna Alta, a series
1114 of surveys were made in different farming terraces. Three burials were found and
1115 consequently an excavation of the area was carried out, identifying a total of 53 burials
1116 (90). The orientation and cover structures indicated an Islamic origin. The excavation
1117 determined that the necropolis had one short phase of occupation, following the
1118 traditional typology without external indications and in some cases with double slate or
1119 flat stone as cover. All these features, which match descriptions in the 16th century book
1120 “Libro de Apeo de Mondújar”, and the finding of a Castilian coin dated to the 16th century
1121 CE above the layer of the site, are consistent with an assignment to the 16th century and
1122 its interpretation as belonging to the *morisco* population (former Muslims converted to
1123 Christianity until their expulsion around 1610 CE). We analyzed eight individuals from
1124 this site:

- 1125 • I3807/Individuo 34: 1500–1600 CE.
- 1126 • I7426/Individuo 32: 1500–1600 CE
- 1127 • I3809/Individuo 5: 1500–1600 CE

- 1128 • I7423/Individuo 34bis: 1500–1600 CE
- 1129 • I3810/Individuo 9: 1500–1600 CE
- 1130 • I7424/Individuo 8: 1500–1600 CE
- 1131 • I3808/Individuo 2: 1500–1600 CE
- 1132 • I7425/Individuo 16: 1500–1600 CE

1133 **Plaza Einstein (Granada, Andalusia, Spain)**

1134 *Contact: Juan Manuel Jiménez Arenas, Isidro Jorge Toro Moyano*

1135 The Roman villa of Camino de Ronda-Plaza Einstein is located in the city of Granada
 1136 and is associated to a necropolis, both dated to the 3rd and 4th centuries CE (89). A final
 1137 phase features several pits cutting the structures of the villa and three silos, all of them
 1138 filled with common ware with comb-incised decoration and African TSA (Terra sigillata
 1139 africana) type D tableware.

1140 We analyzed 4 individuals from this site:

- 1141 • I4054/Sondeo G2/UE217: 200–400 CE. Genetically a brother of I3983.
- 1142 • I4055/Tumba 49: 200–400 CE
- 1143 • I3983/Tumba 19: 265–427 cal CE (1660±25 BP, PSUAMS-2081)
- 1144 • I3982/Tumba 7: 200–400 CE

1145 **Necrópolis de las Delicias (Ventas de Zafarraya, Granada, Andalusia, Spain)**

1146 *Contact: Juan Manuel Jiménez Arenas, Isidro Jorge Toro Moyano*

1147 This necropolis is located within the Ventas de Zafarraya urban area, in the mountainside
 1148 of the Sierra de Alhama close to the El Boquete de Zafarraya, a natural pass from the
 1149 Malaga coast to the interior since antiquity. During the 1985 excavation, 33 tombs were
 1150 found (87, 91, 92). Three of them, not included in this study, were of clear Roman
 1151 tradition.

1152 The funerary rite of all the tombs was inhumation. The number of buried individuals
 1153 varies from one to four, with east-west orientation most common.

1154 A total of 16 graves had grave goods or some object of personal use such as glass bowls,
 1155 belt buckles, shells, iron rings, necklace beads, glasses with horizontal striae decoration,

1156 a rectangular belt brooch with decoration of cells filled with vitreous phase of Ostrogothic
1157 influence, and a brooch and two sheets of Byzantine origin. The funerary ritual, the
1158 constructive typology and the grave goods place this necropolis within the 5th-7th
1159 centuries CE.

1160 We analyzed two individuals from this site:

- 1161 • I3584/Tumba XIX: 400–700 CE
- 1162 • I3585/Tumba XVIII: 677–866 cal CE (1250±25 BP, PSUAMS-2074)

1163 **La Angorrilla (Alcalá del Río, Sevilla, Andalusia, Spain)**

1164 *Contact: Domingo C. Salazar-García, Álvaro Fernández Flores*

1165 The archaeological site of La Angorrilla, which was excavated during the beginning of
1166 the 21st century, is located on the southwest of the municipality of Alcalá del Río (Sevilla,
1167 Spain). Its entire necropolis can be dated from the end of the 8th century to the middle of
1168 the 6th century BCE (93). This "Tartessian" (or "orientalizante") necropolis shows a
1169 variety of burial types in simple pits, mainly inhumations but a few primary and
1170 secondary incinerations are also present. The tombs present rectangular shape and they
1171 are oriented in west-east direction, a common feature amongst the necropolis of the
1172 Phoenician archaic period in the Iberian Peninsula (93).

1173 We analyzed four individuals from this site:

- 1174 • I12173/ROD.03/25; UE 2007: 700–500 BCE
- 1175 • I12171/ROD.03/25; UE 1457: 700–500 BCE
- 1176 • I12560/S-EVA17170, ROD.03/25; UE 404, Tibia: 700–500 BCE
- 1177 • I12561/S-EVA17196, ROD.03/25; UE 1205, Tibia: 700–500 BCE

1178 **Mandubi Zelaia (Ezkio-Itsaso, Gipuzkoa, Basque Country, Spain)**

1179 *Contact: Javier Fernández-Eraso, José Antonio Mujika-Alustiza*

1180 This dolmen was discovered by J. Etxaniz and excavated between 1998–2000 by José
1181 Antonio Mujika-Alustiza (94, 95). During excavation, two levels were discovered in the
1182 interior of the chamber. The upper level contained with several individuals and grave
1183 goods: a bronze awl, four arrowheads, two bone necklace beads and pottery sherds. The
1184 lower level contained burials on the base slab of the chamber, four arrowheads, two bone

1185 awls and one bone chisel. Radiocarbon analysis of four individuals yielded the following
1186 dates: 3502–3105 cal BCE (4585±40 BP, GrA-28313), 3498–3096 cal BCE (4560±50
1187 BP, GrN-26174), 3347–3097 cal BCE (4500±30 BP, Beta 382963), 3348–2938 cal BCE
1188 (4460±50 BP, GrN-26173), 3321–2921 cal BCE (4420±30 BP, Beta 382965).

1189 We analyzed five individuals from this site:

- 1190 • I7605/Mandubi Zelaia-13G-15.4 (x.32; y.9; z.158): 3500–2900 BCE
- 1191 • I7603/Mandubi Zelaia-13G-12.9 (x.10; y.74; z.152): 3500–2900 BCE
- 1192 • I7602/Mandubi Zelaia-13G-12.15 (x.4; y.74; z.151): 3500–2900 BCE
- 1193 • I7604/Mandubi Zelaia-13G-14.5: 3500–2900 BCE
- 1194 • I7606/Mandubi Zelaia-13H-16.37: 3500–2900 BCE

1195 **Jentillarri (Enirio-Aralar, Gipuzkoa, Basque Country, Spain)**

1196 *Contact: Javier Fernández-Eraso, José Antonio Mujika-Alustiza*

1197 Jentillarri is a gallery dolmen formed by 18 slabs. It was excavated in 1917 by José Miguel
1198 de Barandiaran, Enrique de Eguren and Telesforo de Aranzadi (95). Human remains from
1199 27 individuals were excavated, as well as pottery, awls and three arrowheads. We
1200 analyzed four individuals from this site:

- 1201 • I11300/Ar-J11: 3400–3000 BCE
- 1202 • I11301/Ar-J14: 3341–3030 cal BCE (4480±30 BP, Beta 484117)
- 1203 • I11248/Ar-J6: 3400–3000 BCE
- 1204 • I11249/Ar-J10: 3400–3000 BCE

1205 **Ondarre (Aralar, Gipuzkoa, Basque Country, Spain)**

1206 *Contact: Javier Fernández-Eraso, José Antonio Mujika-Alustiza*

1207 This Bronze Age cist was excavated by José Antonio Mujika-Alustiza in 2011 (96). It
1208 contains a small 150 cm long, 90-110 cm wide and 50-60 cm height chamber, formed by
1209 eight disturbed limestone slabs and one sandstone slab.

1210 Fieldwork recovered several human bones corresponding to at least 4 individuals (one
1211 infantile, one juvenile, one young adult and one mature adult), pottery sherds belonging

1212 to 6-7 undecorated vessels (two bowls, a carinated vessel and a S-shaped container), one
1213 deteriorated pendant and a bipyramidal quartz crystal.

1214 We analyzed one individual from this site:

- 1215 • I1982/Ond zis 3D-2.19: 1729–1531 cal BCE (3340±30 BP, Beta-350136)

1216 **La Braña-Arintero (León, Castilla y León, Spain)**

1217 *Contact: Julio Manuel Vidal Encinas*

1218 This site was described in Olalde et al. 2014 (97). We analyzed a phalanx from LaBraña2
1219 individual, who is genetically a brother of LaBraña1.

- 1220 • I0843/LaBraña2: 6010–5796 cal BCE (7030±50 BP, Beta-226473)

1221 **Camino de las Yeseras (San Fernando de Henares, Community of Madrid, Spain)**

1222 *Contact: Corina Liesau, Concepción Blasco, Patricia Ríos*

1223 This site was described in Olalde et al. 2018 (9). We analyzed one new individual from
1224 Funerary Area 3, who corresponds to the only complete skeleton in the tomb:

- 1225 • I4246/RISE697, sample #7, Fondo 5 UE05 Muerto 1: 2473–2030 cal BCE [2473–
1226 2299 cal BCE (3910±30 BP, PSUAMS-2119), 2280–2030 cal BCE (3650±40 BP, Beta-
1227 184837)]

1228 **Fuente la Mora (Valladolid, Castilla y León, Spain)**

1229 *Contact: Domingo C. Salazar-García, Ángel Esparza Arroyo, Javier Velasco Vázquez,*
1230 *Germán Delibes de Castro*

1231 The site of Fuente la Mora is a “pits site” with occupational levels from the Neolithic to
1232 the Early Iron Age. Some of the excavated structures have been attributed to the
1233 archaeological culture Cogotas I (Central Iberian Meseta Middle-Late Bronze Age, ca.
1234 1850-1150 cal BCE). Three of them contained human remains: three primary burials of
1235 an infant and two adults. The individual sampled for DNA analysis was a 20-25-year-old
1236 female:

- 1237 • I3491/S-EVA 26054: 1850–1150 BCE

1238 **La Requejada (San Román de Hornija, Valladolid, Castilla y León, Spain)**

1239 *Contact: Germán Delibes de Castro, Ángel Esparza Arroyo, Javier Velasco Vázquez*

1240 La Requejada is a site located at a fluvial terrace of the river Duero. Excavations revealed
1241 a ‘pits site’ with numerous structures dug on gravel and filled with refuse material such
1242 as ceramic sherds, lithic objects, animal bones, etc (98). Furthermore, a pit burial was
1243 found with the remains of three individuals synchronously buried (61, 99): a young adult
1244 female (SRH-01), a senile female (SRH-02) and an infantile male (SRH-03). All the
1245 materials and structures belonged to a short occupation phase of the Late Bronze Age
1246 Cogotas I culture ~1400–1300 BCE. We generated data from SRH-02 and SRH-03.

1247 • I12208/SRH-02: 1368–1211 BCE

1248 • I12209/SRH-03: 1368–1211 BCE

1249 **Humanejos (Parla, Community of Madrid, Spain)**

1250 *Contact: Rafael Garrido-Pena, Raúl Flores-Fernández. Ana M. Herrero-Corral*

1251 This site was described in Szécsényi-Nagy et al. 2017 (58). A total of 11 Copper Age
1252 individuals from this site were analyzed in Olalde et al 2018 (9). We analyzed one new
1253 individual dated to the Bronze Age.

1254 • I6618/Hume 1A, 443: 1879–1693 cal BCE (3458±24 BP, MAMS-32475)

1255 **Tordillos (Aldeaseca de la Frontera, Salamanca, Castilla y León, Spain)**

1256 *Contact: Domingo C. Salazar-García, Ángel Esparza Arroyo, Javier Velasco Vázquez,*
1257 *Germán Delibes de Castro*

1258 The site of Tordillos presents, like other ‘pits sites’ of the archaeological culture Cogotas
1259 I (Central Iberian Meseta Middle-Late Bronze Age, ca. 1850–1150 cal BCE), contains
1260 hundreds of dug structures that were originally grain storage pits and that are filled with
1261 waste material (potsherds, animal bones, ashes). Nine pits with human remains from 20
1262 skeletons in secondary position were also found, some of which were previously exposed
1263 as indicated by canid bite marks and erosive processes detected during the
1264 bioarchaeological study (100).

1265 We analyzed 2 individuals from this site:

1266 • I3492/S-EVA 26043: 1850–1150 BCE

1267 • I3493/S-EVA 26050: 1420–1283 cal BCE (3090±25 BP, PSUAMS-2072)

1268 **Galls Carboners (Mont-ral, Tarragona, Catalonia, Spain)**

1269 *Contact: Josep Maria Vergès, Marina Lozano*

1270 The Cova dels Galls Carboners site is located in the Prades Mountains, at 965 m a.s.l, on
1271 the western margin of the Brugent river valley. Although the cave is located in a steep
1272 area, it is 10 km away from Camp de Tarragona littoral plain connected with Francolí
1273 river, of which the Brugent river is tributary, and 25 km from the Mediterranean Sea. The
1274 NE oriented cave entrance is open to 5.5 meters high in an almost vertical rocky wall.
1275 The cave is 70 meters long. To get to the inner-most part, where individuals have been
1276 recovered, one has to bend or crawl after passing through a 40 cm diameter crawl. The
1277 collective burial was excavated in different periods, the first in the 1970's and the second
1278 between 2009 and 2010. Along with human remains belonging to a minimum of 17
1279 individuals of different ages (adults and subadults), some ceramic fragments and
1280 ornamentation beads made using shell fragments were recovered (*101*). Our direct dating
1281 of a human tooth points to a Chalcolithic date of 3020-2909 cal BCE (4355±20 BP).
1282 However, direct dates of a human phalanx and human teeth place most of the remains
1283 from this site in the Middle Bronze Age ~1750–1500 BCE.

1284 We analyzed seven individuals from this site:

1285 • I4565/GC.I-1-c.n10: 3020–2909 cal BCE (4355±20 BP, PSUAMS-2866)

1286 • I4558/GC.2.126.n146: 1700–1500 BCE

1287 • I4563/GC.2.150.n170 and GC.2.149.n169: 1700–1500 BCE

1288 • I4559/GC.2.127.n147: 1700–1500 BCE

1289 • I4560/GC.2.132.n152: 1700–1500 BCE

1290 • I4561/GC.2.135.n155: 1700–1500 BCE

1291 • I4562/GC.2.138.n158: 1738–1623 cal BCE (3375±20 BP, PSUAMS-3191)

1292 **Mas Gassol (Alcover, Tarragona, Catalonia, Spain)**

1293 *Contact: Josep Maria Vergès*

1294 The Mas Gassol site is located on the north-western margin of the Camp de Tarragona
1295 plain, at 235 meters a.s.l., at the foothills of the Prades Mountains, 18 km away from the

1296 city of Tarragona on the Mediterranean coast. The human remains reported in this study
1297 come from a small necropolis, dated between the 3rd and 5th centuries CE, associated to
1298 a Roman *villa rustica* (countryside villa), a farm-house that functioned as a residence of
1299 the landowner, his family and his servants (retainers and farm labourers), as well as a
1300 farming management center. Tarragona (*Tarraco*) was the oldest Roman settlement of
1301 the Iberian Peninsula (218 BCE) and became capital of the Roman province of *Hispania*
1302 *Citerior* (197–27 BCE) and later *Hispania Tarraconensis* (27 BCE – 476 CE). Its
1303 hinterland (named *Ager Tarraconensis*) was occupied by many *villae* dedicated to
1304 agriculture and livestock exploitation.

1305 The necropolis of Mas Gassol was composed of six graves, five funerary boxes made
1306 using *tegulae* and limestone slabs from local quarries, and one wood coffin. The graves
1307 contain 10 individuals: 8 adults and 2 children. In three cases, the funerary box contains
1308 more than one individual: 2 adults in two cases and 2 adults and 1 child in the other case.
1309 The wooden coffin contains the remains of a child of 5-6 years of age. All the graves are
1310 oriented NW-SE, with the head on the NW side, looking towards the rising of the sun
1311 (*102*).

1312 We analyzed 4 individuals from this site:

- 1313 • I7158/MGA'92 UE 108: 200–500 CE
- 1314 • I6492/MGA'92 UE 105: 200–500 CE
- 1315 • I6490/MGA'92-Resta II: 200–500 CE
- 1316 • I6491/MGA'92-Resta III: 200–500 CE

1317 **Coveta del Frare (La Font de la Figuera, València/Valencia, Valencian Community,**
1318 **Spain)**

1319 *Contact: Pablo García Borja, Mario Sanz Tormo*

1320 This site is located east of the hill known as “El Frare” or “Moleta del Frare”. It is a 5-
1321 meter-deep, 11-meter-wide rock shelter with a 0.8-1-meter-height entrance oriented
1322 towards the northeast. In 1968, a group of people who lived near the site found many
1323 archaeological remains, including human skulls belonging to at least 4 individuals.
1324 Archaeological study of those materials confirmed the presence of four individuals, two
1325 dated to the Chalcolithic and the other two to the Bronze Age (*103*). The analyzed sample
1326 belonged to a male individual from the Early Bronze Age:

1327 • I3494/CF-1: 1920–1753 cal BCE (3515±30 BP, CNA-1661.1.1)

1328 **Cueva de la Cocina (Dos Aguas, València/Valencia, Valencian Community, Spain)**

1329 *Contact: Oreto García-Puchol, Sarah B. McClure, Joaquim Juan-Cabanilles, Agustín A.*
1330 *Diez-Castillo*

1331 Cocina cave is an archaeological site with Holocene human occupations located in the
1332 municipality of Dos Aguas in eastern Spain. The cave opens to the La Ventana ravine and
1333 is surrounded by the rugged landscape of the southern Iberian ranges, close to the
1334 Mediterranean Sea (ca. 30 km). Humans occupied the site during the Holocene with
1335 evidence of Mesolithic hunter-gatherers as well as several discontinuous archaeological
1336 levels from the Early Neolithic to the Bronze Age (104).

1337 Research at Cocina Cave began in the 1940's (1941 to 1945), when Pericot excavated
1338 roughly 80 square meters at the entrance of the cave. This work produced the rich
1339 archaeological material currently deposited in the Valencian Museum of Prehistory/SIP,
1340 and identified a remarkable collection of portable art (105). In the 1970s, Javier Fortea
1341 leveraged the archaeological materials from Cocina Cave to shed light on the
1342 development of late Mesolithic hunter-gatherers and the transition to agriculture in the
1343 Neolithic (106). The investigation revealed the site's potential for characterizing late
1344 hunter-gatherer socioecological dynamics and the processes linked with the start of the
1345 Neolithic in the region. Fortea also excavated in the cave for seven field seasons (1974 to
1346 1981) in order to investigate the hypothesis of a gradual acculturation process to explain
1347 how last hunter-gatherers became farmers and herders (107). He focused the excavation
1348 in a large area located in the inner part of the cave using up-to-date excavation techniques,
1349 although most of the results remained unpublished (107, 108).

1350 Since 2014, an international research team led by Oreto García-Puchol, Sarah B. McClure
1351 and Joaquim Juan Cabanilles has been working at the site in the framework of two
1352 research projects -*MESO-COCINA* (Har2012-33111) and *EVOLPAST* (Har2015-68962),
1353 funded by government of Spain, to explore the site deposits in the context of the
1354 Neolithization process in Western Mediterranean. These studies are analyzing cultural
1355 and biotic assemblages recovered in the previous archaeological seasons with new
1356 methodological advances including three dimensional environmental modeling (108).
1357 The project also includes new excavations in order to resolve specific questions about
1358 cultural and sedimentary history, chronology, and stratigraphy (104, 109).

1359 This analysis recently produced (*104, 110*) an accurate chronological framework for the
1360 Mesolithic levels making it possible to test hypotheses about the extent to which the early
1361 Neolithic sequence was shaped by acculturation or colonization model (or other possible
1362 scenarios), using data from both Pericot's and Fortea's excavations. The current revision
1363 of Pericot's archaeological and biological record has revealed the presence of human
1364 remains in the Mesolithic deposits.

1365 Briefly, the chronology of archaeological deposits at the site starts with a long Mesolithic
1366 sequence that encompass the 7th millennium and the first centuries of the 6th millennium
1367 BCE including several episodes related to both regional phase A (with trapezes) and
1368 phase B (with triangles). At the moment, the Early Neolithic context is dated not before
1369 the last centuries of the 6th millennium BCE. The current radiocarbon dataset also reflects
1370 some Late Neolithic/Chalcolithic and Bronze Age occupations of the site (*104*).

1371 We analyzed one individual from a tooth recovered in the 1941 Pericot's trench
1372 corresponding to a Mesolithic layer (layer 2):

- 1373 • I8130/C. Cocina-25-7-41-capa 2: 6061-5934 cal BCE (7135±25 BP, PSUAMS-4429)

1374 **Lloma de Betxí (Paterna, València/Valencia, Valencian Community, Spain)**

1375 *Contact: Pablo García Borja, María Jesus de Pedro Michó*

1376 This Bronze Age site was first discovered in 1928 but archaeological work began in 1984
1377 under the direction of María Jesús de Pedro Michó and the patronage of the “Museu de
1378 Prehistòria de València”. It is a small settlement located at a small hill and made out of
1379 stone. Its destruction due to a fire has preserved many domestic objects including pottery,
1380 flints, handmills, metal objects, counterbalance looms and fragments of ornaments.
1381 Different areas were identified including a warehouse and milling and loom spaces. Two
1382 human burials were discovered outside the living space: one senile male buried with a
1383 small dog and a male burial in fetal position with flexed arms and legs and delimited with
1384 a circular stone structure (*111*). The tooth analyzed with aDNA belonged to the second
1385 individual:

- 1386 • I3997/LLBE-30593: 1864–1618 cal BCE (3400±40 BP, Beta-195318)

1387 **Cova de Sant Gomengo (La Font de la Figuera, València/Valencia, Valencian**
1388 **Community, Spain)**

1389 *Contact: Pablo García Borja, Mario Sanz Tormo*

1390 This cave site is located on the northern slope of Mont Capurutxo in La Font de la Figuera.
1391 In 1970 a group of locals found Late Neolithic/Chalcolithic and Iron Age archaeological
1392 materials in the interior of the cave. The Late Neolithic material included pottery, a flint
1393 arrowhead, a hoe made of polished stone and collar beads, and a set of human remains
1394 including two mandibles (112). We analyzed one tooth from one of the mandibles:

- 1395 • I8566/C.560: 3800–2500 BCE

1396 **La Coveta Emparetà (Bocairent, València/Valencia, Valencian Community, Spain)**

1397 *Contact: Pablo García Borja, Isabel Collado Beneyto*

1398 This cave site is located on the northern slope of the “Serra Mariola”. It is a 10-meter-
1399 long, 2.5-meter-wide cave with an irregular layout. It has a wide entrance oriented
1400 towards the west dominating a large part of the valley. At least four burials were deposited
1401 inside the cave (113), two dating to the Bronze Age. Two teeth recovered from the
1402 superficial level and not associated with any mandible were selected for analysis:

- 1403 • I8567/C.E.-1: 3500–3300 BCE
- 1404 • I8568/C.E.-2: 3499-3353 cal BCE (4615±20 BP, PSUAMS-4432)

1405 **La Vital (Gandia, València/Valencia, Valencian Community, Spain)**

1406 *Contact: Yolanda Carrión Marco, David López-Serrano, Pablo García Borja*

1407 This open-air site is located at the river Serpis terraces in the city of Gandia. The
1408 excavation has yielded numerous prehistoric remains dated from the Chalcolithic to the
1409 Iron Age (114). In 2017, archaeological work was undertaken by the rescue archaeology
1410 company “Estrats, Treballs d’Arqueologia SL” due to the construction of the “Acceso
1411 Sur al Puerto de Gandía” by the “Ministerio de Fomento”. During the last dig a series of
1412 prehistoric negative structures dated to the Chalcolithic were excavated. Inside one of
1413 these pits three human skeletons were discovered, two of which were almost complete,
1414 but their anatomic distribution suggested that they had been thrown in. No cultural
1415 artifacts or other ritual signs were found. We sampled three teeth for analysis, two of
1416 which belonged to the same individual:

1417 • I8131/A56-2017-UE5114 Diente 2, Diente 3: 2578–2457 cal BCE (3980±30 BP,
1418 Beta-504712)

1419 • I8132/A56-2017-UE5114 Diente 1: 2600–2400 BCE

1420 **Carrer Sagunto 49 (València, València/Valencia, Valencian Community, Spain)**

1421 *Contact: Pablo García Borja, Guillermo Pascual Berlanga*

1422 Archaeological excavations were carried out at Sagunto street numbers 45, 47 and 49
1423 (city of València) in 1997. An Islamic necropolis dated to the 12th-13th centuries CE was
1424 found on the right banks of the Turia river. We analyzed seven individuals from this site:

1425 • I12644/UE 1617: 1100–1300 CE

1426 • I12645/UE 1813: 1100–1300 CE

1427 • I12646/UE 1637: 1100–1300 CE

1428 • I12647/UE 1996: 1100–1300 CE

1429 • I12648/UE 1117: 1100–1300 CE

1430 • I12649/UE 2194: 1100–1300 CE

1431 • I12650/UE 1384: 1100–1300 CE

1432 **Túmulo Mortòrum (Cabanes, Castelló/Castellón, Valencian Community, Spain)**

1433 *Contact: Gustau Aguilera Arzo, Pablo García Borja*

1434 The Túmulo del Mortòrum is a collective burial dated to the Bronze Age but has feature
1435 that are reminiscent of megalithism, a tradition not attested in the province of
1436 Castelló/Castellón. It is a tumulus structure with a simple chamber, no corridor and stone
1437 cover (I15). The tomb itself was pillaged by grave robbers but it was possible to recover
1438 six individuals buried during the Bronze Age. We analyzed two individuals:

1439 • I8570/ID6: 1800–1000 BCE

1440 • I8571/ID4: 1800–1000 BCE

1441 **Cova dels Diablets (Alcalá de Xivert, Castelló/Castellón, Valencian Community,**
1442 **Spain)**

1443 *Contact: Gustau Aguilera Arzo, Pablo García Borja*

1444 The Cova dels Diablets controls a small interior valley in the foothills of the “Serra d'Irta”
1445 in Alcalá de Xivert. The cave had occupation levels dated to the end of the Paleolithic
1446 (Epi-Magdalenian), Early Neolithic and Chalcolithic (116). The human remains
1447 comprised four individuals from the later Chalcolithic period. We sampled one tooth from
1448 the “nivel 1 cuadro Q1”:

- 1449 • I8569/Q1-N-1: 2871–2626 cal BCE (4141±21 BP, MAMS-18651)

1450 **Palau Castell de Betxí (Betxí, Castelló/Castellón, Valencian Community, Spain)**

1451 *Contact: Gustau Aguilera Arzo, Pablo García Borja*

1452 In 2017, during the restoration works of the Palace-Castle of Betxí, five Islamic
1453 inhumations were discovered. Their chronology was confirmed by radiocarbon dating of
1454 individual UE 119A, and showed that they belonged to a necropolis in use before the
1455 construction of the Medieval fortress during the 14th century CE. We analyzed two
1456 individuals from this site:

- 1457 • I12514/UE 119A: 1020–1155 cal CE (960±30 BP, Beta-459794)
- 1458 • I12515/UE 102: 1000–1200 CE. Genetic data indicate that this individual is a 2nd-
1459 3rd-degree relative of I12514.

1460 **Plaza Parroquial (Vinaròs, Castelló/Castellón, Valencian Community, Spain)**

1461 *Contact: Gustau Aguilera Arzo, Pablo García Borja*

1462 During rescue excavations of the medieval wall of Vinaròs in the Plaza Parroquial, one
1463 inhumation was found. The location suggested that the remains were earlier than the
1464 construction of the wall, which was confirmed by radiocarbon dating:

- 1465 • I12516/UE 30001-3: 901–1116 cal CE (1030±30 BP, Beta-372984)

1466 **Gruta do Medronhal (Arrifana, Coimbra, Portugal)**

1467 *Contact: Ana Maria Silva*

1468 In the 1940s, human bones, metallic artifacts (n=37) and non-human bones were
1469 discovered in the natural cave of Medronhal (Arrifana, Coimbra). All these findings are

1470 currently housed in the Department of Life Sciences of the University of Coimbra and
1471 are analyzed by a multidisciplinary team. The artifacts suggest a date at the beginning of
1472 the 1st millennium BC, which is confirmed by radiocarbon date of a human fibula: 890–
1473 780 cal BCE (2650±40 BP, Beta–223996). This natural cave has several rooms and
1474 corridors with two entrances. No information is available about the context of the human
1475 remains. Nowadays these remains are housed mixed and correspond to a minimum
1476 number of 11 individuals, 5 adults and 6 non-adults.

1477 We analyzed two individuals from this site:

1478 • I7688/GM-23: 1200–700 BCE

1479 • I7687/GM-504: 1200–700 BCE

1480 **Monte da Cabida 3 (São Manços, Évora, Portugal)**

1481 *Contact: Ana Maria Silva*

1482 The Necropolis of Monte da Cabida 3 (São Manços, Évora, Portugal) was discovered in
1483 2004. Excavations performed during the year of 2007 revealed human remains buried in
1484 cists and pit burials, all dated to the Bronze Age (117). The human bone samples we
1485 analyze here were recovered from two pit burials (I7689 and I7691), and one from a
1486 rectangular cist (I7692). This last tomb contained two adults, and the individual analyzed
1487 here was the final interment. Bones from a previous deposition were found dispersed
1488 within the tomb.

1489 We analyzed 3 individuals from this site:

1490 • I7689/MC-3-Sep.14-960: 2200–1700 BCE

1491 • I7691/MC3-945-NÃ_2: 2200–1700 BCE

1492 • I7692/MC3-Sep9: 2200–1700 BCE

1493 **Perdigões (Reguengos de Monsaraz, Évora, Portugal)**

1494 *Contact: Ana Maria Silva, António C. Valera*

1495 At the Perdigões ditched enclosure, twelve pits were identified and excavated during the
1496 field campaigns of 2007/8. In two of them, pits 7 and 11, partial human skeletal remains
1497 were found in primary context and anatomical connection (118).

1498 In pit 11, only a small segment of the west part of the subcircular pit was found
1499 undisturbed. Three very incomplete and highly fragmented non adult skeletons (UE 76,
1500 77 and 78) were unearthed. A Suidae paw and a cockle shell were found associated. UE
1501 76 was a non-adult that died around 16/17 years based on dental age (root development
1502 of third upper molar). This skeleton was deposited on its right side, SW – NE orientated.
1503 A hand bone of this individual confirm the Late Neolithic chronology of these remains
1504 (3020–2910 cal BCE (4370 ± 40 BP, Beta-289263)). Non-adult 77, placed on the left
1505 side, flexed, N – S oriented, died at around age 5, based on dental calcification. With the
1506 exception of two teeth with linear enamel hypoplasia (physiological stress indicator), no
1507 other signs of pathology were detected. Non-adult 78 was lying on its left side, head
1508 orientated north. Age at death estimation of this individual based on several teeth fall
1509 between 12.7 and 14.8 years. The left radius allowed an estimation of 12 years. With the
1510 exception of an enamel hypoplasia in pit form observed in the lower left central incisor,
1511 no other signs of pathology were noted (119).

1512 We analyzed two individuals from this site:

1513 • I3432/Pit 11, UE77: 3082–2909 cal BCE (4365±25 BP, PSUAMS-1882)

1514 • I5429/Pit 11, UE78: 3010–2887 cal BCE (4310±20 BP, PSUAMS-2692)

1515 **Monte Canelas 1 (Alcalar, Faro, Portugal)**

1516 *Contact: Ana Maria Silva*

1517 This site was described in Martiniano et al. 2017 (6). We analyzed one new individual:

1518 • I5076/MCI.228: 3335–3026 cal BCE (4465±25 BP, PSUAMS-3902)

1519 **Cova das Lapas (Alcobaça, Leiria, Portugal)**

1520 *Contact: Ana Maria Silva, Ana Catarina Sousa and Victor S. Gonçalves*

1521 Cova das Lapas is a very small cave located in the Limestone Massif of Estremadura that
1522 was intensively used as a burial space. The excavation fieldworks were directed under
1523 direction of Victor S. Gonçalves in 1984, 1986 and 1987. The sequence of absolute dating
1524 and votive artifacts indicates that this necropolis was used over a relatively short period
1525 between 3245–3263 and 3036–2913 BCE. It was possible to identify several
1526 individualized and coupled burials and a complex sequence of management of the space
1527 with successive depositions and ossuaries. The votive artifacts include the characteristic
1528 elements of the magic-religious complex of the first and second phases of Megalithism:

1529 geometric armatures (all trapezes), blades, daggers, scarce ceramics and one engraved
1530 schist plaque placed in the chest of a young person, which is very uncommon.

1531 We analyzed one individual from this site:

- 1532 • I5428/CLA6: 3300–2900 BCE

1533 **Casas Velhas (Melides, Setúbal, Portugal)**

1534 *Contact: Ana Maria Silva*

1535 The necropolis of Casas Velhas was discovered during the 1970s. Excavations were
1536 undertaken by the Museum of Archaeology and Ethnography of the District of Setúbal
1537 (Portugal) during 1975 and 1996 under the direction of Carlos Tavares da Silva and
1538 Joaquina Soares. This necropolis is composed by 35 graves, mostly small stone cists. The
1539 cists, highly disturbed by agriculture, were mostly composed of four upright slabs of
1540 limestone or ferruginous breccia. The maximum lengths of these tombs were less than
1541 1m. The cemetery belongs to the Southwest Iberian Bronze Age that was widespread
1542 across the south of Portugal (Alentejo and Algarve) and southwest Spain, including the
1543 regions of Huelva, Badajoz and Seville (*120, 121*). In funerary terms, this culture was
1544 characterized by individual burials deposited in lateral fetal position, mostly inside small
1545 stone cists, sometimes with funerary ceramic vessels, metallic objects and/or faunal
1546 remains. These burials are predominantly individual, but double, triple and quadruple
1547 (usually not simultaneous) interments are also documented (*122*). Casas Velhas
1548 represents the site with best preserved human remains in Portugal for this culture and
1549 period (*122, 123*). Radiocarbon dating of human bones from two cists confirmed the
1550 Bronze Age chronology of these remains (cist 14 - 1670-1410 cal BCE (3255±55BP,
1551 OxA-5531); and cist 35 - 1680-1415 cal BCE (3260±60BP, Beta-127904)) (*124, 125*).

1552 Preliminary results indicate that of the 35 graves, 20 contained human bone, 19 of which
1553 were available for detailed anthropological analysis. Of these, 15 were individual tombs,
1554 3 double and 1 triple, corresponding to a minimum number of 24 individuals, 22 adults
1555 and 2 non-adults. Cist 30 contained the bones of two adults. The last interment of this
1556 tomb belonged to an adult female more than 30 years old, the sample analyzed here
1557 (I8045). This female was deposited in crouched position, lying on the right side,
1558 orientated East (head) – West. In front of the pelvic region of this skeleton a ceramic
1559 vessel was recovered. The bones from the left forelimb of an adult individual of *Bos*
1560 *taurus* (radius, ulna, lunate and scaphoid bone) were also recovered from this cist,
1561 although only the exact position of the *Bos* radius is known, apparently associated with

1562 the last interment. The other individual was identified through the duplication of some
1563 teeth, belonging to an adult of unknown sex.

- 1564 • I8045/CV-Sep30.8: 1700–1300 BCE

1565 **Bolores (Torres Vedras, Lisboa, Portugal)**

1566 *Contact: Katina Lillios*

1567 This site is described in Szécsényi-Nagy et al (58). We successfully analyzed 2
1568 individuals:

- 1569 • I11614/MS024: 2800–2600 BCE
- 1570 • I11592/MS002: 2800–2600 BCE

1571 **Cabeço da Arruda I (Torres Vedras, Lisboa, Portugal)**

1572 *Contact: Ana Maria Silva*

1573 This site is described in Martiniano et al (6). We successfully analyzed 3 individuals:

- 1574 • I11599/MS009: 3400–2800 BCE [layer date based on a long bone from a likely
1575 different individual 3330–2885 cal BCE (4370±70 BP, Beta-123363)]
- 1576 • I11601/MS011: 3400–2800 BCE [layer date based on a long bone from a likely
1577 different individual 3330–2885 cal BCE (4370±70 BP, Beta-123363)]
- 1578 • I11600/CA122A, CabecoArruda122A: 3400–2800 BCE [layer date based on a long
1579 bone from a likely different individual 3330–2885 cal BCE (4370±70 BP, Beta-123363)].
1580 This is a sample from the same individual as CabecoArruda122A, who was analyzed in
1581 Martiniano et al (6).

1582 **Tholos of Paimogo I (Lourinhã, Lisboa, Portugal)**

1583 *Contact: Ana Maria Silva*

1584 Paimogo I (or Pai Mogo I) is a corbel-vaulted tomb located in Lourinhã (Portugal), 1 km
1585 from the Atlantic coast. The site was discovered in 1968, and excavated in 1971 (126).
1586 The tomb consists of a nearly elliptic burial chamber (diameter 4.85 m East-West and 4.5
1587 m North-South) and a corridor 6.6 m length. An extensive array of objects, dated to the
1588 Late Neolithic and Chalcolithic were recovered, such as decorated pre-Beaker and Beaker
1589 ceramics, groundstones and flaked stone tools, bone tools, limestone idols, other

1590 limestone objects, and copper implements (*126, 127*). Several radiocarbon dates were
1591 obtained on human bones, which produced consistent date ranges between the end of 4th
1592 millennium to the middle of 3rd millennium: 3095–2575 cal BCE (4250±90 BP, Sac-
1593 1556) and 2619–2475 cal BCE (4030±25 BP, UGAM-22150) (*128*).

1594 Little information is available about the context of the human remains recovered from
1595 this burial. These were found commingled and fragmented but with good preservation.
1596 The first anthropological study performed by Silva revealed a minimal number of 413
1597 individuals: 290 adults and 123 non-adults (*128, 129*). This collection was further
1598 analyzed for dietary evidences using stable isotopic data (*130*), strontium isotope analysis
1599 to identify territorial mobility patterns (*131*), physiological stress indicators (*132*),
1600 fractures patterns, among others.

1601 We successfully analyzed 2 individuals from this site:

1602 • I11604/MS014: 3100–2500 BCE

1603 • I11605/MS015: 3100–2500 BCE

1604

1605 **SI 2 - Direct AMS ¹⁴C Bone Dates**

1606 Bone samples for the newly reported direct AMS ¹⁴C dates (Table S3) from Penn State
1607 (PSUAMS) were manually cleaned to remove sediment, conservants and adhesives. Parts
1608 of bones with obvious signs of glues, written catalog numbers, etc. were avoided for
1609 sampling. All samples were physically broken down to 1-3 mm pieces to aid
1610 demineralization and then sonicated in successive solvent washes of methanol, acetone
1611 and dichloromethane (a substitute for the more toxic chloroform) and rinsed repeatedly
1612 in 18.2 MΩ·cm⁻¹ water. Samples were demineralized in 0.5N HCl for 2-3 days at ~5°C,
1613 and soaked in 0.1N NaOH at room temperature to remove contaminating soil humates.
1614 Samples were then rinsed to neutrality in 18.2 MΩ·cm⁻¹ water and gelatinized in 0.01N
1615 HCL for 12 hrs at 60°C (133). The resulting gelatin was lyophilized and weighed to
1616 determine percent crude gelatin yield as a measure of collagen preservation. After
1617 assessing gelatin yield and qualitative indicators of preservation (e.g., persistent
1618 coloration suggestive of incomplete humate removal, gelatin was further purified by
1619 ultrafiltration, using precleaned Centriprep® filters retaining >30 kDa gelatin. More
1620 poorly preserved samples were hydrolyzed in 1.5 mL of 6N HCl at 100°C for 24 hrs, and
1621 then run through Supelco ENVI-Chrom° solid phase extraction columns to remove
1622 humates and other polar contaminants (“XAD” purification; detailed methods described
1623 in Lohse et al. 2014 (134)).

1624 The resulting material, >30 kDa gelatin or purified amino acid hydrolyzate, was
1625 submitted to the Yale Analytical and Stable Isotope Center for EA-IRMS analysis, with
1626 %C, %N and C:N ratios and δ¹³C and δ¹⁵N evaluated before AMS ¹⁴C dating. C:N ratios
1627 for well-preserved samples fall between 2.9 and 3.6, indicating good collagen
1628 preservation (135); in practice the observed range tends to be between 3.1 and 3.4.

1629 Pretreated samples were converted to CO₂ in 6 mm OD clear fused quartz tubing prebaked
1630 at 900°C for 3 hrs, along with ~60 mg of CuO wire and ~3 mm of Ag wire, and sealed
1631 under vacuum on a line backed with an oil free turbopump system. Ultrafiltered gelatin
1632 (~2.2 mg) was packed into 6” tubes and combusted for 3 hrs at 900°C, while hydrolyzed
1633 amino acids (~4.0 mg) were packed into 8” tubes and combusted for 3 hrs at 800°C.
1634 Sample CO₂ was converted to graphite by hydrogen reduction onto an Fe catalyst (5.5-
1635 6.5 mg) at 550°C for 3 hrs (136) with reaction water is drawn off with Mg(ClO₄)₂ (137).
1636 Sample graphite is pressed into Al targets for AMS measurement along with graphite of
1637 6 OXII primary standards, and bone backgrounds (SR-5156 Beaufort Whale) and
1638 secondaries (AD 1800s cow bone, 1850 BP bison bone, and 5670 BP sea lion bone) for

1639 each run. AMS ¹⁴C measurements were made on a modified NEC 500kV 1.5SDH-1
1640 compact AMS at the Penn State AMS ¹⁴C laboratory. Conventional ¹⁴C ages were
1641 corrected for fractionation during graphitization and measurement with δ¹³C values
1642 measured on the AMS following the conventions of Stuiver and Polach 1977 (138).

1643 **SI 3 - Ancient DNA laboratory work**

1644 We performed laboratory work in dedicated clean rooms at the Reich's lab (Harvard
1645 Medical School). We extracted DNA (139–141) and built double-stranded and single-
1646 stranded DNA libraries (Table S2). Libraries were subjected to a partial uracil-DNA-
1647 glycosylase (UDG half) treatment to remove most of the ancient DNA damage while
1648 preserving the signal in the terminal nucleotides (1, 142–144). For single-stranded
1649 libraries we used E.coli UDG (USER from NEB) with the ssDNA2.0 protocol to achieve
1650 this; Adapter CL78 was replaced by TL181 (5'-
1651 AGATCGGAAGAAA[A][A][A][A][A][A]-3'; [A] = ortho methyl RNA), Splinter
1652 TL110 was replaced by TL159a (5'-[A][A][A]CTTCCGATCTNNNNNNNN[A]-3', [A]
1653 = ortho methyl RNA) and the extension primer CL130 was replaced by CL128 5'-
1654 GTGACTGGAGTTCAGACGTGTGCTCTTCC*G*A*T*C*T-3'; * = phosphor thioate.
1655 A subset of the double-stranded libraries were prepared with an automated liquid handler
1656 that uses silica magnetic beads instead of MinElute columns for cleanup steps). DNA
1657 libraries were enriched for human DNA using probes that target 1,233,013 SNPs ('1240k
1658 capture') (3, 12) and the mitochondrial genome. Captured libraries were sequenced on an
1659 Illumina NextSeq500 instrument with 2x76 cycles and 2x7 cycles (2x8 for single-
1660 stranded libraries) to read out the two indices (145).

1661 Sampling and DNA extraction at the University of Huddersfield

1662 We processed six samples (I11614, I11592, I11599, I11601, I11604, I11605) in clean
1663 rooms in the specialized Ancient DNA Facility at the University of Huddersfield, wearing
1664 full body suits, hairnets, gloves and face masks at all times. We constantly cleaned all
1665 tools and surfaces with LookOut® DNA Erase (SIGMA Life Sciences), as well as with
1666 bleach, ethanol and long exposures to UV light. We subjected six samples to UV-
1667 radiation for a total of 60 minutes (30 minutes each side) and cleaned sampling surfaces
1668 with 5µm aluminum oxide powder using a compressed air abrasive system. For the four
1669 petrous samples (two each from Bolores and Cabeço da Arruda I), we targeted the densest
1670 part of the bone; for the two tooth samples (both from Paimogo I), we removed the tooth
1671 root, using a circular saw attached to a hobby drill. We obtained bone and tooth root
1672 powder by crushing the excised petrous portion or tooth root in a MixerMill (Retsch

1673 MM400). We extracted DNA from ~150 mg of powder following the protocol of Yang
1674 et al. 1998 (146), with modifications by MacHugh et al. 2000 (147). We included blank
1675 controls throughout extractions to monitor for possible modern DNA contamination.
1676 DNA extracts were shipped to Reich's lab.

1677 **SI 4 - Bioinformatics processing**

1678 Reads for each sample were extracted from raw sequence data according to sample-
1679 specific indices added during wetlab processing, allowing for one mismatch. Adapters
1680 were trimmed and paired-end sequences were merged into single ended sequences
1681 requiring 15 base pair overlap (allowing one mismatch) using a modified version of
1682 *SeqPrep 1.1* (<https://github.com/jstjohn/SeqPrep>) which selects the highest quality base
1683 in the merged region. Unmerged reads are discarded prior to alignment to both the human
1684 reference genome (hg19) and the RSRS version of the mitochondrial genome (148) using
1685 the 'samse' command in *bwa v0.6.1* (149). Duplicates were removed based on the
1686 alignment coordinates of aligned reads, as well as their orientation. Libraries were
1687 sequenced to saturation across multiple sequencing lanes where necessary, with
1688 complexity metrics established using *preseq* (150), merging where necessary. Subsequent
1689 authenticity of ancient DNA is established using several criteria: we discarded from
1690 further analysis libraries with a rate of deamination at the terminal nucleotide below 3%.
1691 We computed the ratio of X-to-Y chromosome reads, estimated mismatch rates to the
1692 consensus mitochondrial sequence, using *contamMix-1.0.10* (151) and ran X-
1693 chromosome contamination estimates using *ANGSD* (152) in males with sufficient
1694 coverage (Table S2). Libraries with evidence of contamination were discarded from
1695 genome-wide analyses or, in cases with sufficient data, restricted to sequences with
1696 cytosine deamination to remove potential contaminating sequences (Table S1).

1697 We merged libraries from the same individual and required a minimum of 10,000 SNPs
1698 with at least one overlapping sequence for inclusion in genome-wide analyses.
1699 Individuals that were first-degree relatives of others in the dataset with higher coverage
1700 were also excluded for genome-wide analyses (Table S1).

1701 **SI 5 - Mitochondrial and Y-chromosome haplogroup** 1702 **determination**

1703 We determined mitochondrial DNA haplogroups (Table S1) for each individual using
1704 Haplogrep2 (153).

1705 We performed Y-chromosome haplogroup determination (Table S4) using the
1706 nomenclature of the International Society of Genetic Genealogy (<http://www.isogg.org>)
1707 version 11.110 (21 April 2016). We restricted to sequences with mapping quality ≥ 30
1708 and bases with quality ≥ 30 .

1709 We comment here on the striking Y-chromosome patterns observed during the Copper
1710 Age-Bronze Age transition in Iberia. All the Bronze Age males from Iberia with sufficient
1711 coverage ($n=30$) belonged to R1b-M269 (R1b1a1a2). Furthermore, all the R1b-M269
1712 males with sufficient coverage ($n=15$) could be further classified as R1b-P312
1713 (R1b1a1a2a1a2). Only one Bronze Age male, esp005.SG (7), had DNA sequences
1714 overlapping R1b-DF27 (R1b1a1a2a1a2a) and he was positive for the mutation. Two
1715 Bronze Age males, I6470 and I3997, had DNA sequences overlapping R1b-Z195
1716 (R1b1a1a2a1a2a1), with I6470 being negative and I3997 positive. Eleven Bronze Age
1717 males had DNA sequences overlapping R1b-Z225 (R1b1a1a2a1a2a5), with only
1718 VAD001 being positive for the mutation (one Iron Age male, I3320, is also positive for
1719 this mutation). We thus detect three Bronze Age males who belonged to DF27 (154, 155),
1720 confirming its presence in Bronze Age Iberia. The other Iberian Bronze Age males could
1721 belong to DF27 as well, but the extremely low recovery rate of this SNP in our dataset
1722 prevented us to study its true distribution. All the Iberian Bronze Age males with
1723 overlapping sequences at R1b-L21 were negative for this mutation. Therefore, we can
1724 rule out Britain as a plausible proximate origin since contemporaneous British males are
1725 derived for the L21 subtype.

1726 **SI 6 - Kinship analysis**

1727 We looked for kinship relationships between the individuals included in our study. We
1728 followed the same strategy as in Kennett et al 2017 (156) and Loosdrecht et al 2018 (15),
1729 which is similar to that in Monroy Kuhn et al 2018 (157). For each pair of individuals,
1730 we computed the mean mismatch rate using all the autosomal SNPs with at least one
1731 sequencing read for both individuals in the comparison. In the cases with more than one
1732 read at a particular SNP for a given individual, we randomly sample one read for analysis.
1733 We then estimated relatedness coefficients r as in Kennett et al 2017 (156):

$$1734 \quad r = 1 - ((x-b)/b)$$

1735 with x being the mismatch rate and b the base mismatch rate expected for two genetically
1736 identical individuals, which we estimated by computing intra-individual mismatch-rates.

1737 We also computed 95% confidence intervals using block jackknife standard errors. The
1738 inferred kinship relationships for each pair can be viewed in Table S1.

1739 We illustrate this procedure with our Iberian Mesolithic individuals. We first split them
1740 into two groups according to their genomic population affinities (Table S7): one group
1741 comprised of individuals with lower affinity to El Mirón individual: LaBraña1, LaBraña2
1742 and Canes1. The other group comprised of individuals with high El Mirón affinity: Car1,
1743 CMN2, CC1 and Chan. We computed pairwise mismatch rates between individuals in
1744 each of the groups and intra-individual mismatch rates (Table S6).

1745 Then, we computed relatedness coefficients (Fig. S1) using base mismatch rates of
1746 0.1138323 and 0.1069545 for the first and second groups, respectively. These values were
1747 obtained by averaging intra-individual mismatch rates of individuals with more than
1748 100,000 SNPs to avoid extremely noisy estimates.

1749 We obtained a relatedness coefficient of 0.51 for LaBraña1 and LaBraña2 (two males
1750 with overlapping radiocarbon dates and found at the same cave), which indicates that they
1751 were 1st-degree relatives. They had the same mtDNA and Y-chromosome haplotypes,
1752 suggesting a sibling relationship, which we confirm by the presence of long IBD segments
1753 on the X-chromosome (Fig. S2). This is not expected for a father-son relationship as the
1754 X-chromosome is inherited from the mother.

1755 **SI 7 - Genome-wide analysis datasets**

1756 We built two datasets for genome-wide analyses:

1757 - HO dataset, which includes 1331 ancient individuals together with 2562 present-
1758 day individuals from worldwide populations genotyped on the Human Origins
1759 Array (10, 11, 158). The ancient set includes newly reported individuals from
1760 Iberia and individuals that had previously been published (2, 4–10, 12, 13, 15, 17,
1761 20, 97, 158–181) (Table S1), both from Iberia and other regions. We kept 591,642
1762 autosomal SNPs after intersecting autosomal SNPs in the 1240k enrichment with
1763 the analysis set of 594,924 SNPs from a previous publication (10).

1764 - HOIII dataset, which includes the same set of ancient individuals, 300 present-day
1765 individuals from 142 populations sequenced to high coverage as part of the
1766 Simons Genome Diversity Project (182), and 2535 present-day individuals
1767 sequenced as part of the 1000 Genomes Project Phase 3 (183). For this dataset,

1768 we used 1,054,671 autosomal SNPs, excluding SNPs of the 1240k array with
1769 known functional effects or located on sex chromosomes.

1770 For each individual, each genomic position was represented by a randomly sampled
1771 sequence, removing the first and the last two nucleotides of each sequence if the
1772 sample was treated with UDG half and the first and the last ten nucleotides for
1773 samples from the literature that were not treated with UDG.

1774 We repeated key analyses after removing 284,013 SNPs in CpG context (Table S5)
1775 that could potentially be affected by aDNA damage, as methylated cytosines are
1776 deaminated into thymines which are not removed by UDG half treatment.

1777 **SI 8 - Principal component analysis**

1778 We performed principal component analysis on the HO dataset using the ‘smartpca’
1779 program in EIGENSOFT (184). We projected ancient individuals onto the components
1780 computed on present-day individuals with lsqproject:YES and shrinkmode:YES. We ran
1781 three analyses with different sets of present-day individuals:

1782 -A set with 989 present-day West Eurasians (Fig. 1C-D).

1783 -A set with 989 present-day West Eurasians and 70 present-day North Africans (Fig. S3).

1784 -A set with 989 present-day West Eurasians, 70 present-day North Africans and 136
1785 present-day sub-Saharan Africans (Fig. S4).

1786 **SI 9 - f -statistics**

1787 We computed f_4 -statistics in ADMIXTOOLS (11) using the program *qpDstat* and *f4mode*:
1788 YES. To assess statistical significance, we compute standard errors using a weighted
1789 block jackknife approach (185) over 5 Mb blocks.

1790 **SI 10 - Estimation of F_{ST} coefficients**

1791 We estimated F_{ST} using smartpca (184) with parameters *inbreed*: YES and *fstonly*: YES.

1792 **SI 11 - *qpAdm* admixture modeling**

1793 In this section we use *qpAdm* (12) (<https://github.com/DReichLab>) to fit the ancestry of
1794 populations in the Iberia genetic time transect as a mixture of other populations from the
1795 same area or from neighboring regions. This method models the ancestry of a *test*
1796 population as mixture of a set of *source* populations that are differentially related to a set
1797 *outgroup* populations. The software fits a matrix of f_4 -statistics relating the *test*, *source*
1798 and *outgroup* populations and outputs mixture proportions and formal P-values for

1799 whether the tested model is a good fit to the data. For a more detailed explanation of this
1800 methodology see Supplementary Information section 7 of ref (158).

1801 Following a similar strategy to the one in ref (167), we started with a set of populations
1802 that includes groups distantly related, both geographically and temporally, to our Iberian
1803 individuals, and more proximate groups that are plausible sources for the ancestry in
1804 them. We tested all possible 1-way, 2-way and 3-way combinations of populations in our
1805 initial set, using them as sources and leaving the remaining populations as outgroups in
1806 the model. We then checked whether a 1-way model was sufficient to explain the ancestry
1807 in the *test* population. If no 1-way model showed a good fit ($p>0.05$), we looked for
1808 plausible 2-way models and if not, for 3-way models. Unless otherwise noted, this is the
1809 strategy followed throughout SI 11.

1810 ***Mesolithic period***

1811
1812 To increase resolution, we decided to merge the data for the two Mesolithic individuals
1813 from the southeast (CMN2 and CC1), both with fewer than 25,000 covered SNPs. This
1814 prevented us from studying differences between these two roughly contemporaneous
1815 individuals.

1816 Using f_4 -statistics (Fig. S5) we showed that Iberian Mesolithic hunter-gatherers are
1817 differentially related to the El Mirón (4) individual (northwestern Spain, ~16000 cal BCE)
1818 and to contemporaneous individuals from central Europe such as KO1 (186),
1819 demonstrating the presence of genetic structure during this period. Therefore, we included
1820 KO1 and El Mirón in our *outgroup* population set together with other Upper Palaeolithic
1821 and later West Eurasians, an ancient East African (Mota) (168) and the oldest East Asian
1822 (Tianyuan) (177) and North African (Morocco_Iberomaurusian) (15) individuals with
1823 available genome-wide data.

1824 *Outgroup* set: Mota, Ust_Ishim, Kostenki14, GoyetQ116-1, Vestonice16, MA1, El
1825 Mirón, EHG, KO1, Iran_N, Israel_Natufian, Morocco_Iberomaurusian, Tianyuan.

1826
1827 None of the possible 1-way models fit the data, meaning that our *test* populations do not
1828 form a clade with any population in the *outgroup* set. The model El Mirón+KO1 is the
1829 only 2-way model that fits the data for the Iberian Mesolithic individuals and Loschbour
1830 (Table S7). We repeated the analysis substituting KO1 by Villabruna as representative of
1831 the WHG cluster. The model El Mirón+Villabruna does not fit the data for the La Braña
1832 brothers and Canes1 and thus we present in the main text models featuring El
1833 Mirón+KO1.

1834 The Iberian hunter-gatherer with the strongest shift towards KO1 is Canes1. Unlike the
1835 other Mesolithic Iberians who belong to mtDNA U5b, this individual belongs to mtDNA
1836 haplogroup U5a, which is more common in central European hunter-gatherers.

1837 ***Neolithic and Copper Age***

1838
1839 The Early Neolithic period in Europe is characterized by the arrival of farmers from
1840 Anatolia. Therefore, we added Anatolia_N as a possible source in the *outgroup* set.

1841 *Outgroup* set: Mota, Ust_Ishim, Kostenki14, GoyetQ116-1, Vestonice16, MA1, El
1842 Mirón, EHG, KO1, Iran_N, Israel_Natufian, Morocco_Iberomaurusian, Tianyuan,
1843 Anatolia_N

1844
1845 Again, we were not able to successfully model any Neolithic/Copper Age group using
1846 one population from the *outgroup* set. Central European populations can be modeled as
1847 a 2-way mixture between Anatolia_N and KO1, with the exception of Germany_MN
1848 (Table S8). In the case of populations from Iberia, southern France and Britain, no 2-way
1849 combination fit the data, and most of them can only be modeled as a mixture of
1850 Anatolia_N, El Mirón and KO1 (Table S8).

1851 ***Copper Age outlier from Camino de las Yeseras***

1852
1853 One Copper Age individual (C_Iberia_CA_Afr; ID I4246) excavated at Camino de las
1854 Yeseras in central Iberia clusters with North Africans and not with Europeans in PCA
1855 (Fig. 1C, Fig. S3-4), and we wanted to check whether *qpAdm* detects the same genetic
1856 signal. Previous studies have reported the presence of ancestry related to Early Neolithic
1857 Europeans in Late Neolithic North Africans (8). Therefore, we included in our *outgroup*
1858 set several Early Neolithic Europeans (Croatia_EN, Iberia_EN, Macedonia_N,
1859 Serbia_EN, LBK_EN, Romania_EN, Hungary_EN) under the population name
1860 Europe_EN to act as a possible ancestry source.

1861 *Outgroup* set: Mota, Ust_Ishim, Kostenki14, GoyetQ116-1, Vestonice16, MA1, El
1862 Mirón, Villabruna, WHG, EHG, Iran_N, Israel_Natufian, Levant_N, Europe_EN,
1863 Morocco_Iberomaurusian, Tianyuan

1864
1865 The best 2-way and 3-way models both feature Europe_EN and
1866 Morocco_Iberomaurusian, with ancestry proportion for Mota not significantly different
1867 from 0 in the 3-way model (Table S9). This supports the conclusion that
1868 C_Iberia_CA_Afr, like Late Neolithic North Africans (8), has ancestry related to both
1869 Early Neolithic Europeans and earlier North Africans, supporting a North African origin
1870 for this individual.

1871 Next, we added Early and Late Neolithic North Africans (8) to the *outgroup* set and found
1872 that all the successful models included Morocco_LN as the main source of ancestry
1873 (Table S10). This confirms that C_Iberia_CA_Afr was genetically close to populations
1874 living in Morocco during the Late Neolithic, but with less ancestry related to Early
1875 Neolithic Europeans as compared to the available Morocco_LN individuals.

1876 A North African origin is further supported by uniparental markers: Y-chromosome
1877 E1b1b1a and mtDNA haplogroup M1a1b1 (tables S1 and S4). Both E1b1b1a, and the
1878 higher ranking clade M1a occur most frequently in present-day North and East Africans
1879 (187, 188). Also, haplogroups M1 (albeit M1b) and E1b1b1 have been found in Late
1880 Pleistocene and Early Neolithic North Africans (8, 15) but are completely absent or very
1881 rare in Neolithic and Copper Age Iberians.

1882 ***Bronze and Iron Ages***

1883
1884 We started by modeling the earliest individuals with steppe ancestry in Iberia
1885 (Iberia_CA_Stp), dated to ~2500-2000 BCE. We used an *outgroup* set that included
1886 Neolithic and Copper Age populations from Europe that could be a source for the non-
1887 steppe-related ancestry in Iberia_CA_Stp, as well as European groups that could be a
1888 proximate source for the population that introduced steppe ancestry into Iberia.

1889 *Outgroup set:* Mota, Ust_Ishim, Kostenki14, GoyetQ116-1, Vestonice16, MA1, El
1890 Mirón, EHG, Iran_N, Israel_Natufian, Morocco_Iberomaurusian, Anatolia_N,
1891 Steppe_EBA, Iberia_EN, LBK_EN, England_Beaker, Germany_Beaker,
1892 Netherlands_Beaker, France_Beaker, Iberia_CA, Globular_Amphora_Poland

1893
1894 Only one 2-way model fits the ancestry in Iberia_CA_Stp with P-value>0.05:
1895 Germany_Beaker + Iberia_CA (Table S11). Finding a Bell Beaker-related group as a
1896 plausible source for the introduction of steppe ancestry into Iberia is consistent with the
1897 fact that some of the individuals in the Iberia_CA_Stp group were excavated in Bell
1898 Beaker associated contexts (9). Models with Iberia_CA and other Bell Beaker groups
1899 such as France_Beaker (P-value=7.31E-06), Netherlands_Beaker (P-value=1.03E-03)
1900 and England_Beaker (P-value=4.86E-02) failed, probably because they have slightly
1901 higher proportions of steppe ancestry than the true source population. We can also discard
1902 Beaker complex individuals from the island of Britain as a plausible directly source for
1903 the steppe ancestry in Iberia because all the analyzed males with enough resolution in this
1904 group are derived for R1b-L21, a SNP for which Iberian males are ancestral.

1905 For Iberia_BA, we added Iberia_CA_Stp to the *outgroup* set as a possible source. The
1906 same Germany_Beaker + Iberia_CA model shows a good fit, but with less ancestry

1907 attributed to Germany_Beaker (Table S11). Another working model is
1908 Iberia_CA+Iberia_CA_Stp, suggesting that Iberia_BA is a mixture between the local
1909 Iberia_CA population and the earliest individuals with steppe ancestry in Iberia.

1910 To model Iron Age Iberian groups, we added three preceding populations:
1911 England_MBA, Unetice_EBA and Iberia_BA (including NE_Iberia_BA, N_Iberia_BA
1912 and C_Iberia_BA when modeling E_Iberia_IA and N_Iberia_IA, and SW_Iberia_BA and
1913 SE_Iberia_BA when modeling SW_Iberia_IA) as possible sources in the population set.
1914 The three Iron Age groups, E_Iberia_IA from a non-Indo-European-speaking area,
1915 SW_Iberia from a Tartessian cultural context and N_Iberia_IA from an Indo-European-
1916 speaking area, show a poor fit (P-values of 1.72E-04, 3.46E-02 and 4.37E-15,
1917 respectively) when modeled with Iberia_BA as the only source, indicating some degree
1918 of genetic discontinuity between the Bronze Age and the Iron Age in the three areas.
1919 Several models successfully fit (Table S11), most featuring either Iberia_CA or
1920 Iberia_BA and populations from outside Iberia with high levels of steppe ancestry.
1921 Interestingly, N_Iberia_IA is always modeled with a higher contribution from
1922 populations outside Iberia than E_Iberia_IA or SW_Iberia_IA (Fig. S6).

1923 For all the populations in this section with good coverage (Iberia_CA_Stp, Iberia_BA,
1924 E_Iberia IA, N_Iberia_IA), the model Iberia_CA + Steppe_EBA shows a poor fit (P-
1925 value<2.24E-02). This is not surprising because in this model all the European Neolithic-
1926 related ancestry in those populations is attributed to Iberia_CA, when in fact a portion of
1927 it must be derived from incoming populations that were not entirely Steppe_EBA in
1928 ancestry. However, using a fixed set of outgroups less sensitive to the differences between
1929 Neolithic European populations we can try to estimate the proportion of Steppe_EBA-
1930 related ancestry in our populations of interest. Table S12 and Fig. S6 show these estimates
1931 using the following set of *outgroups*: Mota, Ust_Ishim, Kostenki14, GoyetQ116-1,
1932 Vestonice16, MA1, EHG, Iran_N, Israel_Natufian, Anatolia_N, LBK_EN.

1933 To study possible genetic differences between Bronze Age groups from different
1934 geographic areas, we repeated the *qpAdm* model in Table S12 stratifying by geographic
1935 region (Table S13). We found that Bronze Age groups in the south had less steppe
1936 ancestry (~15%) than groups in central and northern Iberia (~20%).

1937 ***Sex bias in Bronze Age Iberia***

1938
1939 Based on the observation of the complete replacement of Neolithic/Copper Age Y-
1940 chromosome haplogroups by haplogroup R1b-M269 during the Bronze Age, we tried to

1941 study sex-biased admixture in the formation of the Iberian Bronze Age population. Given
1942 that males carry one X-chromosome and two copies of each of the autosomes, if the
1943 incoming population that admixed with the local Iberia_CA population was heavily male-
1944 biased, the Iberian Bronze Age population is expected to have lower ancestry proportions
1945 from the incoming population on the X-chromosome than on the autosomes. Thus, we
1946 computed ancestry proportions with *qpAdm* on the autosomes and on the X-chromosome
1947 using Iberia_CA as a local source of ancestry and Germany_Becker as a non-local source.
1948 This Germany_Becker group was very likely not genetically identical to the actual group
1949 that arrived in Iberia between 2500-2000 BCE, but due to the lack of data from closer
1950 regions such as southern France, we think that it is a useful proxy both chronologically
1951 and genetically. We used the conservative fixed set of *outgroups* with the addition of
1952 Steppe_EBA: Mota, Ust_Ishim, Kostenki14, GoyetQ116-1, Vestonice16, MA1, EHG,
1953 Iran_N, Israel_Natufian, Anatolia_N, LBK_EN, Steppe_EBA. We computed standard
1954 errors over 10-Mb blocks. We obtained lower proportions of ancestry related to
1955 Germany_Becker on the X-chromosome than on the autosomes (Table S14), although the
1956 Z-score for the differences between the estimates is 2.64, likely due to the large standard
1957 error associated to the mixture proportions in the X-chromosome.

1958 Using the estimated admixture proportions on the X-chromosome and autosomes, we
1959 estimated the proportion of female and male ancestors in Iberia_BA that were local, i.e.
1960 from the Iberia_CA population, following the same approach as in (169). The computed
1961 log-likelihood surface (Fig. S7) points to a low proportion of male ancestors from the
1962 Iberia_CA population, which agrees with the observed Y-chromosome pattern.

1963 ***Admixture proportions for individuals in the Iberia_CA_Stp, Iberia_BA and Iberia_IA*** 1964 ***groups***

1965
1966 We computed admixture proportions (Table S15, Fig. 2B) for each individual in the
1967 Iberia_CA_Stp, Iberia_BA and Iberia_IA groups, using Iberia_CA and Germany_Becker
1968 as sources and the same fixed *outgroup* set as in the previous section: Mota, Ust_Ishim,
1969 Kostenki14, GoyetQ116-1, Vestonice16, MA1, EHG, Iran_N, Israel_Natufian,
1970 Anatolia_N, LBK_EN, Steppe_EBA.

1971 ***Bronze Age outlier from Loma del Puerco***

1972
1973 In PCA analysis (Fig. 1C-D, Fig. S3), one Bronze Age individual (ID I7162) from Loma
1974 del Puerco (Chiclana de la Frontera, Cádiz), a site located in the southern tip of Spain,
1975 appears somewhat shifted from the main Bronze Age cluster. This shift cannot be

1976 attributed to statistical noise from low coverage because we recovered 366,033 genomic
1977 positions. Therefore, we tried to understand the underlying cause of this shift with *qpAdm*
1978 using the following *outgroup* set.

1979 *Outgroup* set: Mota, Ust_Ishim, Kostenki14, GoyetQ116-1, Vestonice16, MA1, El
1980 Mirón, EHG, Iran_N, Israel_Natufian, Morocco_Iberomaurusian, Anatolia_N,
1981 Steppe_EBA, Iberia_EN, LBK_EN, Germany_Becker, Iberia_CA,
1982 Globular_Amphora_Poland, Iberia_BA, C_Iberia_CA_Afr, Morocco_LN

1983

1984 Given that Loma del Puerco lies only 70 kilometers north of the North African coast, we
1985 included in the *outgroup* set the outlier individual from Camino de las Yeseras with a
1986 North African origin (C_Iberia_CA_Afr) and Morocco_LN to account for the possibility
1987 of recent North African ancestry in I7162 as the reason for the shift observed in the PCA.

1988 None of the 1-way models show a good fit, including Iberia_BA (P-value=6.93E-08),
1989 confirming that this individual does not form a clade with the rest of the Bronze Age
1990 samples from Iberia. We found five 2-way models with a good fit (Table S16), all of the
1991 them featuring Iberia_BA and either an African individual/population or the Natufians.
1992 Similar models including Iberia_CA instead of Iberia_BA show a very poor fit,
1993 demonstrating that this individual has steppe ancestry like the rest of the Bronze Age
1994 Iberians. Taking into account archaeological context, the most plausible model is a
1995 mixture between Iberia_BA-related ancestry and ancestry related to individuals like
1996 C_Iberia_CA_Afr, who could have been present not only in central Iberia like the one we
1997 have sampled, but also in southern Iberia during the second half of the 3rd millennium
1998 BCE and the first half of 2nd millennium BCE.

1999 ***The past 2500 years in northeast Iberia***

2000

2001 Many of our individuals with working genome-wide data from northeast Iberia and dated
2002 to the past ~2500 years were excavated from the site of Empúries, the most important
2003 Greek colony in the Iberian Peninsula and later occupied by the Romans.

2004 In PCA (Fig. 1C-D), most of the individuals from Empúries form two clusters: one (which
2005 we call Empúries1) plotting close to the Iron Age Iberia cluster that includes samples
2006 from the nearby site of Ullastret and the other (which we call Empúries2) plotting close
2007 to Bronze Age samples from the eastern Mediterranean such as the Mycenaean samples
2008 from Greece (I67). The presence of two genetically distinct populations is further
2009 supported by different patterns of F_{ST} estimated with present-day populations (Fig. S8)
2010 and by Y-chromosome haplogroup composition (Table S4). Empúries2 was least
2011 differentiated from populations from the central and eastern Mediterranean region and

2012 was dominated by Y-chromosome haplogroup J, present in high frequencies precisely in
2013 those regions, whereas Empúries1 was least differentiated from western European
2014 populations and contained only R1b lineages, similar to the Bronze and Iron Age
2015 populations from Iberia. We find the two clusters in the three periods of the site for which
2016 we have genetic data: the Greek, Hellenistic and Roman periods. This demonstrates that
2017 the ancient town of Empúries was inhabited by local Iberians as well as by colonists from
2018 the Eastern Mediterranean, which agrees with historical sources and archaeological
2019 evidence.

2020 We confirm the eastern Mediterranean origin of the second cluster of individuals
2021 (Empuries2) using *qpAdm* and the following *outgroup* set:

2022 *Outgroup* set: Mota, Ust_Ishim, Kostenki14, GoyetQ116-1, Vestonice16, MA1, El
2023 Mirón, EHG, Iran_N, Israel_Natufian, Morocco_Iberomaurusian, Anatolia_N,
2024 Steppe_EBA, Iberia_EN, LBK_EN, Iberia_CA, Globular_Amphora_Poland, Iberia_BA,
2025 Iberia_IA, Mycenaean, Minoan_Lasithi

2026
2027 Using this setup, all the 1-way models failed (P-value<3.69E-14) except for the
2028 Mycenaean (P-value==8.81E-01), indicating that Empuries2 and the Mycenaean
2029 samples form a clade with respect to the rest of the groups in the populations set to the
2030 limits of our resolution. This result is perhaps not surprising given that the available
2031 Mycenaean samples from southern Greece lived only ~700 years before the founding of
2032 Empúries by Greeks from Phocaea ~575 BCE, according to historical sources.

2033 Next, we wished to study whether the different peoples that established themselves in
2034 northeast Iberia over the past ~2500 years and dominated parts or the whole territory had
2035 a significant impact on the overall Iberian gene pool. We analyzed individuals from
2036 L'Esquerda (Roda de Ter, Barcelona) dated to the 7th-8th century CE and individuals
2037 from Pla de l'Horta (Sarrià de Ter, Girona) dated to the 6th century CE, both from the
2038 period of Visigoth domination and postdating the Greek and Roman presence in Iberia.
2039 We began with the individuals from L'Esquerda (NE_Iberia_c.6-8CE_ES) and used the
2040 following *outgroup* set for our admixture modeling.

2041 *Outgroup* set: Mota, Ust_Ishim, Kostenki14, GoyetQ116-1, Vestonice16, MA1, El
2042 Mirón, EHG, Iran_N, Israel_Natufian, Morocco_Iberomaurusian, Anatolia_N,
2043 Steppe_EBA, Iberia_EN, LBK_EN, Iberia_CA, Globular_Amphora_Poland, Iberia_BA,
2044 Iberia_IA, Empuries2, England_Saxon.SG, Bavaria_Early_Medieval.SG, TSI, Greek,
2045 Bergamo

2046
2047 To increase resolution, we added to the Iberia_IA group the samples from Empúries that
2048 cluster within the Iberia_IA cluster. The other group of samples from Empúries with

2049 Eastern Mediterranean origin (Empuries2) was included in the *outgroup* set because they
2050 could have contributed ancestry to later populations in northeast Iberia. Due to the lack
2051 of published aDNA data from the first millennium CE, we included present-day European
2052 populations such as TSI (Tuscans from the 1000 Genomes project), Greek and Bergamo
2053 that could serve as a proxy for the ancestry in our samples of interest. Modeling
2054 NE_Iberia_c.6-8CE_ES as 1-way mixture with any of the populations from the set fails,
2055 including Iberia_IA (P-value=3.01E-07). This demonstrates that the individuals from
2056 L'Esquerda do not form a clade with Iberia_IA, and therefore additional layers of ancestry
2057 are needed to explain their genetic makeup. In Table S17 we show all 2-way models that
2058 include Iberia_IA as one of the sources. The only models with good fit are those featuring
2059 present-day populations from Italy and Greece. This suggests that NE_Iberia_c.6-
2060 8CE_ES has ancestry related to populations from the central and eastern Mediterranean
2061 that is not present in Iberia_IA. The eastern outliers from Empúries showed a poor fit (P-
2062 value= 4.48E-04), suggesting that they were likely not the source of the central/eastern
2063 Mediterranean ancestry in NE_Iberia_c.6-8CE_ES.

2064 Next, we wanted to study the individuals from Pla de l'Horta (NE_Iberia_c.6CE_PL),
2065 adding NE_Iberia_c.6-8CE_ES to the population set as a possible source of ancestry. In
2066 fact, all the successful models include NE_Iberia_c.6-8CE_ES as one of the sources
2067 (Table S18), confirming that both sites have similar ancestry makeup although they do
2068 not form a clade with respect to the other populations in the population set (P-value=
2069 1.29E-03). The best 2-way models feature NE_Iberia_c.6-8CE_ES and either
2070 Steppe_EBA, Bavaria_Early_Medieval or Saxon, indicating that the individuals from Pla
2071 de l'Horta had higher steppe ancestry than the individuals from L'Esquerda, probably
2072 mediated by contemporaneous populations from central/northern Europe where this type
2073 of ancestry was present in higher proportions than in Iberia.

2074 Finally, to explore the genetic impact of the Muslim conquest in northeast Iberia, we
2075 studied individuals from Sant Julià de Ramis (Girona), dated between the 8th and 12th
2076 centuries CE (NE_Iberia_c.8-12CE) and therefore largely postdating Muslim political
2077 control of the area. We added to the *outgroup* set the preceding population from the area
2078 (NE_Iberia_c.6-8CE_ES) and, to account for a possible genetic contribution of the
2079 Muslim conquest, a North African ancient group (Morocco_LN) and the individuals from
2080 southeast Iberia during the period of Muslim rule (SE_Iberia_c.10-16CE):

2081 Mota, Ust_Ishim, Kostenki14, GoyetQ116-1, Vestonice16, MA1, El Mirón, EHG,
2082 Iran_N, Israel_Natufian, Morocco_Iberomaurusian, Anatolia_N, Steppe_EBA,

2083 Iberia_EN, LBK_EN, Iberia_CA, Globular_Amphora_Poland, Iberia_BA, Iberia_IA,
2084 Empuries2, NE_Iberia_c.6-8CE_ES, SE_Iberia_c.10-16CE, Morocco_LN
2085
2086 No 1-way model fits the data, including the one featuring NE_Iberia_c.6-8CE_ES (P-
2087 value=7.58E-04). Three 2-way models fit, with two being (Table S19) historically more
2088 plausible: NE_Iberia_c.6-8CE_ES + SE_Iberia_c.10-16CE and NE_Iberia_c.6-8CE_ES
2089 + Morocco_LN. This suggests that the individuals from Sant Julià de Ramis harbored
2090 North African-related ancestry not present in the populations from the same area before
2091 the Muslim conquest.

2092 ***The past 2000 years in southeast Iberia***

2093
2094 We recovered aDNA data from individuals excavated at 13 sites in the present-day
2095 provinces of Granada, València/Valencia and Castelló/Castellón, and dated between the
2096 3rd and 16th centuries CE, covering the periods of Roman, Visigothic, Byzantine and
2097 Islamic domination in southeast Iberia.

2098 We grouped the individuals under three population names: SE_Iberia_c.3-4CE,
2099 SE_Iberia_c.5-8CE and SE_Iberia_c.10-16CE. All the individuals that we analyzed are
2100 clearly shifted towards present-day and ancient North Africans in PCA (Fig. S3-4), which
2101 suggests that North African genetic input was already present in this region several
2102 centuries before the Islamic conquest of the Iberian Peninsula beginning in the 8th century
2103 CE. Two individuals from SE_Iberia_c.10-16CE plot on a very different position (Fig.
2104 S3-4) and thus were not included in the three groups. For *qpAdm* analysis, we began by
2105 using the following *outgroup* set:

2106 *Outgroup* set: Mota, Ust_Ishim, Kostenki14, GoyetQ116-1, Vestonice16, MA1, El
2107 Mirón, EHG, Iran_N, Israel_Natufian, Morocco_Iberomaurusian, Anatolia_N,
2108 Steppe_EBA, Iberia_EN, LBK_EN, Iberia_CA, Globular_Amphora_Poland, Iberia_BA,
2109 Iberia_IA/NE_Iberia_c.6-8CE_ES, Guanche, Morocco_LN, Levant_EBA

2110
2111 This set includes Upper Paleolithic North Africans (Morocco_Iberomaurusian),
2112 Late_Neolithic North Africans (Morocco_LN) and indigenous Canary Islanders
2113 (Guanche), all of which could serve as a proxy for North African populations before the
2114 Arab expansion, and Levant_EBA to account for Levantine-related ancestry. We also use
2115 either Iron Age Iberia (Iberia_IA) or early Medieval Iberian individuals from the
2116 northeast (NE_Iberia_c.6-8CE_ES) to act as a proxy for Iberia-related ancestry. For the
2117 three groups, the best 2-way models include NE_Iberia_c.6-8CE and the Guanche or
2118 Morocco_LN (Table S20). However, with the exception of SE_Iberia c.3-4 CE, these
2119 models show a poor fit to the data, meaning that they do not successfully explain the

2120 ancestry in these groups. Using present-day North Africans such as Mozabite or Saharawi
2121 instead of the ancients does not improve the fit. Instead, the models slightly improve when
2122 Levant_EBA is used as a third source, although they do not achieve a P-value >0.05 for
2123 SE_Iberia_c.5-8CE (Table S20).

2124 The lack of models with a good fit to the data might be a consequence of the limited
2125 number of available proximate sources of ancestry in key regions. For instance, in North
2126 Africa the only ancient populations with available data are Morocco_Iberomaurusian,
2127 Morocco_EN, Morocco_LN and the Guanches, and we use Morocco_LN and the
2128 Guanches as proxies for North African populations before the Arab expansion. However,
2129 they might not be good representatives of the true North African population that
2130 contributed ancestry to our Iberian test populations. Similarly, the local Iberian ancestry
2131 component in our test populations could have some genetic differences to the populations
2132 that we are using as sources for this component. Another potential issue is the presence
2133 of genetic heterogeneity within the populations we are trying to model. In PCA (Fig. S3-
2134 4), all the individuals in SE_Iberia_c.3-4CE, SE_Iberia_c.5-8CE and SE_Iberia_c.10-
2135 16CE plot in an intermediate position between present-day populations from Europe, the
2136 Levant and North Africa, but they do not form a tight cluster, which could represent
2137 significant ancestry differences. Thus, we analyzed each individual separately, with the
2138 caveat that for low-coverage individuals we had less power to reject poorly-fitting models
2139 and to estimate admixture proportions. We used a fixed set of *outgroups*: Mota,
2140 Ust_Ishim, Kostenki14, GoyetQ116-1, Vestonice16, MA1, El Mirón, EHG, Iran_N,
2141 Israel_Natufian, Morocco_Iberomaurusian, Anatolia_N, Steppe_EBA, Iberia_EN,
2142 LBK_EN, Iberia_CA, Globular_Amphora_Poland, Iberia_BA; and tested models
2143 including either Iberia_IA or NE_Iberia_c.6-8CE_ES as a local Iberian ancestry source,
2144 the Guanches or Morocco_LN as a North African ancestry source and one of the
2145 following Levantine populations as proxies for the extra ancestry not modeled by the
2146 Iberian and North African populations: present-day Palestinian, present-day Druze,
2147 present-day Jordanian and Levant_EBA. In Table S21 we provide the best-fitting model
2148 for each individual. An interesting observation is the fact that many individuals require
2149 ancestry from Levantine populations on top of the Iberian and North African-related
2150 ancestry for the model to fit. This could represent eastern Mediterranean ancestry input
2151 into the region, either independently or through North African populations with more
2152 Levantine-related ancestry than the one we used as a North African ancestry source.

2153 As previously mentioned, two individuals dated to the 10th (I7427) and 16th (I3810)
2154 century CE plot on a very different position in the PCA (Fig. S3-4), reflecting a very
2155 different ancestry profile. We were able to model them as mixture of ancestry related to
2156 previous populations from the same region (SE_Iberia c.3-4CE) and ancestry related to
2157 present-day sub-Saharan African populations (Table S22). The high proportions of sub-
2158 Saharan African ancestry explain their marked shift in PCA and agree with uniparental
2159 markers with sub-Saharan African origin in both individuals.

2160 **SI 12 - Allele frequency estimation of SNPs of phenotypic** 2161 **importance**

2162 Our dense genetic time transect allowed us to follow the trajectory of genetic variants
2163 with phenotypic importance over time. Due to the presence of missing data in ancient
2164 individuals, chances are high that a particular SNP will not be covered by any DNA
2165 sequence in several individuals. Therefore, we group our Iberian individuals in 5 broad
2166 time periods to increase the accuracy of the allele frequency estimation. The groups are
2167 Mesolithic, Neolithic, Copper Age, Bronze-Iron Age and Historical (which includes
2168 individuals from 500 BCE to 1600 CE). We used allele counts at each SNP to perform
2169 maximum likelihood estimations of allele frequencies in ancient populations as in ref. (2),
2170 and computed confidence intervals using the Agresti-Coull method implemented in the
2171 `binom.confint` function of the R-package *binom*.

2172 In Fig. S9, we show derived allele frequency estimates for four SNPs with functional
2173 importance: SNP rs4988235 in *LCT* responsible for lactase persistence, SNP rs12913832
2174 in *HERC2/OCA2* responsible for blue eyes, and SNPs rs16891982 and rs1426654 in
2175 *SLC45A2* and *SLC24A5*, respectively, associated with reduced skin pigmentation in
2176 Europeans. A striking observation is the complete absence of the lactase persistence allele
2177 in Iberia (present at 0.46 frequency in present-day Iberians) until recent historical times,
2178 which suggests very recent selection.

2179 We wished to examine whether the obtained allele frequencies could be affected by
2180 reference bias (i.e., the preferential recovery of the allele present in the reference genome
2181 over the alternative allele). To estimate this possible bias, we identified ancient
2182 individuals with 1240k data from previous studies that presented at least one read with
2183 the reference allele and one read with the derived allele at the SNP of interest, which
2184 indicates that they were very likely heterozygous at that position. Then, we counted the
2185 number of reads with the reference and alternative allele in those individuals and

2186 computed a reference bias estimate. In the case of rs4988235 it was not possible to
2187 estimate reference bias due to the limited number of heterozygous individuals. For
2188 rs12913832 (152 reference reads, 145 alternative reads; 0.5118) and rs16891982 (946
2189 reference reads, 947 alternative reads; 0.4997) we found no evidence of reference bias.
2190 In contrast, for rs4988235 (102 reference reads, 45 alternative reads; 0.6939) we found
2191 evidence of reference bias as ~70% of the reads in heterozygous individuals carried the
2192 reference allele. Thus, we applied a correction for this bias in the maximum likelihood
2193 estimation of rs4988235, shown in Fig. S9.

2194 **SI 13 - Date of the Carigüela pre-Neolithic individual**

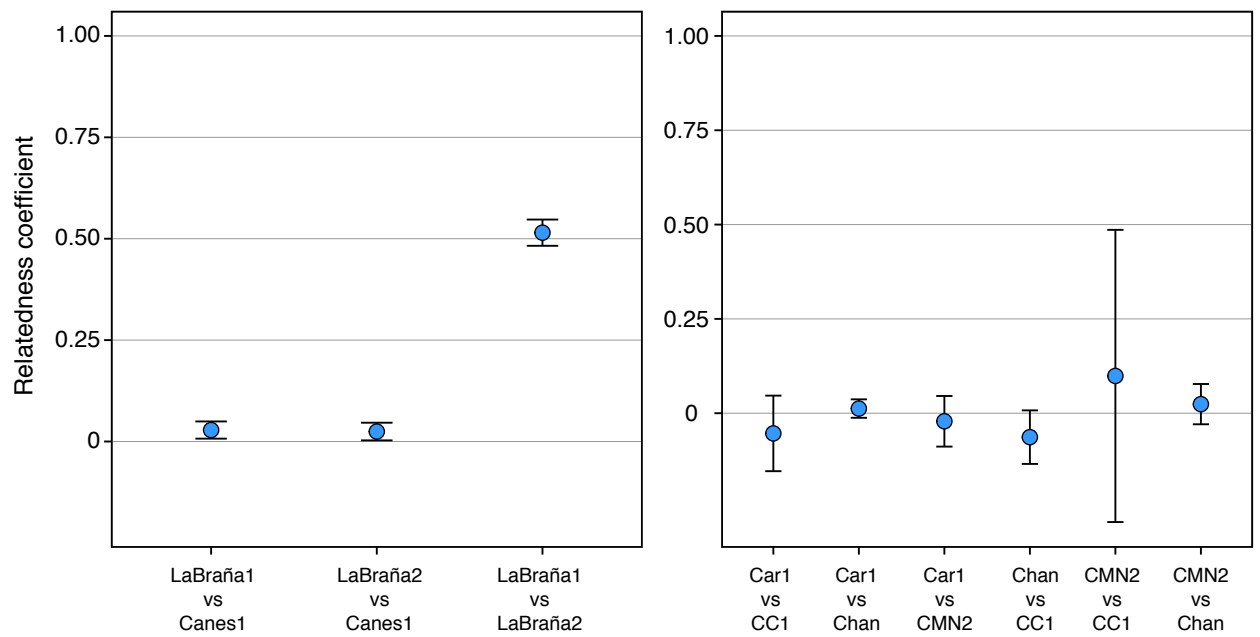
2195 We successfully obtained sequencing data from the Car1 individual from the Carigüela
2196 cave in Piñar, Granada Province. The archaeological excavation strongly points to a pre-
2197 Neolithic context, but several attempts to generate a radiocarbon date have not been
2198 successful. Therefore, we tried to narrow down the age of this individual using the genetic
2199 data.

2200 In PCA, the Car1 individual plots close to the other Iberian Mesolithic individuals (Fig.
2201 1C), confirming that his genome-wide ancestry signal is the one expected for an
2202 individual who lived before the arrival of Neolithic farmers.

2203 It has been previously shown (4) that Neanderthal ancestry has steadily decreased during
2204 the last 45,000 years. Thus, we computed the % of Neanderthal introgression for the
2205 ancient European individuals analyzed in Fu et al. 2016 (4) with at least 200,000 SNPs
2206 and for the Car1 individual, using f_4 -statistics as in Fu et al. 2016 (4). We obtained 2.22%
2207 of Neanderthal ancestry for Car1 (Fig. S10), similar to other European individuals that
2208 lived around 8000 BCE.

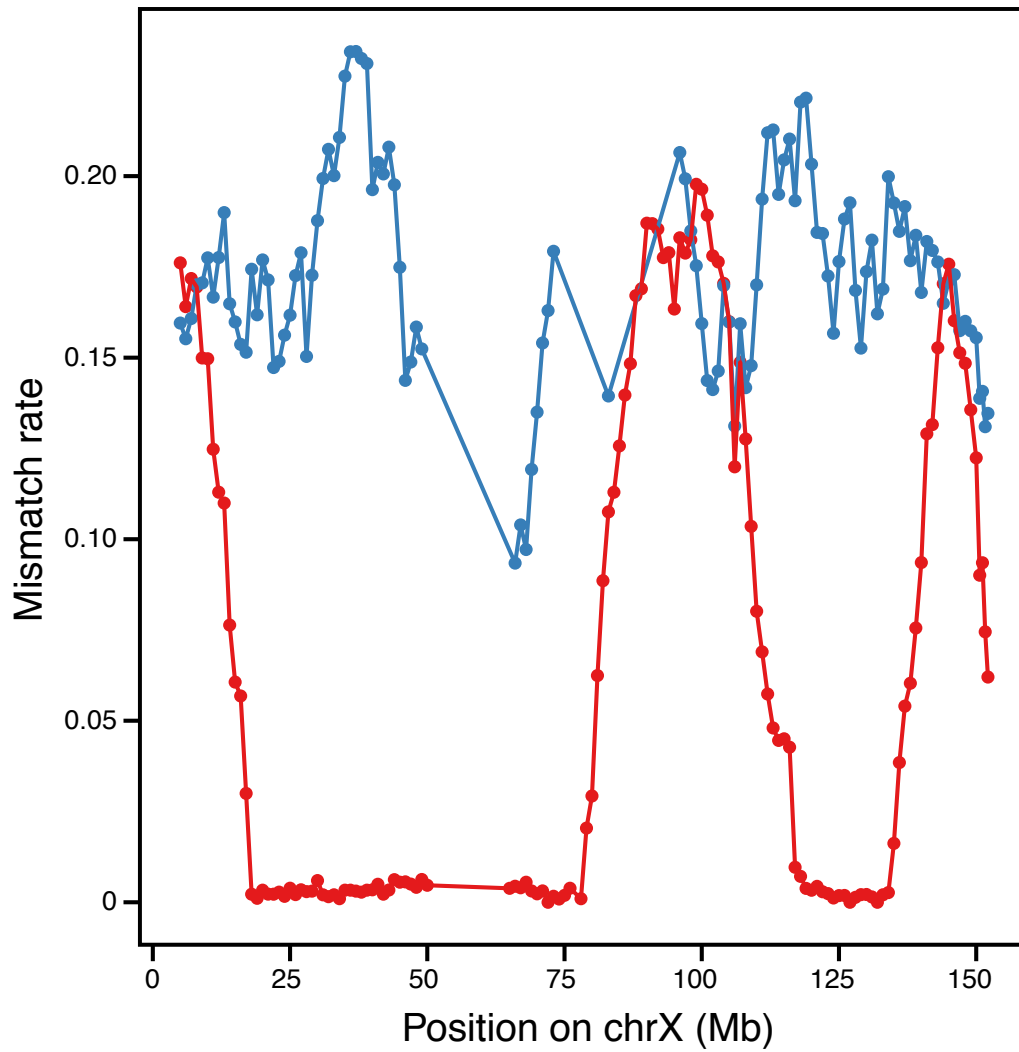
2209 Lastly, we looked at the mitochondrial genome of Car1. He belonged to haplogroup
2210 U5b1, also present in one Iberian Mesolithic sample from Cingle del Mas Nou
2211 (Castelló/Castellón, Spain). The appearance of the U5b1 lineage has been dated to
2212 15530 ± 4890 years ago (148) using data from present-day individuals. In the ancient DNA
2213 literature, the oldest known U5b1 individuals to date are from Late Glacial Oberkassel
2214 (Germany, 12220–11920 and 11620–11340 BCE) (151, 189) and Bichon (Switzerland,
2215 11820–11610 BCE) (164), becoming prevalent in Europe during the Mesolithic (4).

2216 Based on these lines of evidence, we conclude that the Car1 individual likely lived during
2217 the Mesolithic period, 9700–5500 BCE. We caution, however, that a direct radiocarbon
2218 date would provide the most accurate estimation of the age of this individual.



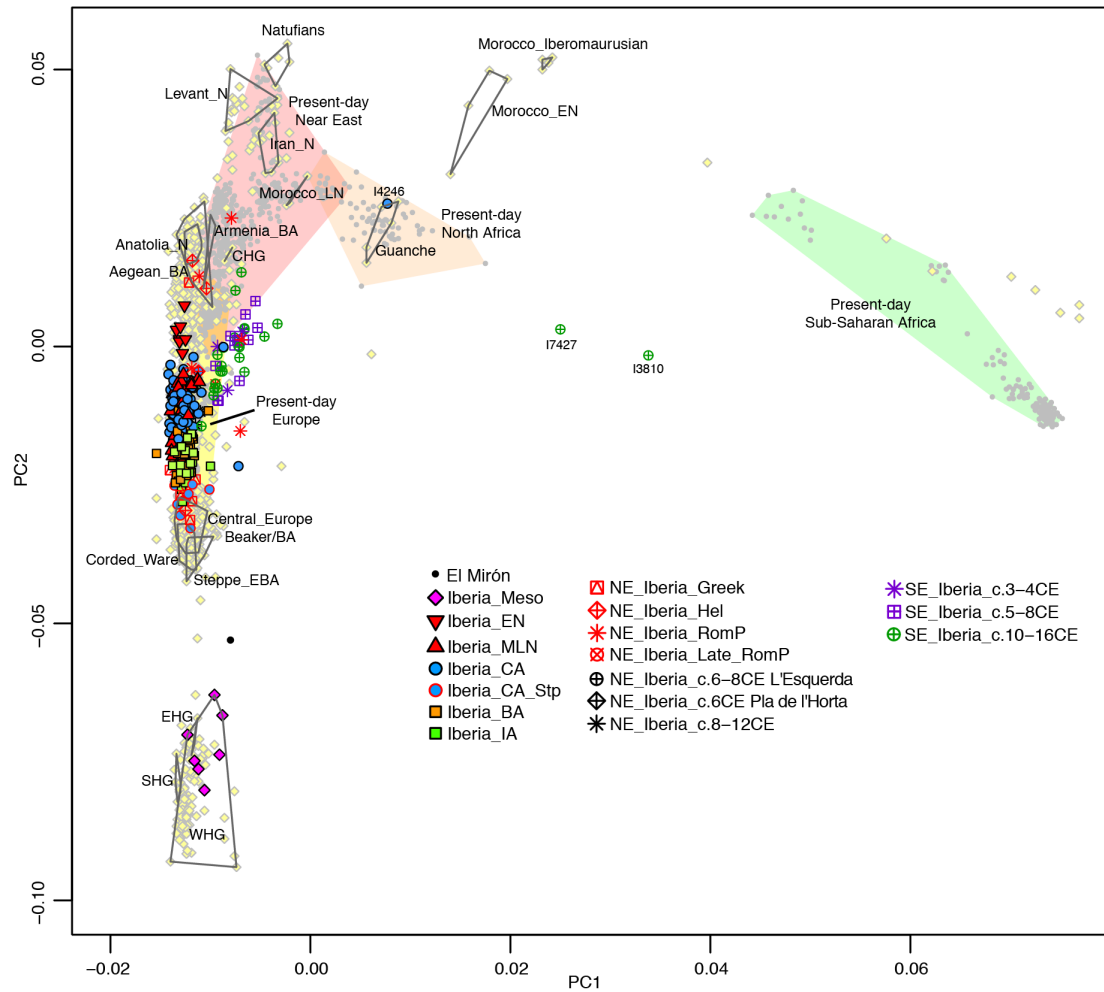
2221
 2222
 2223
 2224
 2225

Fig. S1. Genetic relatedness among Mesolithic individuals. Relatedness coefficients estimated on the autosomes for pairs of Iberian Mesolithic individuals. Error bars correspond to 95% confidence intervals.



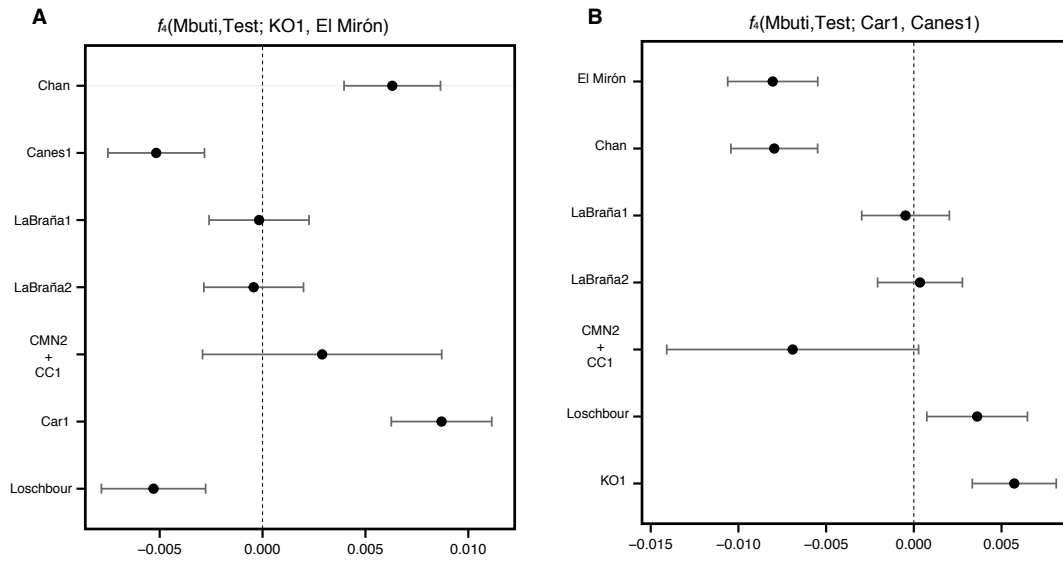
2226

2227 **Fig. S2.** Mismatch rate at 1240k sites between LaBraña1 and LaBraña2 males (red) and
 2228 between two unrelated Iberian hunter-gatherers (blue) along the X chromosome. Analysis
 2229 was performed on sliding windows of 10 Mb, moving by 1 Mb each step.
 2230



2240
 2241
 2242
 2243
 2244
 2245
 2246
 2247
 2248

Fig. S4. Principal component analysis of 1,195 present-day west Eurasian, North African and Sub-Saharan African individuals (grey dots), with ancient individuals from Iberia and other regions (pale yellow) projected onto the first two principal components. WHG, western hunter-gatherers; EHG, eastern hunter-gatherers; SHG, Scandinavian hunter-gatherers; CHG, Caucasus hunter-gatherers; E, Early; M, Middle; L, Late; N, Neolithic; CA, Copper Age; BA, Bronze Age; IA, Iron Age; Meso, Mesolithic; Hel, Hellenistic; RomP, Roman Period; NE, Northeast; SE, Southeast.



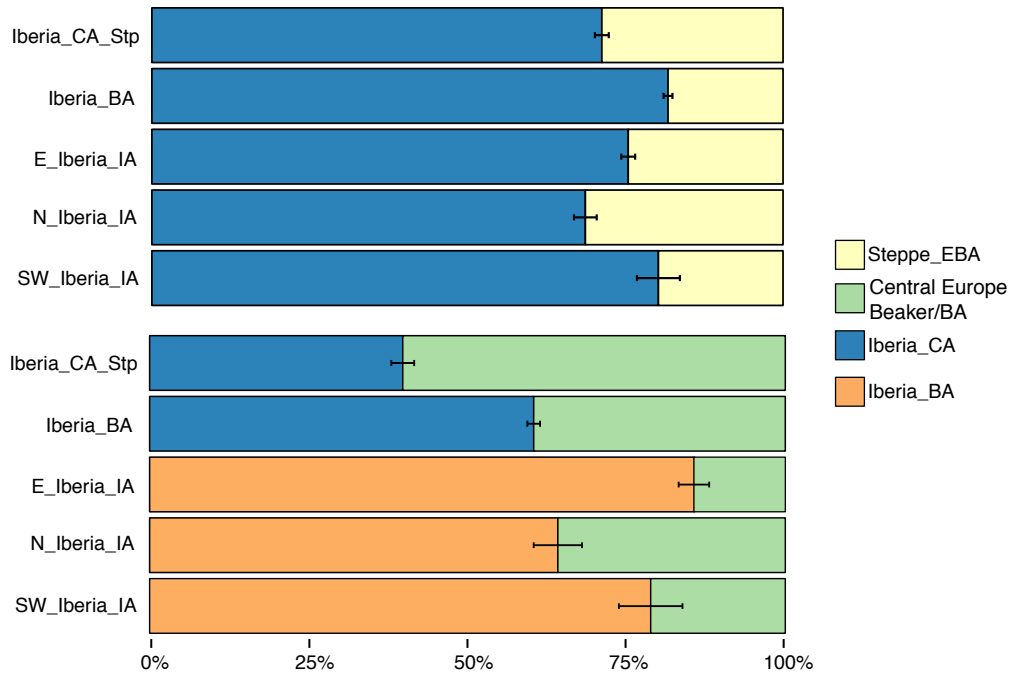
2249

2250

2251

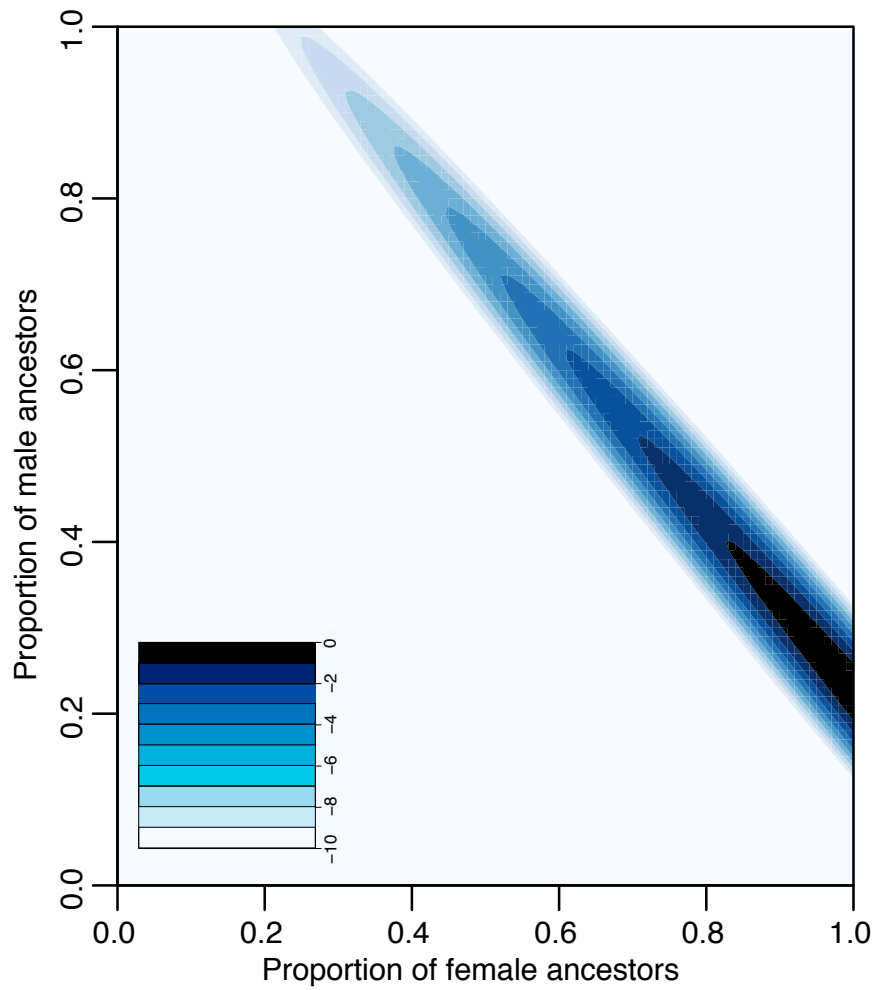
2252

Fig. S5. f_4 -statistics of the form (A) $f_4(\text{Mbuti, Test; KO1, El Mirón})$ and (B) $f_4(\text{Mbuti, Test; Car1, Canes1})$. Bars indicate ± 3 standard errors.



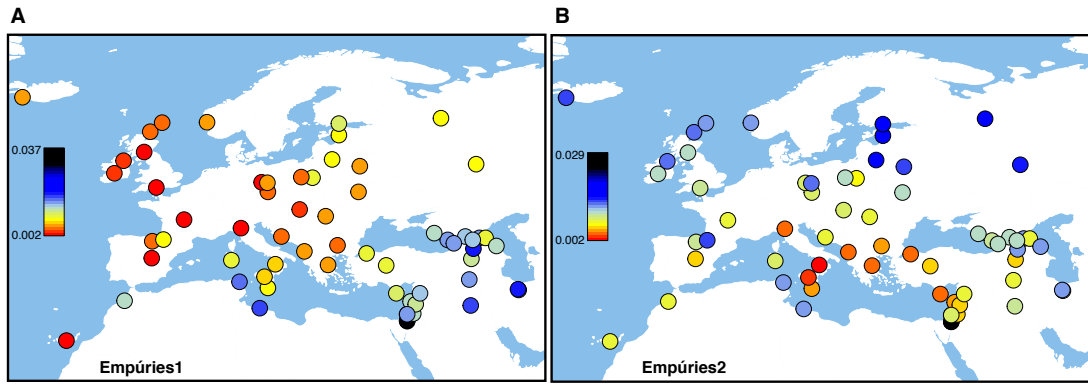
2253
 2254
 2255
 2256
 2257
 2258

Fig. S6. Genome-wide admixture proportions using *qpAdm*. The top panel shows the model Iberia_CA+Steppe_EBA and the bottom panel shows more proximate admixture models for the same five populations. Error bars indicate ± 1 standard errors. CA, Copper Age; EBA, Early Bronze Age; BA, Bronze Age; IA, Iron Age; SW_Iberia, southwest Iberia; N_Iberia, northern Iberia; E_Iberia, eastern Iberia.



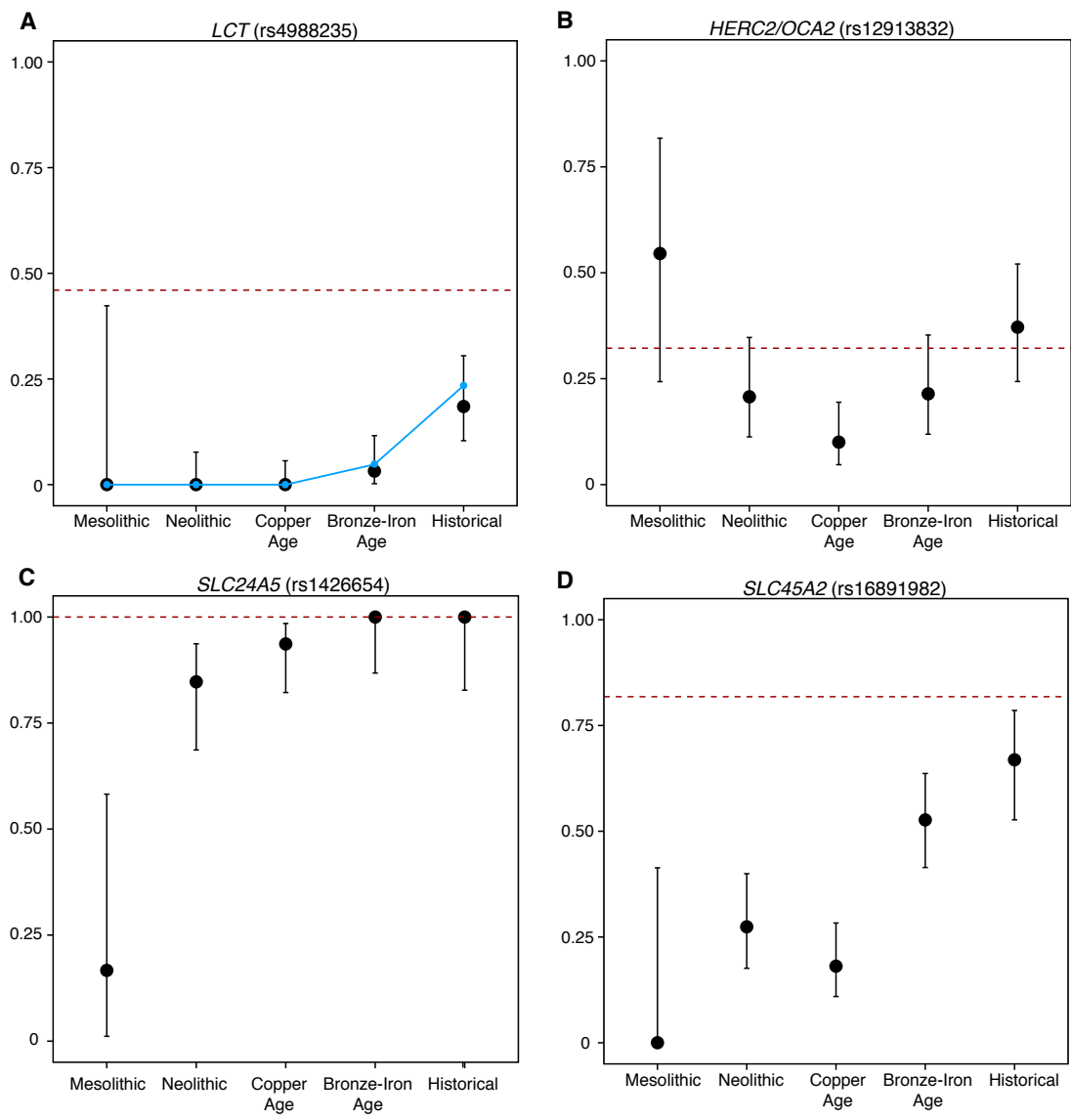
2259
 2260
 2261
 2262
 2263
 2264

Fig. S7. Sex bias in Bronze Age Iberia. Log-likelihood surface for the proportion of female (x axis) and male (y axis) ancestors from the Iberia_CA population. The log-likelihood scale ranges from 0 to -10, in which 0 is the feasible point with the highest likelihood.



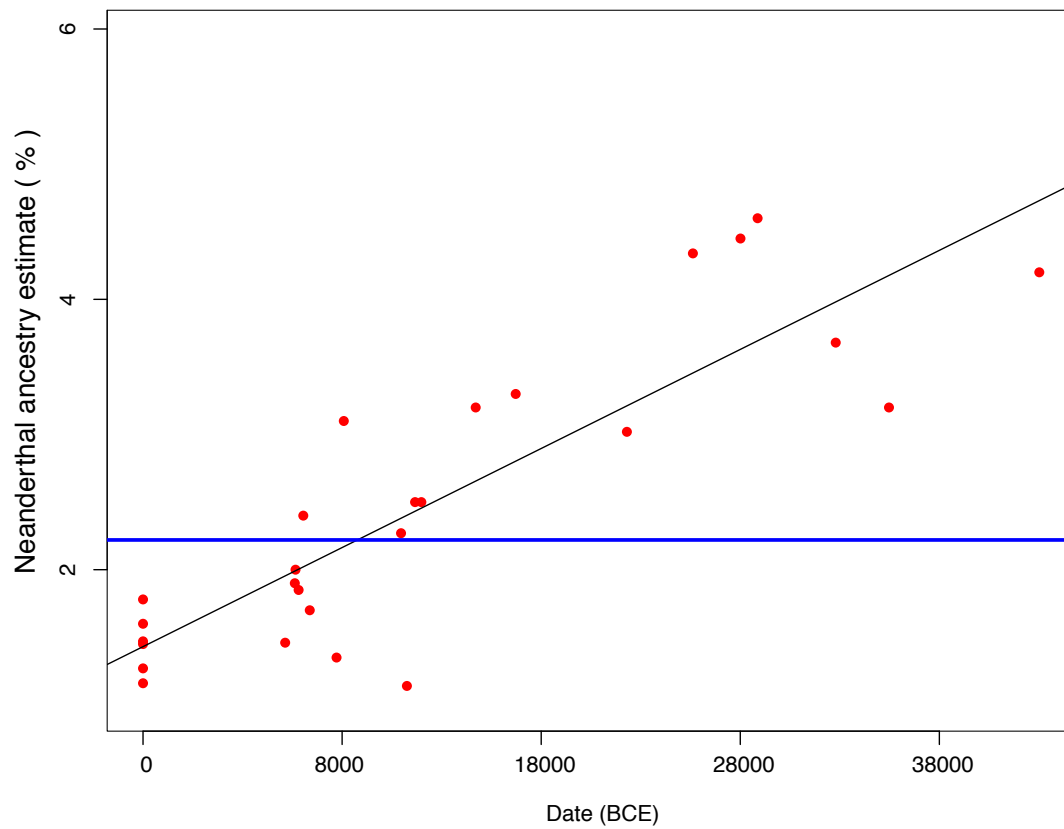
2265
 2266
 2267
 2268

Fig. S8. Genetic differentiation measured by F_{ST} between present-day West Eurasians and (A) Empúries1 or (B) Empúries2 groups.



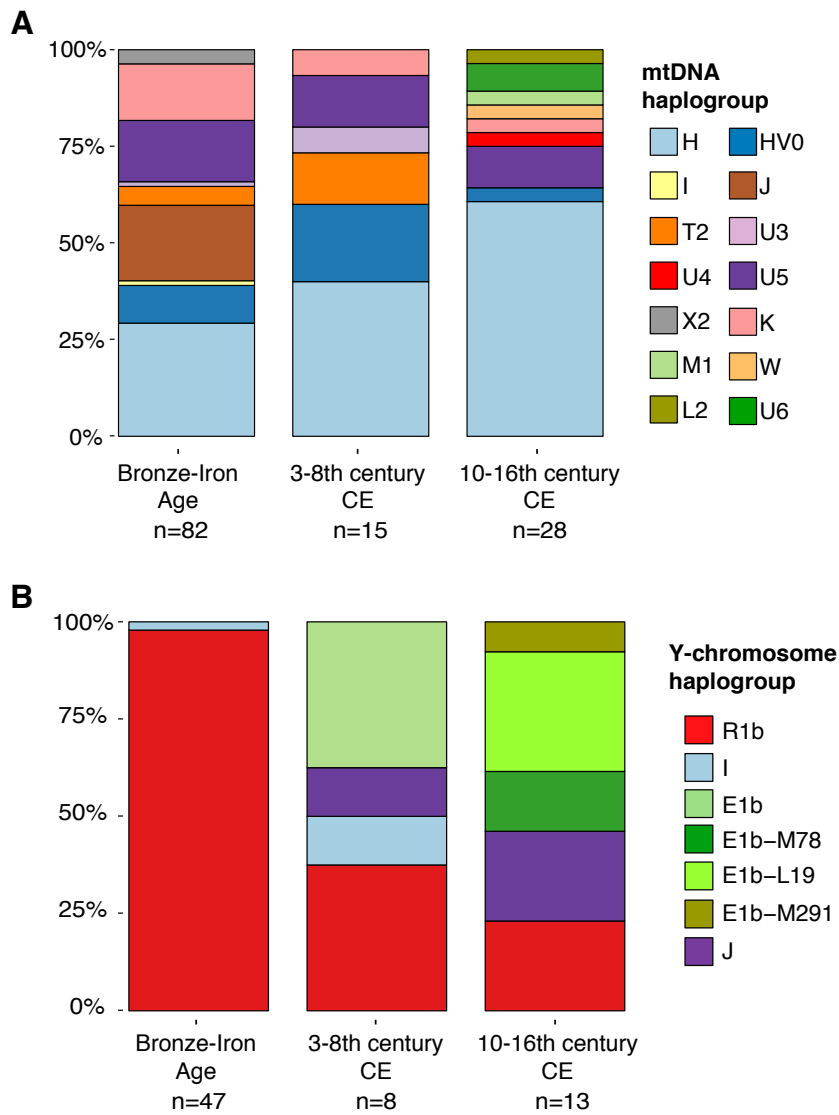
2269

2270 **Fig. S9. Derived allele frequencies at four SNPs of functional importance.** Error bars
 2271 represent 95% confidence intervals. The red dashed lines show allele frequencies in the
 2272 1000 Genomes Project (<http://www.internationalgenome.org/>) ‘IBS’ population (present-
 2273 day people from Spain). The blue solid line in (A) represents the derived allele
 2274 frequencies after correcting for reference bias.
 2275



2276
 2277
 2278
 2279
 2280
 2281
 2282
 2283

Fig. S10. Neanderthal ancestry for the Car1 individual from Carigüela cave in the context of other ancient and present-day Europeans. Neanderthal ancestry for 21 ancient Europeans and six present-day populations (Dai, Han, French, Karitiana, English and Sardinian). Each dot represent one individual. The black line represents the least squares fit. The blue horizontal line represents the estimated Neanderthal ancestry for the Car1 individual.



2284
2285
2286
2287

Fig. S11. (A) Mitochondrial and (B) Y chromosome haplogroup composition of individuals from southeast Iberia during the past 2000 years. The general Iberian Bronze and Iron Age population is included for comparison.

2288 **Table S1.** Ancient individuals from the Iberian Peninsula included in this study.
2289
2290 **Table S2.** New DNA libraries sequenced in this study.
2291
2292 **Table S3.** New radiocarbon dates generated in this study.
2293
2294 **Table S4.** Y-chromosome calls for the Iberian males.
2295
2296 **Table S5.** Comparison between key statistics computed using all SNPs and after
2297 removing SNPs in CpG context.

2298 **Table S6.** Mismatch rates between Iberian Mesolithic individuals.

Individual 1	Individual 2	Mismatch rate	SE	SNPs
LaBraña2	LaBraña2	0.1148088	0.00102	804276
LaBraña1	LaBraña1	0.1106495	0.00095	857356
Canes1	Canes1	0.1160385	0.00102	579144
LaBraña1	LaBraña2	0.1690504	0.00188	892225
LaBraña2	Canes1	0.2248682	0.00126	738526
LaBraña1	Canes1	0.2244443	0.00123	752748
Car1	Car1	0.1068768	0.00123	156133
CMN2	CMN2	0.0704225	0.00998	710
CC1	CC1	0.0374449	0.00944	454
Chan	Chan	0.1070321	0.00106	948893
Car1	CMN2	0.2161954	0.00366	12979
Car1	Chan	0.2125906	0.00133	450321
Car1	CC1	0.2196306	0.00546	6388
Chan	CC1	0.2206930	0.00387	12497
CMN2	Chan	0.2113349	0.00291	23432
CMN2	CC1	0.2033426	0.02113	359

2299
2300

2301 **Table S7.** Working 2-way models for Iberian Mesolithic hunter-gatherers and Loschbour. These
 2302 values were used for Fig. 2A.

<i>Test</i>	<i>Source1</i>	<i>Source2</i>	<i>P-value</i>	Mixture proportions		SE	
				<i>Source1</i>	<i>Source2</i>	<i>Source1</i>	<i>Source2</i>
LaBraña1	El Mirón	KO1	2.34E-01	0.448	0.552	0.046	0.046
LaBraña2	El Mirón	KO1	1.63E-01	0.490	0.510	0.042	0.042
Canes1	El Mirón	KO1	1.17E-01	0.268	0.732	0.047	0.047
Chan	El Mirón	KO1	6.26E-01	0.874	0.126	0.045	0.045
CMN2+CC1	El Mirón	KO1	5.22E-01	0.801	0.199	0.137	0.137
Car1	El Mirón	KO1	5.10E-01	0.927	0.073	0.046	0.046
Loschbour	El Mirón	KO1	8.65E-01	0.320	0.680	0.051	0.051

2303
 2304

2305 **Table S8.** Working 2-way and 3-way models for Neolithic and Copper Age groups from Iberia,
 2306 central Europe and Britain. These values were used for Fig. 2A.
 2307
 2308

<i>Test</i>	<i>Source1</i>	<i>Source2</i>	<i>Source3</i>	<i>P-value</i>	Mixture proportions			SE		
					<i>Source 1</i>	<i>Source 2</i>	<i>Source 3</i>	<i>Source 1</i>	<i>Source 2</i>	<i>Source3</i>
C_Iberia_MLN	El Mirón	KO1	Anatolia_N	9.07E-01	0.118	0.218	0.664	0.025	0.027	0.022
C_Iberia_CA	El Mirón	KO1	Anatolia_N	9.35E-01	0.079	0.216	0.705	0.016	0.019	0.013
NE_Iberia_EN	GoyetQ116-1	KO1	Anatolia_N	5.89E-01	0.083	0.087	0.831	0.026	0.024	0.021
	Ust_Ishim	KO1	Anatolia_N	5.04E-01	0.061	0.136	0.803	0.017	0.019	0.025
	Vestonice16	KO1	Anatolia_N	4.93E-01	0.089	0.091	0.820	0.026	0.024	0.022
	El Mirón	KO1	Anatolia_N	3.27E-01	0.079	0.076	0.845	0.025	0.026	0.021
	Iran_N	KO1	Anatolia_N	2.40E-01	0.061	0.120	0.819	0.033	0.019	0.038
	Tianyuan	KO1	Anatolia_N	2.23E-01	0.053	0.132	0.815	0.019	0.019	0.025
	Kostenki14	KO1	Anatolia_N	1.98E-01	0.074	0.102	0.824	0.026	0.023	0.023
	Morocco Iberomaurusian	KO1	Anatolia_N	1.96E-01	0.048	0.161	0.791	0.016	0.021	0.031
	EHG	KO1	Anatolia_N	1.24E-01	0.026	0.151	0.823	0.027	0.034	0.025
	El Mirón	EHG	Anatolia_N	6.29E-02	0.103	0.063	0.834	0.023	0.022	0.020
	Israel_Natufian	KO1	Anatolia_N	5.70E-02	0.066	0.141	0.793	0.052	0.024	0.069
NE_Iberia_MLN	El Mirón	KO1	Anatolia_N	3.86E-01	0.058	0.188	0.754	0.021	0.022	0.016
NE_Iberia_CA	El Mirón	KO1	Anatolia_N	6.88E-01	0.089	0.175	0.736	0.031	0.032	0.025
	GoyetQ116-1	KO1	Anatolia_N	1.50E-01	0.134	0.188	0.677	0.034	0.032	0.024
N_Iberia_EN	El Mirón	KO1	Anatolia_N	9.76E-01	0.000	0.106	0.893	0.035	0.036	0.031
	El Mirón	EHG	Anatolia_N	1.32E-01	0.060	0.037	0.904	0.035	0.033	0.030
	GoyetQ116-1	KO1	Anatolia_N	7.26E-02	0.061	0.115	0.824	0.037	0.035	0.030
N_Iberia_MLN	GoyetQ116-1	KO1	Anatolia_N	9.31E-02	0.100	0.263	0.636	0.022	0.022	0.016
	EHG	KO1	Anatolia_N	7.64E-02	0.008	0.379	0.613	0.021	0.027	0.020
	El Mirón	KO1	Anatolia_N	4.73E-02	0.066	0.264	0.670	0.020	0.023	0.016
N_Iberia_CA	El Mirón	KO1	Anatolia_N	5.99E-01	0.095	0.233	0.672	0.018	0.020	0.015
NW_Iberia_MLN	El Mirón	EHG	Anatolia_N	2.22E-01	0.208	0.264	0.528	0.114	0.098	0.092
	EHG	KO1	Anatolia_N	1.03E-01	0.182	0.446	0.372	0.110	0.131	0.112
	El Mirón	KO1	Anatolia_N	2.35E-02	0.365	-0.016	0.651	0.212	0.195	0.102
SE_Iberia_MLN	El Mirón	KO1	Anatolia_N	3.75E-01	0.114	0.143	0.742	0.021	0.022	0.017
SE_Iberia_CA	El Mirón	KO1	Anatolia_N	3.72E-01	0.097	0.157	0.746	0.019	0.022	0.015
SW_Iberia_EN	El Mirón	KO1	Anatolia_N	8.53E-01	0.052	0.074	0.874	0.049	0.051	0.040
	El Mirón	EHG	Anatolia_N	7.23E-01	0.070	0.070	0.860	0.044	0.043	0.038
	El Mirón	Iran_N	Anatolia_N	5.76E-01	0.133	0.005	0.862	0.038	0.060	0.066
	GoyetQ116-1	KO1	Anatolia_N	4.55E-01	0.075	0.096	0.829	0.049	0.047	0.038
	MA1	ElMirón	Anatolia_N	4.32E-01	0.023	0.100	0.877	0.044	0.042	0.040
	Iran_N	KO1	Anatolia_N	3.44E-01	0.001	0.156	0.843	0.063	0.037	0.068
	Tianyuan	KO1	Anatolia_N	3.30E-01	0.024	0.138	0.838	0.037	0.036	0.046
	Kostenki14	KO1	Anatolia_N	3.14E-01	0.031	0.132	0.836	0.048	0.043	0.042
	Vestonice16	KO1	Anatolia_N	3.13E-01	0.025	0.136	0.839	0.051	0.047	0.041
	Ust_Ishim	KO1	Anatolia_N	3.12E-01	0.000	0.147	0.853	0.036	0.035	0.047
SW_Iberia_MLN	El Mirón	KO1	Anatolia_N	6.18E-03	0.078	0.132	0.790	0.028	0.032	0.024
SW_Iberia_CA	El Mirón	KO1	Anatolia_N	6.83E-01	0.124	0.155	0.721	0.017	0.019	0.014
England_N	El Mirón	KO1	Anatolia_N	9.78E-01	0.058	0.202	0.740	0.018	0.020	0.015
Scotland_N	El Mirón	KO1	Anatolia_N	2.97E-01	0.041	0.201	0.758	0.015	0.017	0.012
France_MLN	El Mirón	KO1	Anatolia_N	7.35E-01	0.054	0.205	0.741	0.028	0.032	0.023
	GoyetQ116-1	KO1	Anatolia_N	2.18E-01	0.093	0.214	0.692	0.027	0.030	0.022
LBK_EN	KO1	Anatolia_N		6.71E-01	0.076	0.924		0.009	0.009	
Germany_MN	Tianyuan	KO1	Anatolia_N	4.40E-01	0.096	0.245	0.659	0.023	0.023	0.029
	mota	KO1	Anatolia_N	1.96E-01	0.043	0.298	0.659	0.020	0.024	0.036
	Iran_N	KO1	Anatolia_N	1.09E-01	0.110	0.240	0.650	0.037	0.024	0.042
	KO1	Anatolia_N		1.55E-03	0.263	0.737		0.024	0.024	

Hungary_EN	KO1	Anatolia_N	4.43E-01	0.090	0.910	0.012	0.012
Hungary_LCA	KO1	Anatolia_N	9.31E-01	0.164	0.836	0.010	0.010
Globular_Amphora Poland	KO1	Anatolia_N	1.51E-01	0.280	0.720	0.020	0.020

2309
2310

2311 **Table S9.** Best 2-way and 3-way model for the Iberian Copper Age outlier (C_Iberia_CA_Afr).
 2312

<i>Source1</i>	<i>Source2</i>	<i>Source3</i>	<i>P-value</i>	Mixture proportions			SE		
				<i>Source1</i>	<i>Source2</i>	<i>Source3</i>	<i>Source1</i>	<i>Source2</i>	<i>Source3</i>
Europe_ EN	Morocco Iberomaurusian		1.60E-02	0.451	0.549		0.027	0.027	
Mota	Europe_ EN	Morocco Iberomaurusian	5.85E-02	0.034	0.549	0.417	0.060	0.054	0.102

2313
 2314

2315 **Table S10.** Working models for the Iberian Copper Age outlier (C_Iberia_CA_Afr) when
 2316 including Morocco_EN and Morocco_LN in the *outgroup* set.
 2317

<i>Source1</i>	<i>Source2</i>	<i>Source3</i>	P-value	Mixture proportions			SE		
				<i>Source1</i>	<i>Source2</i>	<i>Source3</i>	<i>Source1</i>	<i>Source2</i>	<i>Source3</i>
Morocco									
Iberomaurusian	Morocco_EN	Morocco_LN	7.36E-01	0.021	0.164	0.814	0.084	0.105	0.037
Mota	Israel_Natufian	Morocco_LN	3.51E-01	0.039	0.065	0.895	0.022	0.055	0.068
Mota	Morocco_EN	Morocco_LN	3.38E-01	0.013	0.024	0.963	0.021	0.012	0.021
Mota	Morocco								
Mota	Iberomaurusian	Morocco_LN	3.07E-01	0.013	0.015	0.972	0.022	0.014	0.020
Mota	Morocco LN		2.32E-01	0.024	0.976		0.020	0.020	

2318
 2319

2320 **Table S11.** Working models for Iberia_CA_Stp, Iberia_BA and Iberia IA groups. Models in bold
 2321 were used for Fig. S6 and mentioned in the main text.
 2322

<i>Test</i>	<i>Source1</i>	<i>Source2</i>	P-value	Mixture proportions		SE		
				<i>Source1</i>	<i>Source2</i>	<i>Source1</i>	<i>Source2</i>	
Iberia_CA_Stp	Germany_Beaker	Iberia_CA	6.06E-01	0.602	0.398	0.018	0.018	
Iberia_BA	Germany_Beaker	Iberia_CA	3.90E-01	0.396	0.604	0.010	0.010	
	Iberia_CA	Iberia_CA_Stp	2.96E-01	0.332	0.668	0.024	0.024	
E_Iberia_IA	England_MBA	Iberia_BA	6.64E-01	0.135	0.865	0.022	0.022	
	England_Beaker	Iberia_BA	6.03E-01	0.123	0.877	0.020	0.020	
	Netherlands_Beaker	Iberia_BA	5.87E-01	0.114	0.886	0.019	0.019	
	France_Beaker	Iberia_BA	5.32E-01	0.144	0.856	0.024	0.024	
	Unetice_EBA	Iberia_BA	3.10E-01	0.119	0.881	0.021	0.021	
	Steppe_EBA	Iberia_BA	2.73E-01	0.059	0.941	0.011	0.011	
	France_Beaker	Iberia_CA	2.71E-01	0.493	0.507	0.017	0.017	
	Germany_Beaker	Iberia_BA	2.69E-01	0.143	0.857	0.026	0.026	
	EHG	Iberia_BA	2.36E-01	0.048	0.952	0.009	0.009	
	England_Beaker	Iberia_CA	2.09E-01	0.434	0.566	0.013	0.013	
	Netherlands_Beaker	Iberia_CA	1.92E-01	0.422	0.578	0.012	0.012	
	England_MBA	Iberia_CA	1.87E-01	0.474	0.526	0.014	0.014	
	N_Iberia_IA	England_MBA	Iberia_BA	5.59E-01	0.322	0.678	0.034	0.034
		Netherlands_Beaker	Iberia_BA	3.09E-01	0.286	0.714	0.029	0.029
France_Beaker		Iberia_BA	2.43E-01	0.358	0.642	0.038	0.038	
France_Beaker		Iberia_CA	2.35E-01	0.639	0.361	0.026	0.026	
Netherlands_Beaker		Iberia_CA	2.25E-01	0.545	0.455	0.022	0.022	
England_Beaker		Iberia_BA	2.14E-01	0.300	0.700	0.03	0.03	
England_MBA		Iberia_CA	2.10E-01	0.604	0.396	0.023	0.023	
England_Beaker		Iberia_CA	1.10E-01	0.562	0.438	0.021	0.021	
Steppe_EBA		Iberia_BA	5.50E-02	0.162	0.838	0.017	0.017	
SW_Iberia_IA		Unetice_EBA	Iberia_CA	8.34E-01	0.395	0.605	0.040	0.040
	Germany_Beaker	Iberia_BA	6.99E-01	0.260	0.740	0.059	0.059	
	Unetice_EBA	Iberia_BA	6.78E-01	0.192	0.808	0.047	0.047	
	Steppe_EBA	Iberia_BA	6.77E-01	0.105	0.895	0.028	0.028	
	France_Beaker	Iberia_BA	6.77E-01	0.212	0.788	0.050	0.050	
	Steppe_EBA	Iberia_CA	5.71E-01	0.228	0.772	0.026	0.026	
	MA1	Iberia_BA	5.27E-01	0.110	0.890	0.028	0.028	
	Netherlands_Beaker	Iberia_BA	5.11E-01	0.179	0.821	0.044	0.044	
	England_Beaker	Iberia_BA	5.09E-01	0.171	0.829	0.047	0.047	
	Germany_Beaker	Iberia_CA	4.94E-01	0.479	0.521	0.047	0.047	
	England_MBA	Iberia_BA	4.69E-01	0.197	0.803	0.051	0.051	
	EHG	Iberia_BA	3.72E-01	0.089	0.911	0.024	0.024	
	Iran_N	Iberia_BA	3.48E-01	0.147	0.853	0.037	0.037	
	France_Beaker	Iberia_CA	3.11E-01	0.410	0.590	0.042	0.042	

Netherlands_Beaker	Iberia_CA	2.44E-01	0.362	0.638	0.037	0.037
England_Beaker	Iberia_CA	1.94E-01	0.368	0.632	0.038	0.038
England_MBA	Iberia_CA	1.42E-01	0.401	0.599	0.041	0.041
ElMiron	Iberia_BA	1.28E-01	0.081	0.919	0.042	0.042
EHG	Iberia_CA	1.00E-01	0.199	0.801	0.021	0.021
Kostenki14	Iberia_BA	7.91E-02	0.073	0.927	0.031	0.031

2323
2324

2325 **Table S12.** Mixture proportions for the model Iberia_CA+Steppe_EBA. These values were used
 2326 for Fig. S6.

<i>Test</i>	<i>Source1</i>	<i>Source2</i>	<i>P-value</i>	Mixture proportions		SE	
				<i>Source1</i>	<i>Source2</i>	<i>Source1</i>	<i>Source2</i>
Iberia_CA_Stp	Iberia_CA	Steppe_EBA	4.01E-01	0.713	0.287	0.011	0.011
Iberia_BA	Iberia_CA	Steppe_EBA	1.66E-01	0.818	0.182	0.007	0.007
E_Iberia_IA	Iberia_CA	Steppe_EBA	1.24E-01	0.754	0.245	0.011	0.011
N_Iberia_IA	Iberia_CA	Steppe_EBA	2.57E-01	0.687	0.313	0.018	0.018
SW_Iberia_IA	Iberia_CA	Steppe_EBA	9.30E-01	0.803	0.197	0.034	0.034

2327

2328

2329 **Table S13.** Mixture proportions for the model Iberia_CA+Steppe_EBA in Bronze Age groups
 2330 from different regions.

<i>Test</i>	<i>Source1</i>	<i>Source2</i>	P-value	Mixture proportions		SE	
				<i>Source1</i>	<i>Source2</i>	<i>Source1</i>	<i>Source2</i>
C_Iberia_BA	Iberia_CA	Steppe_EBA	1.29E-01	0.808	0.192	0.012	0.012
N_Iberia_BA	Iberia_CA	Steppe_EBA	2.69E-01	0.799	0.201	0.012	0.012
NE_Iberia_BA	Iberia_CA	Steppe_EBA	9.19E-02	0.806	0.194	0.012	0.012
SE_Iberia_BA	Iberia_CA	Steppe_EBA	4.35E-01	0.854	0.146	0.014	0.014
SW_Iberia_BA	Iberia_CA	Steppe_EBA	7.64E-03	0.856	0.144	0.017	0.017

2331
 2332

2333 **Table S14.** Mixture proportions for Iberia_BA using the model Iberia_CA+ Germany_Beaker.
 2334

	<i>Source1</i>	<i>Source2</i>	P-value	Mixture proportions		SE	
				<i>Source1</i>	<i>Source2</i>	<i>Source1</i>	<i>Source2</i>
Autosomes	Iberia_CA	Germany_Beaker	6.14E-01	0.611	0.389	0.012	0.012
X-chromosomes	Iberia_CA	Germany_Beaker	1.27E-01	0.827	0.173	0.081	0.081

2335

2336

2337
2338
2339

Table S15. Admixture proportions for individuals in the Iberia_CA_Stp, Iberia_BA and Iberia_IA populations. These values were used for Fig. 2B.

Ind	Label	P-value	Iberia_CA	Germany Beaker	SE
I0462	C_Iberia_CA_Stp	2.53E-01	0.229	0.771	0.111
EHU002	C_Iberia_CA_Stp	9.30E-01	0.371	0.629	0.049
I3239	NW_Iberia_CA_Stp	9.39E-01	0.226	0.774	0.085
I3243	NW_Iberia_CA_Stp	7.54E-01	0.239	0.761	0.094
I3238	NW_Iberia_CA_Stp	8.81E-01	0.365	0.635	0.056
I0461	C_Iberia_CA_Stp	5.19E-02	0.544	0.456	0.046
I6471	C_Iberia_CA_Stp	7.81E-01	-0.145	1.145	0.097
I6472	C_Iberia_CA_Stp	4.89E-01	0.499	0.501	0.057
I6539	C_Iberia_CA_Stp	5.74E-01	0.485	0.515	0.048
I6588	C_Iberia_CA_Stp	4.02E-01	0.270	0.730	0.067
EHU001	C_Iberia_CA_Stp	8.76E-01	0.096	0.904	0.049
I5665	C_Iberia_CA_Stp	3.69E-01	0.501	0.499	0.045
I3484	C_Iberia_CA_Stp	6.19E-01	0.644	0.356	0.075
I7689	SW_Iberia_BA	9.71E-01	0.840	0.160	0.188
I7691	SW_Iberia_BA	2.64E-01	0.678	0.322	0.073
I7692	SW_Iberia_BA	2.40E-01	0.645	0.355	0.077
I3756	C_Iberia_BA	4.28E-01	0.655	0.345	0.044
I6623	C_Iberia_CA_Stp	1.86E-01	0.297	0.703	0.046
I3494	SE_Iberia_BA	4.60E-01	0.744	0.256	0.042
I12809	C_Iberia_BA	6.54E-01	0.507	0.493	0.083
I12855	C_Iberia_BA	5.09E-01	0.677	0.323	0.124
I6618	C_Iberia_BA	4.73E-02	0.681	0.319	0.046
I8144	SE_Iberia_BA	4.64E-01	0.534	0.466	0.064
VAD001	N_Iberia_BA	3.12E-02	0.498	0.502	0.047
I1310	NE_Iberia_BA	7.15E-02	0.654	0.346	0.048
I1312_d	NE_Iberia_BA	5.84E-01	0.499	0.501	0.056
I1313_d	NE_Iberia_BA	9.26E-01	0.688	0.312	0.049
I3997	SE_Iberia_BA	1.81E-03	0.694	0.306	0.044
I4562	NE_Iberia_BA	2.48E-01	0.559	0.441	0.042
I3487	SE_Iberia_BA	2.42E-01	0.754	0.246	0.065
I6470	C_Iberia_BA	5.11E-01	0.522	0.478	0.045
I10939	SW_Iberia_BA	6.27E-01	0.702	0.298	0.049
I10940	SW_Iberia_BA	3.45E-01	0.544	0.456	0.095
I10941	SW_Iberia_BA	1.18E-01	0.638	0.362	0.050
VAD005	N_Iberia_BA	3.67E-01	0.524	0.476	0.050
I1982	N_Iberia_BA	7.70E-01	0.462	0.538	0.141
VAD002	N_Iberia_BA	1.64E-01	0.583	0.417	0.070
VAD003	N_Iberia_BA	3.33E-01	0.575	0.425	0.109
I3486	SE_Iberia_BA	1.13E-01	0.650	0.350	0.089
I3488	SE_Iberia_BA	3.52E-01	0.793	0.207	0.074
I4559	NE_Iberia_BA	6.19E-01	0.545	0.455	0.048
I4560	NE_Iberia_BA	9.25E-01	0.549	0.451	0.045
I4561	NE_Iberia_BA	4.25E-01	0.552	0.448	0.044
I1836	NE_Iberia_BA	2.71E-01	0.597	0.403	0.050
I2471	N_Iberia_BA	9.37E-01	0.577	0.423	0.059
I1840	N_Iberia_BA	6.19E-01	0.610	0.390	0.046
I1977	N_Iberia_BA	3.42E-02	0.585	0.415	0.064
I2472	N_Iberia_BA	5.35E-01	0.677	0.323	0.060
I8136	SE_Iberia_BA	1.43E-01	0.685	0.315	0.044

I3490	C_Iberia_BA	4.09E-01	0.585	0.415	0.053
I3491	C_Iberia_BA	1.09E-01	0.606	0.394	0.071
I3492	C_Iberia_BA	4.43E-01	0.483	0.517	0.058
I8045	SW_Iberia_BA	7.14E-01	0.627	0.373	0.104
VAD004	N_Iberia_BA	1.75E-02	0.572	0.428	0.050
I8570	SE_Iberia_BA	9.86E-01	0.648	0.352	0.048
I8571	SE_Iberia_BA	4.70E-01	0.766	0.234	0.095
I3493	C_Iberia_BA	1.76E-02	0.518	0.482	0.048
I2470	N_Iberia_BA	1.14E-01	0.583	0.417	0.049
I12208	C_Iberia_BA	7.83E-02	0.598	0.402	0.043
I12209	C_Iberia_BA	3.93E-01	0.581	0.419	0.043
I7687	SW_Iberia_BA	7.75E-01	0.537	0.463	0.117
I7688	SW_Iberia_BA	9.49E-01	0.391	0.609	0.123
I2469	N_Iberia_BA	7.79E-01	0.420	0.580	0.069
I12641	E_Iberia_IA	5.82E-01	0.430	0.570	0.071
I12640	E_Iberia_IA	3.94E-01	0.461	0.539	0.073
I12171	SW_Iberia_IA	7.90E-01	0.505	0.495	0.068
I12561	SW_Iberia_IA	7.87E-01	0.582	0.418	0.091
I4556	E_Iberia_IA	9.24E-01	0.412	0.588	0.060
I3322	E_Iberia_IA	9.22E-01	0.504	0.496	0.045
I12642	E_Iberia_IA	4.83E-01	0.678	0.322	0.172
I12879	E_Iberia_IA	2.83E-03	0.359	0.641	0.053
I12410	E_Iberia_IA	9.18E-01	0.499	0.501	0.043
I12877	E_Iberia_IA	4.13E-01	0.596	0.404	0.093
I12878	E_Iberia_IA	5.67E-01	0.562	0.438	0.057
I3757	N_Iberia_IA	3.59E-01	0.467	0.533	0.060
I3323	E_Iberia_IA	5.89E-01	0.548	0.452	0.049
I3758	N_Iberia_IA	6.02E-01	0.307	0.693	0.043
I3759	N_Iberia_IA	6.13E-01	0.407	0.593	0.044
I3324	E_Iberia_IA	1.49E-01	0.389	0.611	0.049
I3326	E_Iberia_IA	5.81E-01	0.021	0.979	0.070
I3327	E_Iberia_IA	4.46E-01	0.495	0.505	0.053
I3320	E_Iberia_IA	3.68E-01	0.434	0.566	0.045
I3321	E_Iberia_IA	9.25E-01	0.518	0.482	0.044

2340
2341

2342 **Table S16.** Working 2-way model for the Iberian Bronze Age outlier (ID I7162).
 2343

			Mixture proportions		SE	
<i>Source1</i>	<i>Source2</i>	P-value	<i>Source1</i>	<i>Source2</i>	<i>Source1</i>	<i>Source2</i>
Iberia_BA	Morocco_LN	7.40E-01	0.534	0.466	0.050	0.050
Morocco						
Iberomaurusian	Iberia_BA	5.50E-01	0.112	0.888	0.018	0.018
Iberia_BA	C_Iberia_CA_Afr	5.65E-01	0.759	0.241	0.031	0.031
Israel_Natufian	Iberia_BA	3.54E-01	0.292	0.708	0.039	0.039
mota	Iberia_BA	8.33E-02	0.133	0.867	0.016	0.016

2344
 2345

2346 **Table S17.** 2-way models for NE_Iberia_c.6-8CE_ES (L'Esquerda) including Iberia_IA as one
 2347 of the sources. The models in bold were used for Fig. 2C.
 2348

<i>Source1</i>	<i>Source2</i>	P-value	Mixture proportions		SE	
			<i>Source1</i>	<i>Source2</i>	<i>Source1</i>	<i>Source2</i>
Iberia_IA	Greek	3.29E-01	0.794	0.206	0.027	0.027
Iberia_IA	Bergamo	1.33E-01	0.731	0.269	0.039	0.039
Iberia_IA	TSI	4.89E-02	0.737	0.263	0.043	0.043
Iberia_IA	Bavaria_Early Medieval.SG	5.70E-03	0.819	0.181	0.033	0.033
Iberia_IA	Saxon.SG	2.87E-03	0.818	0.182	0.034	0.034
Iberia_IA	Steppe_EBA	1.14E-03	0.926	0.074	0.018	0.018
Iberia_IA	Empuries2	4.48E-04	0.858	0.142	0.034	0.034
Iberia_IA	Iran_N	2.64E-04	0.908	0.092	0.019	0.019
Iberia_IA	MA1	9.93E-05	0.955	0.045	0.013	0.013
Iberia_IA	EHG	3.68E-05	0.959	0.041	0.014	0.014
Iberia_IA	Anatolia_N	7.38E-06	-0.009	1.009	0.024	0.024
Iberia_IA	Kostenki14	1.79E-06	0.987	0.013	0.014	0.014
Iberia_IA	Israel_Natufian	1.04E-06	0.985	0.015	0.020	0.020
Iberia_IA	LBK_EN	7.62E-07	0.975	0.025	0.025	0.025
Iberia_IA	Ust_Ishim	8.73E-09	0.976	0.024	0.012	0.012
Iberia_IA	mota	8.46E-11	0.986	0.014	0.009	0.009
Iberia_IA	Morocco Iberomaurusian	6.07E-13	0.970	0.030	0.011	0.011

2349
 2350

2351 **Table S18.** Best 2-way and 3-way models for NE_Iberia_c.6CE_PL (Pla de l'Horta). The models
 2352 in bold were used for Fig. 2C.

<i>Source1</i>	<i>Source2</i>	<i>Source3</i>	P-value	Mixture proportions			SE		
				<i>Source1</i>	<i>Source2</i>	<i>Source3</i>	<i>Source1</i>	<i>Source2</i>	<i>Source3</i>
NE_Iberia_c.6-8CE_ES	Steppe_EBA		1.22E-01	0.914	0.086		0.020	0.020	
NE_Iberia_c.6-8CE_ES	Bavaria_Early Medieval.SG		3.61E-02	0.832	0.168		0.042	0.042	
NE_Iberia_c.6-8CE_ES	Saxon.SG		2.87E-02	0.864	0.136		0.045	0.045	
NE_Iberia_c.6-8CE_ES	Steppe_EBA	LBK_EN	1.96E-01	0.853	0.114	0.033	0.069	0.033	0.040
NE_Iberia_c.6-8CE_ES	Steppe_EBA	TSI	9.35E-02	0.781	0.091	0.127	0.059	0.019	0.054
NE_Iberia_c.6-8CE_ES	Bavaria_Early Medieval.SG	TSI	9.20E-02	0.732	0.226	0.041	0.067	0.050	0.054
NE_Iberia_c.6-8CE_ES	Steppe_EBA	Bavaria_Early Medieval.SG	6.19E-02	0.881	0.069	0.050	0.053	0.036	0.080
NE_Iberia_c.6-8CE_ES	Steppe_EBA	Empuries2	5.58E-02	0.819	0.104	0.077	0.054	0.022	0.040
NE_Iberia_c.6-8CE_ES	Steppe_EBA	Anatolia_N	5.39E-02	0.792	0.136	0.072	0.059	0.030	0.033

2353

2354

2355 **Table S19.** Working 2-way models for NE_Iberia_c.8-12CE (Sant Julià de Ramis). The models
 2356 in bold were used for Fig. 2C.

			Mixture proportions		SE	
<i>Source1</i>	<i>Source2</i>	P-value	<i>Source1</i>	<i>Source2</i>	<i>Source1</i>	<i>Source2</i>
NE_Iberia_c.6-8CE_ES	SE_Iberia_c.10-16CE	3.33E-01	0.678	0.322	0.059	0.059
NE_Iberia_c.6-8CE_ES	Morocco_LN	1.36E-01	0.827	0.173	0.038	0.038
NE_Iberia_c.6-8CE_ES	Israel Natufian	1.21E-01	0.888	0.112	0.023	0.023

2357
 2358

2359 **Table S20.** 2-way and 3-way admixture models for populations from the southeast over the past
 2360 2000 years.

<i>Test</i>	<i>Source1</i>	<i>Source2</i>	<i>Source3</i>	<i>P-value</i>	<i>Mixture proportions</i>			<i>SE</i>		
					<i>Source 1</i>	<i>Source 2</i>	<i>Source 3</i>	<i>Source 1</i>	<i>Source 2</i>	<i>Source 3</i>
SE_Iberia c.3-4 CE	NE_Iberia c.6-8CE_ES	Morocco _LN		7.87E-02	0.554	0.446		0.031	0.031	
SE_Iberia c.5-8 CE	NE_Iberia c.6-8CE_ES	Morocco _LN		1.22E-06	0.532	0.468		0.026	0.026	
SE_Iberia c.10-16CE	NE_Iberia c.6-8CE_ES	Guanche		2.76E-02	0.773	0.227		0.012	0.012	
SE_Iberia c.3-4 CE	NE_Iberia c.6-8CE_ES	Morocco _LN	Levant_ EBA	9.45E-02	0.542	0.393	0.065	0.031	0.047	0.041
SE_Iberia c.5-8 CE	NE_Iberia c.6-8CE_ES	Guanche	Levant_ EBA	6.92E-05	0.699	0.193	0.108	0.026	0.018	0.036
SE_Iberia c.10-16CE	NE_Iberia c.6-8CE_ES	Guanche	Levant_ EBA	2.11E-01	0.699	0.188	0.113	0.022	0.015	0.030

2361
 2362

2363 **Table S21.** Admixture models for individuals in the SE_Iberia_c.3-4CE, SE_Iberia_c.5-8CE and
 2364 SE_Iberia_c.10-16CE populations. These ancestry proportions were used for Fig. 2D.
 2365

Ind ID	Population	Source1	Source2	Source3	P-value	Mixture proportions			SE		
						Source 1	Source 2	Source 3	Source 1	Source 2	Source 3
I3982	SE_Iberia c.3-4CE	NE_Iberia c.6-8CE_ES	Morocco_LN	Levant_EBA	1.03E-01	0.543	0.435	0.022	0.046	0.067	0.050
I3983	SE_Iberia c.3-4CE	NE_Iberia c.6-8CE_ES	Morocco_LN	Levant_EBA	6.51E-02	0.480	0.410	0.110	0.041	0.068	0.058
I4055	SE_Iberia c.3-4CE	NE_Iberia c.6-8CE_ES	Morocco_LN		3.88E-01	0.433	0.567	0.000	0.102	0.102	0.000
I3980	SE_Iberia c.5-8CE	NE_Iberia c.6-8CE_ES	Morocco_LN	Levant_EBA	7.73E-01	0.269	0.568	0.162	0.041	0.080	0.077
I3981	SE_Iberia c.5-8CE	NE_Iberia c.6-8CE_ES	Morocco_LN	Levant_EBA	1.28E-01	0.489	0.504	0.007	0.048	0.090	0.067
I3574	SE_Iberia c.5-8CE	NE_Iberia c.6-8CE_ES	Morocco_LN		4.63E-01	0.539	0.461	0.000	0.092	0.092	0.000
I3575	SE_Iberia c.5-8CE	NE_Iberia c.6-8CE_ES	Morocco_LN		4.68E-01	0.331	0.669	0.000	0.043	0.043	0.000
I3581	SE_Iberia c.5-8CE	NE_Iberia c.6-8CE_ES	Morocco_LN		4.60E-01	0.459	0.541	0.000	0.042	0.042	0.000
I3576	SE_Iberia c.5-8CE	NE_Iberia c.6-8CE_ES	Morocco_LN	Levant_EBA	1.62E-01	0.481	0.447	0.071	0.041	0.066	0.058
I3583	SE_Iberia c.5-8CE	NE_Iberia c.6-8CE_ES	Morocco_LN	Levant_EBA	7.42E-01	0.281	0.668	0.051	0.058	0.105	0.082
I3577	SE_Iberia c.5-8CE	NE_Iberia c.6-8CE_ES	Morocco_LN		1.75E-01	0.290	0.710	0.000	0.086	0.086	0.000
I3578	SE_Iberia c.5-8CE	NE_Iberia c.6-8CE_ES	Guanche		3.41E-01	0.681	0.319	0.000	0.043	0.043	0.000
I3579	SE_Iberia c.5-8CE	NE_Iberia c.6-8CE_ES	Morocco_LN	Levant_EBA	4.46E-01	0.548	0.229	0.223	0.102	0.204	0.143
I3582	SE_Iberia c.5-8CE	NE_Iberia c.6-8CE_ES	Morocco_LN	Levant_EBA	2.34E-01	0.442	0.557	0.001	0.048	0.090	0.066
I3585	SE_Iberia c.5-8CE	NE_Iberia c.6-8CE_ES	Morocco_LN	Levant_EBA	6.20E-02	0.662	0.317	0.022	0.058	0.091	0.056
I7500	SE_Iberia c.10-16CE	NE_Iberia c.6-8CE_ES	Guanche		1.28E-01	0.795	0.205	0.000	0.060	0.060	0.000
I12516	SE_Iberia c.10-16CE	NE_Iberia c.6-8CE_ES	Morocco_LN		1.89E-01	0.699	0.301	0.000	0.066	0.066	0.000
I12514	SE_Iberia c.10-16CE	NE_Iberia c.6-8CE_ES	Morocco_LN		7.59E-01	0.556	0.444	0.000	0.047	0.047	0.000
I12515	SE_Iberia c.10-16CE	NE_Iberia c.6-8CE_ES	Morocco_LN		3.28E-01	0.602	0.398	0.000	0.051	0.051	0.000
I7497	SE_Iberia c.10-16CE	NE_Iberia c.6-8CE_ES	Morocco_LN	Levant_EBA	5.51E-01	0.466	0.464	0.070	0.071	0.115	0.112
I7498	SE_Iberia c.10-16CE	NE_Iberia c.6-8CE_ES	Morocco_LN	Levant_EBA	1.39E-01	0.589	0.294	0.117	0.050	0.078	0.062
I7499	SE_Iberia c.10-16CE	NE_Iberia c.6-8CE_ES	Morocco_LN	Jordanian	5.00E-02	0.431	0.286	0.283	0.042	0.081	0.079
I7457	SE_Iberia c.10-16CE	NE_Iberia c.6-8CE_ES	Guanche	Levant_EBA	9.74E-02	0.678	0.242	0.080	0.052	0.037	0.068
I12644	SE_Iberia c.10-16CE	Iberia IA	Morocco_LN	Jordanian	3.04E-02	0.333	0.486	0.181	0.038	0.073	0.059
I12645	SE_Iberia c.10-16CE	NE_Iberia c.6-8CE_ES	Morocco_LN	Levant_EBA	3.84E-01	0.327	0.478	0.195	0.118	0.171	0.128

I12647	SE_Iberia c.10-16CE	NE_Iberia c.6-8CE_ES	Guanche	Levant_EBA	8.15E-02	0.753	0.150	0.097	0.047	0.031	0.060
I12648	SE_Iberia c.10-16CE	NE_Iberia c.6-8CE_ES	Guanche		8.20E-02	0.936	0.064	0.000	0.085	0.085	0.000
I12649	SE_Iberia c.10-16CE	NE_Iberia c.6-8CE_ES	Morocco_LN		9.68E-01	0.674	0.326	0.000	0.089	0.089	0.000
I8145	SE_Iberia c.10-16CE	NE_Iberia c.6-8CE_ES	Morocco_LN		9.14E-01	0.571	0.429	0.000	0.176	0.176	0.000
I8146	SE_Iberia c.10-16CE	NE_Iberia c.6-8CE_ES	Guanche	Levant_EBA	3.15E-01	0.445	0.358	0.197	0.068	0.045	0.086
I8147	SE_Iberia c.10-16CE	Iberia IA	Guanche	Levant_EBA	4.12E-01	0.720	0.176	0.103	0.124	0.100	0.172
I3808	SE_Iberia c.10-16CE	NE_Iberia c.6-8CE_ES	Morocco_LN	Levant_EBA	4.39E-02	0.379	0.367	0.255	0.046	0.079	0.065
I3809	SE_Iberia c.10-16CE	NE_Iberia c.6-8CE_ES	Morocco_LN		1.16E-01	0.461	0.539	0.000	0.133	0.133	0.000
I7423	SE_Iberia c.10-16CE	Iberia IA	Morocco_LN	Levant_EBA	8.51E-01	0.317	0.637	0.045	0.056	0.116	0.088
I7424	SE_Iberia c.10-16CE	NE_Iberia c.6-8CE_ES	Morocco_LN	Levant_EBA	1.19E-01	0.559	0.336	0.105	0.051	0.090	0.065
I7425	SE_Iberia c.10-16CE	NE_Iberia c.6-8CE_ES	Guanche	Levant_EBA	1.98E-01	0.629	0.286	0.086	0.046	0.033	0.057

2366

2367

2368 **Table S22.** Admixture models for the two outlier individuals from the SE_Iberia_c.10-16CE
 2369 population. These ancestry proportions were used for Fig. 2D.

<i>Test</i>	<i>Source1</i>	<i>Source2</i>	<i>P-value</i>	Mixture proportions		SE	
				<i>Source1</i>	<i>Source2</i>	<i>Source1</i>	<i>Source2</i>
I7427	SE_Iberia c.3-4CE	Gambian	6.61E-01	0.630	0.370	0.021	0.021
I3810	SE_Iberia c.3-4CE	Gambian	2.68E-01	0.517	0.483	0.023	0.023

2370